Fundamental Chemistry of Carbon Dioxide Capture

James Ernest Wheatley

Submitted in accordance with the requirements for the degree of Doctor of Philosophy.

The University of Leeds

School of Chemistry

May, 2017

The candidate confirms that the work is his own and appropriate credit has been given where reference is made to the work of others.

Acknowledgements

First and foremost, I would like to thank my supervisor, Professor Christopher Rayner, for giving me the opportunity to do this work, for his sound guidance, advice and support throughout, and at times extreme patience. I couldn't have done this one without you.

I would like to thank C-Capture Ltd. for their funding support and access to their vapour-liquid equilibrium cells on which much of the work laid out in Chapters 4 and 5 relied. I am indebted to the staff of C-Capture, Dr Douglas Barnes, Caspar Schoolderman, Dr Gergely Jakab and Dave Lawlor, for their help in many aspects, as well as numerous illuminating discussions.

Special thanks go also to everyone from the Rayner group and Keracol Ltd. with whom I have had the pleasure of working over the past few years – Dr Balazs Kulik, Dr Meryem Benohoud, Dr Henry Spurr, Muhammad Wathon, Rachel Hollis, Lissie Dufton, Diarmaid Clery, Gillian Finnerty, Sannia Farooque and Lauren Ford.

None of the work that goes on in the School would be possible without the tireless efforts of its technical staff. I owe thanks to Simon Barrett for his help with the NMR, and Matt Broadbent from the Mechanics Workshop, as well the staff of Chemistry Stores – Francis Billinghurst (now enjoying a richly-deserved retirement), Richard Roper, Steven Chowney and Jake Roberts.

I would like to thank my family for their backing and support in every aspect, and everyone who has brightened up my time at Leeds. I am deeply grateful for the help and support of Dr Adrian Chaplin and Dr Vas Stavros, without whom I would never have come here in the first place. Finally, I owe thanks to Peter Holloway who helped me access the Nimbus 4 satellite data, to Ben Jennings, Rachel Player, Sophie Clayton and Darren Mason for many fine evenings together, and to Catherine Oughtibridge, without whose unfailing moral support this work would never have come into existence.

Abstract

Carbon dioxide capture is an urgently needed pathway to mitigation of climate change, yet the amine-based solvents currently considered the leading industrial technologies suffer from many shortcomings; namely their high operating cost, poor stability and potentially damaging environmental impact from emission of degradation products. This work is a study of possible routes to improved CO_2 capture technologies from a fundamental chemistry perspective.

Initial work focused on the development of a straightforward and adaptable protocol for studying the species formed by CO_2 capture into amine solvents, using ^{1}H NMR spectroscopy for its combination of speed and accuracy. The applicability of this approach to diverse blended-amine solvents was demonstrated.

This method was then applied to the study of phenoxide as a novel possible capture agent in conjunction with amines. Blends of potassium phenoxide with monoethanolamine were found to have an excellent capture capacity and favourable speciation that suggests a low energy consumption in practical use. This demonstrates the feasibility of blended solvents with a reduced amine component.

Finally, a possible amine-free route to CO_2 capture, exploiting the high susceptibility of carboxylate acidity to solvation, was explored. The first systematic study of the pK_a of CO_2 in mixtures of organic solvent and water was carried out, finding that this value is relatively insensitive to the makeup of the solvent and therefore in organic-rich solutions, carboxylate salts can be used as a CO_2-absorbing base. CO_2 capture using a system developed along these principles was demonstrated, and the possible basis for the observed insensitivity was discussed with particular emphasis given to the thermodynamics of the process.

Contents

List of Figures

List of Tables

List of Schemes

List of Abbreviations

°C	degrees Celsius
Ac	acetyl
AMP	2-amino-2-methyl-propan-1-ol
BECCS	bioenergy with carbon dioxide capture and storage
CCS	carbon dioxide capture and storage
DEA	diethanolamine
DMSO	dimethylsulfoxide
DSS	sodium 4,4-dimethyl-4-silapentane-1-sulfonate
EGBE	ethylene glycol monobutyl ether
EOR	enhanced oil recovery
g	grams
GJ	gigajoule
HPLC	high performance liquid chromatography
Hx	hexyl
IR	infrared
K	Kelvin
L	litres
M	moles per litre
MDEA	*N*-methyldiethanolamine
MEA	monoethanolamine
MHz	megahertz
mL	millilitres
MOF	metal-organic framework
mol	moles
mol%	mole percent
MΩ	megaohms
Mta	million tons per annum
NMR	nuclear magnetic resonance
NRTL	non-random two-liquid
PE	2-piperidineethanol

Ph	phenyl
pK_a	acid dissociation constant
ppm	parts per million
PZ	piperazine
TEDAM	tetraethyldiaminomethane
UV	ultraviolet
Vis	visible
wt%	weight percent
δ	chemical shift

1 Introduction to Carbon Dioxide Capture and Storage

1.1 Properties of carbon dioxide

Carbon dioxide was first isolated by the Scottish chemist Joseph Black in 1754.[1] Black observed that treatment of limestone (calcium carbonate) with acids yielded a colourless, odourless gas in which neither flames nor animals could survive, and that calcium carbonate could be recovered by passage of the gas through limewater (calcium hydroxide). The substance was termed "fixed air," but is now known to be carbon dioxide or CO_2.

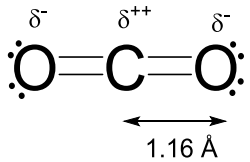

Figure 1.1: Structure and bonding of carbon dioxide.

CO_2 consists of two oxygen atoms double-bonded to a central carbon atom (Figure 1.1). Despite the high polarity of these bonds, the molecule has no dipole moment due to its centrosymmetric nature. As the most oxidised form of carbon, CO_2 exhibits high stability. Though it might superficially be described as a C1 dicarbonyl, and like carbonyl compounds its chemistry is dominated by nucleophilic attacks on its electropositive carbon atom, carbon dioxide is much more resistant to reduction than most carbonyls.[2]

CO_2 is present in relatively small quantities in the Earth's atmosphere, at a concentration of *ca.* 404 ppm,[3] though its occurrence in the atmospheres of other terrestrial planets is dramatically higher, and the same is likely to have been true of the early Earth prior to the development of life. Carbon dioxide is fundamental for life on earth as a source of carbon. Photosynthesis in autotrophs reduces carbon dioxide to sugars, oxidation of which provides energy for living organisms and releases CO_2 once again.

1.2 Carbon dioxide and climate change

Carbon dioxide's two C=O bonds give rise to strong absorptions in its infrared spectrum at 2349 cm^{-1} and 667 cm^{-1}, which can be used to determine the concentration of CO_2 in the atmosphere.[4] Svante Arrhenius was the first to propose that this absorption may also play a significant role in the Earth's atmosphere, and thereby originated the concept of the greenhouse effect.[5] The greenhouse effect describes the warming effect of radiation-absorbing gases on the temperature of the atmosphere. The surface temperature of the Earth resembles a steady state, in which visible radiation received from the sun is balanced by black-body infrared radiation emitted into space from the Earth. The presence of IR-absorbing gases (known as *greenhouse gases*) in the atmosphere adjusts this balance by absorbing some of the infrared radiation emitted from the planet's surface, thus trapping additional heat and increasing the surface temperature of the Earth.

The principal greenhouse gases in the Earth's atmosphere are water and CO_2, as is readily evident from the infrared emission spectrum of the Earth, which displays significant troughs at wavelengths corresponding to the infrared absorption spectra of these two molecules (Figure 1.2). The CO_2 absorption at 667 cm^{-1} is particularly important, as it falls within the region of highest radiance from the Earth, and therefore exerts a disproportionate effect upon the temperature of the atmosphere relative to its concentration.[6]

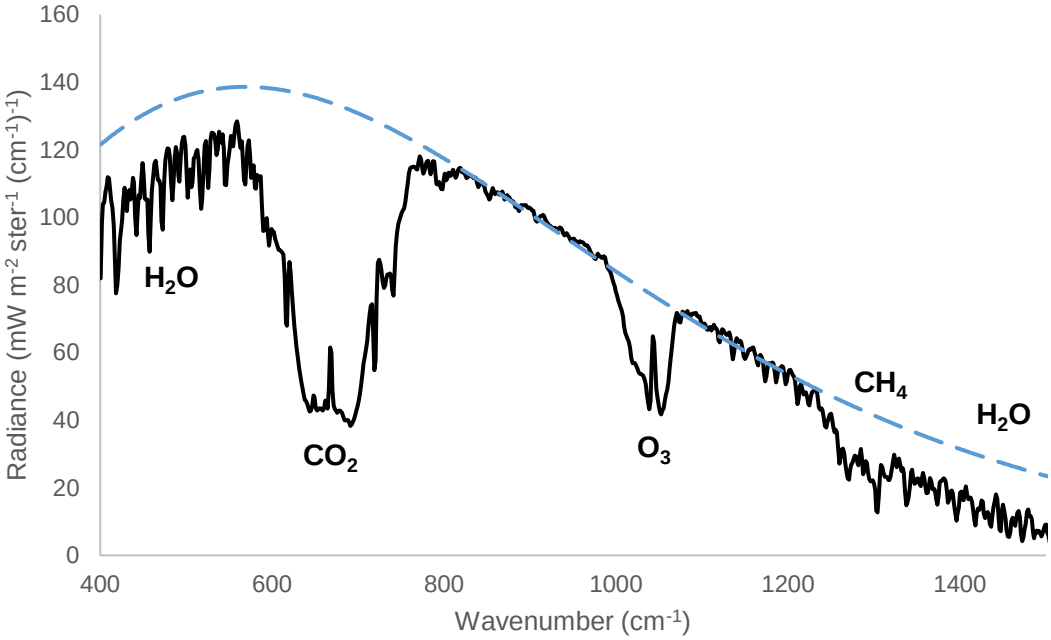

Figure 1.2: Infrared emission spectrum of the Earth, showing major absorbances and the gases attributed to them, as measured by the Nimbus 4 satellite.[6] *Dashed line indicates the theoretical emission of a black body (computed from the Planck equation) at 290 K.*

These observations are borne out by study of the history of the Earth's climate and atmosphere. Figure 1.3 compares the surface temperature and concentration of CO_2 in the atmosphere over the previous 420,000 years, as measured by study of the composition of air trapped in Antarctic ice.[7–10] A strong correlation between the two is evident. Relatively low levels of atmospheric CO_2 (*ca.* 190 ppm) coincide with significant cooling, whereas high levels (*ca.* 290 ppm) correlate with interglacial periods more similar to the present day climate.

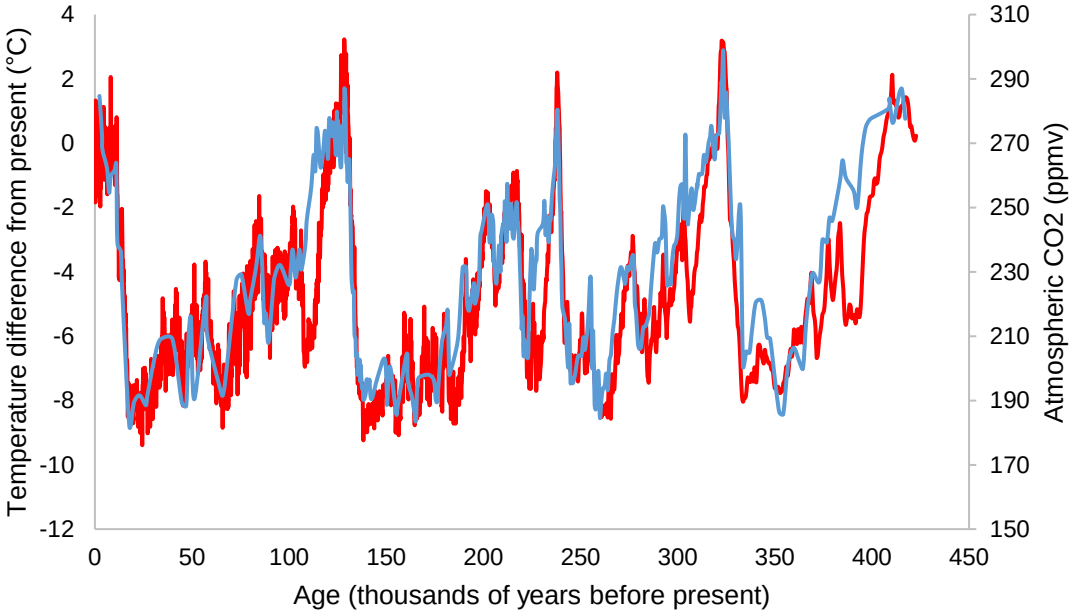

Figure 1.3: Historical temperature (red) and CO_2 concentration (blue) data derived from analysis of the Vostok ice core.[7–10]

This correlation is of very high concern, as CO_2 levels in recent history have been rising with extreme rapidity. This was first observed at Mauna Loa in studies of atmospheric composition carried out from 1958 onwards by Keeling and coworkers, and has since been repeated many times over worldwide.[3] Atmospheric CO_2 concentration recently surpassed 400 ppm, an unprecedented increase of 100 ppm in less than a century, and continues to increase (Figure 1.4) at a steady rate.

This alarming increase in atmospheric CO_2 is almost certainly due to human activity. Beginning in eighteenth-century Britain and spreading steadily across the globe, fossil fuels replaced renewable wood, water and animal power as the main energy source for industry. This industrialisation led to tremendous increases in energy demand and exponential population growth. Combustion of fossil fuels releases large amounts of carbon that had previously been isolated from the surface for millions of years, creating a large source of CO_2 for which there is no comparable sink. It is estimated that fossil fuel use since 1751 has released approximately 337 billion tonnes of CO_2 into the atmosphere with annual emissions now at 8 billion tonnes per year.[11]

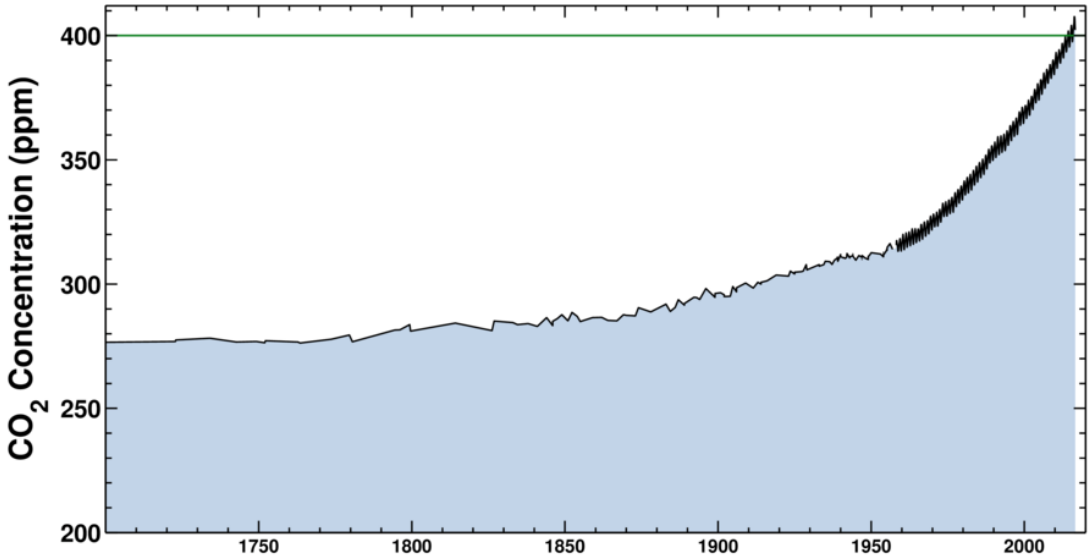

Figure 1.4: Atmospheric concentration of CO_2, 1700-present. Data 1700-1958 is derived from ice core analysis, 1958-present from direct atmospheric observations.[3]

The likely consequence of an increase in atmospheric CO_2 concentrations is a significant increase in the surface temperature of the Earth, on the order of multiple degrees Celsius, referred to variously as "global warming" or "climate change," the latter name having been adopted to reflect the fact that an increase in the average global surface temperature would not correspond to an even warming across the planet - redistribution of air and water currents may cause pronounced cooling in certain areas. For example, the climate of Western Europe is currently warmed by ocean currents in the North Atlantic, but melting of polar glaciers, especially in Greenland, may alter or disrupt these currents.

Indeed, the climate is already changing. Analysis of temperature data over recent decades shows an increase in the global temperature of approximately 0.5 °C since 1970. Unusual climate patterns have occurred with increasing frequency in recent decades. The extent of ice caps worldwide has seen reductions due to the warming climate.[12]

The effects of climate change are predicted to be catastrophic on many different levels. Likely effects include: melting of polar ice caps, resulting in sea level rises and flooding of low-lying land; droughts and desertification; spread of harmful insects, including malarial mosquitos and crop pests, into higher latitudes; increases in energetic weather events including hurricanes and storms; and extinction of species and habitats which cannot adapt to the changes.

Most serious of all is the risk of "runaway" climate change, wherein initial climate change induces further release of greenhouse gases into the atmosphere from natural sources (in particular, methane currently trapped beneath subarctic permafrost) and a positive feedback loop develops, resulting in a far greater temperature increase than might have been expected from the amount of CO_2 initially released. This presents the danger of a "tipping point" in CO_2 emissions, beyond which dramatic climate change is irreversible. It is possible that such a tipping point has already passed, but if it has not, emissions reduction is of the highest priority.

A full analysis of climate change together with its causes and effects has been prepared by the Intergovernmental Panel on Climate Change.[12]

1.3 Carbon dioxide capture and storage (CCS)

1.3.1 The case for CCS

The majority of anthropogenic CO_2 emissions originate from the burning of fossil fuels to provide energy, and a significant reduction is needed in order to minimise climate change. In the long term this may be accomplished by replacement of fossil fuels with low-carbon alternatives, such as nuclear or solar power production, but this transition is likely to require significant political will (not necessarily forthcoming in all major CO_2-producing countries) and decades of work to achieve, and is therefore insufficient when change is needed as urgently as possible.

The transition can be eased by application of carbon capture and storage (CCS) technology.[13–15] The goal of CCS is to prevent carbon dioxide, produced from fossil fuel burning and other industrial sources, from reaching the atmosphere. To this end, the CO_2 would be selectively captured from such sources, then pressurised and stored in a suitable location over a geological timespan.

CCS would allow fossil fuels to remain in use while minimising the amount of CO_2 thereby released into the atmosphere, providing sufficient time for low-carbon alternatives to be implemented worldwide. It is a solution particularly relevant to developing countries which are currently dependent on coal for their electrical power and cannot necessarily afford cleaner, more

expensive sources in the medium term. CCS also provides a means of reducing CO_2 emissions from industrial processes, such as cement and steel manufacture, which produce CO_2 from sources other than fossil fuels.

Additionally, combination of bioenergy with CCS (commonly abbreviated as BECCS) is one of the few viable means by which the removal of CO_2 already present in the atmosphere could be achieved. This approach would use plants to capture CO_2 from the atmosphere, allowing the high thermodynamic cost of CO_2 capture at such small concentrations to be paid by photosynthesis. Subsequent biomass combustion with CCS then produces energy while sequestering the carbon. Such "negative emissions" may provide a means of reversing past emissions before the climatic effects are felt, though large-scale deployment of BECCS would be needed in order to achieve this.[16]

1.3.2 Description of the process

Successful implementation of CCS requires three connected processes. Firstly, a means of selectively capturing CO_2 from source emissions is needed. This separation is necessary in order to reduce the volume of gas that is to be handled, as well as to avoid the numerous major difficulties (both of differing physical properties, as well as chemical reactivity, flammability and corrosion) that would arise from handling disparate gas mixtures.

Secondly, CCS requires a transport infrastructure to move pressurised CO_2 from capture sites to storage locations. This can be developed from existing pipeline technology developed for natural gas, though the differing physical and chemical properties of CO_2 must be taken into account. In particular, CO_2 poses a corrosion hazard in the presence of water due to the formation of carbonic acid. Economically, this favours the development of CO_2 capture sites in geographical clusters in order to take advantage of shared infrastructure.[17]

The third component is a suitable storage site that is sufficiently stable to retain CO_2 over timescales of millions of years. Various different geological formations have been proposed, ranging from saline aquifers to oil wells. Several pilot projects have been carried out in order to demonstrate the principle of CO_2 storage. Since 1996, the Sleipner project in Norway has

sequestered 0.8 million tonnes of CO_2 per annum (Mta) in the Utsira Sands saline aquifer,[18,19] while in 2015 the Quest project in Canada began the sequestration of 1 Mta in the Athabasca oil sands. Concerns remain regarding the long-term stability of CO_2 storage sites, and in particular, where the liability for any leakages may lie.[14,20,21]

Oil wells are particularly attractive storage sites due to the possibility of using captured CO_2 for enhanced oil recovery (EOR), a process in which pressurised CO_2 is pumped in at one location in order to force additional oil out of production wells. EOR provides an economic value to captured CO_2, and has been in use since the 1970s using CO_2 derived from natural gas sweetening. It has been suggested that EOR may provide a financial impetus for CCS development; however, this is disputed since the amount of CO_2 that would be available from large scale deployment of CCS is likely to far exceed the amount required for EOR.[22,23] Furthermore, use of CCS to increase fossil fuel production risks undermining the core goal of reducing CO_2 emissions.

1.3.2.1 Carbon dioxide capture

CO_2 separation from industrial emissions is a significant technical challenge. These emissions are mostly composed of nitrogen, oxygen, water, and relatively low partial pressures of CO_2 (<15%), and therefore CO_2 capture from such a mixture is thermodynamically disfavoured. Nevertheless, a number of technologies have been developed for this purpose, with varying degrees of success, as fully described below (section 1.4). Carbon dioxide capture direct from emissions is termed *post-combustion CO_2 capture*, and the advantage of such a system over other approaches (see below) is that once successfully developed, carbon capture units can be applied to a wide variety of emission sources with only limited modification. This could allow relatively rapid implementation of CCS, a necessary feature if it is to be used to smooth the transition away from fossil fuels. Such a transitional technology would be of little use if it requires the same lengthy period of research and engineering as the low-carbon energy sources intended to replace it.

An alternate approach to CO_2 capture is to modify the processes that generate CO_2 in order to ensure that pure carbon dioxide, or at least a highly CO_2-rich mixture, is produced, obviating the need for a difficult capture step. Several methods to accomplish this have been developed for combustion processes. The first, termed *pre-combustion CO_2 capture*, employs chemical

processes to convert hydrocarbon fuel into a mixture of CO_2 and hydrogen. Since CO_2 in this mixture is present at high partial pressures, its separation is comparatively easy, while the hydrogen is then burnt to produce energy. However, the required gasification processes introduce significant complexity into the system, necessitating very high capital costs.[24,25]

The second method, termed *oxy-fuel combustion*, employs pure oxygen in place of air for hydrocarbon combustion. The advantage of doing so is that the 78% N_2 normally found in air is not present to dilute the exhaust gas, which therefore is an easily separable mixture of CO_2 and H_2O. Furthermore, absence of nitrogen from the combustion chamber prevents formation of harmful and reactive nitrogen oxides. On the other hand, oxy-fuel combustion requires a source of pure oxygen, entailing costly air separation. Combustion in pure oxygen (commonly diluted in CO_2 recycled from the exhaust in order to achieve a more controllable reaction) is physically different to traditional combustion in air in numerous ways, and significant research is underway into achieving a proper understanding of these differences.

1.3.2.2 Carbon dioxide transport

Transportation of CO_2 from capture to storage site may be carried out either as a gas a liquid, or a supercritical fluid. CO_2 transport as a liquid in general is projected to be the most economically viable option. Gaseous transport allows compression costs to be reduced, but require a larger pipeline diameter in order to compensate for the lower density of the gas, which translates into a more expensive pipeline. Thus, gaseous transport is only competitive with liquid transport over short distances or for very high flow rates – situations where compression costs dominate. As for supercritical transport, this has usually been dismissed on the grounds that the heating or insulation required in order to maintain CO_2 above the critical temperature of 31 °C are prohibitively costly over the length of a pipeline.[26] Since CO_2 is relatively inert, safe transport can be carried out using technology originally designed for natural gas transportation. The rigorous exclusion of water is highly important, however, in order to avoid corrosion associated with carbonic acid formation.[17]

The required inlet pressure for CO_2 transportation is approximately 100 bar. Pressurisation of CO_2 to such a high level is a comparatively costly process, and therefore imposes an important

requirement on the capture process; namely, that CO_2 be captured at the highest possible pressure in order to minimise compression costs.

1.3.2.3 Carbon dioxide storage

The key criterion for CO_2 storage is that locations used must retain CO_2 over geological periods of time, in order to replicate the geological store of carbon formerly provided in the form of fossil fuels. Hence, existing geological formations are most attractive. Possible sites include saline aquifers and oil fields, which have already proven their ability to trap liquids and gases for extended periods. However, the suitability of such sites is not unqualified, particularly in the case of oil fields, due to the punctures created by previous exploitation. Oil fields are also prone to collapse into the void left by extraction of their oil, which together with the high capital cost of new drilling limits CO_2 injection to existing wells that are approaching the end of their lifespan.

Alternative approaches also exist. In order to entirely eliminate the risk of CO_2 leakage, underground mineralisation of CO_2 into carbonate rock formations has been trialled. This provides exceptional stability, and takes only 2 years for the rocks to form, but also requires very large amounts of water.[27] A diametric opposite approach would be deep ocean storage, in which liquid CO_2 is simply pumped to the bottom of the ocean where it is retained by the pressure of the seawater above it. This would be a comparatively simple and cheap approach that could be implemented quickly and unlike other methods would also allow the CO_2 to be easily recovered if a future use is found for it. The drawback of deep ocean storage is that it would be an inherently less stable means of CO_2 storage, cause tremendous damage to ecosystems on the sea floor, and pose a long-term risk of ocean acidification due to the steady diffusion of CO_2 through the water.

1.4 Methods for carbon dioxide capture

Carbon dioxide capture technology has been in use over many decades for the purpose of natural gas sweetening – removal of CO_2 and H_2S from natural gas in order to improve its flammability and avoid corrosion from carbonic and sulfuric acids. Cost pressures on gas sweetening are comparatively limited since the result is a valuable product. CCS applications on the other hand,

EOR notwithstanding, do not produce any product of economic value and therefore cost minimisation is extremely important. Significant improvements from existing gas sweetening technologies are therefore required for application to CCS.

A critical aspect relating to CO_2 capture for CCS is the tremendous scale at which the process must be conducted. An average coal-fired power plant produces 10-20 million tons of CO_2 per year, and CCS must be applied to many of these in order to be effective. This requires the use of cheap commodity chemicals, and precludes the use of advanced materials or rare elements. Furthermore, robustness of the process is of considerable importance since regular replacement of solvents or materials is a costly inconvenience at this scale.

1.4.1 Chemical absorption methods

1.4.1.1 Alkanolamine absorption process

The most mature approach to CO_2 capture uses an aqueous amine solution, the prototypical example being 30 wt% monoethanolamine (MEA, Figure 1.5). This has been in commercial use for many decades, though not for CO_2 capture and storage.[28] The solution is contacted with the gas stream in an absorption column with a high surface area. CO_2 is selectively absorbed into the solvent (in this industry, "solvent" is a commonly used term to denote the whole CO_2 capture solution) via an acid-base reaction that is more fully described in Chapter 2. The loaded solvent is then passed to a separate stripper column where it is heated to 120 °C to force the CO_2 out of solution. The CO_2 stream is collected while the solvent is returned to the absorber for repeated cycles (Figure 1.6).

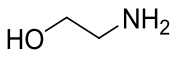

Figure 1.5: Structure of monoethanolamine (MEA).

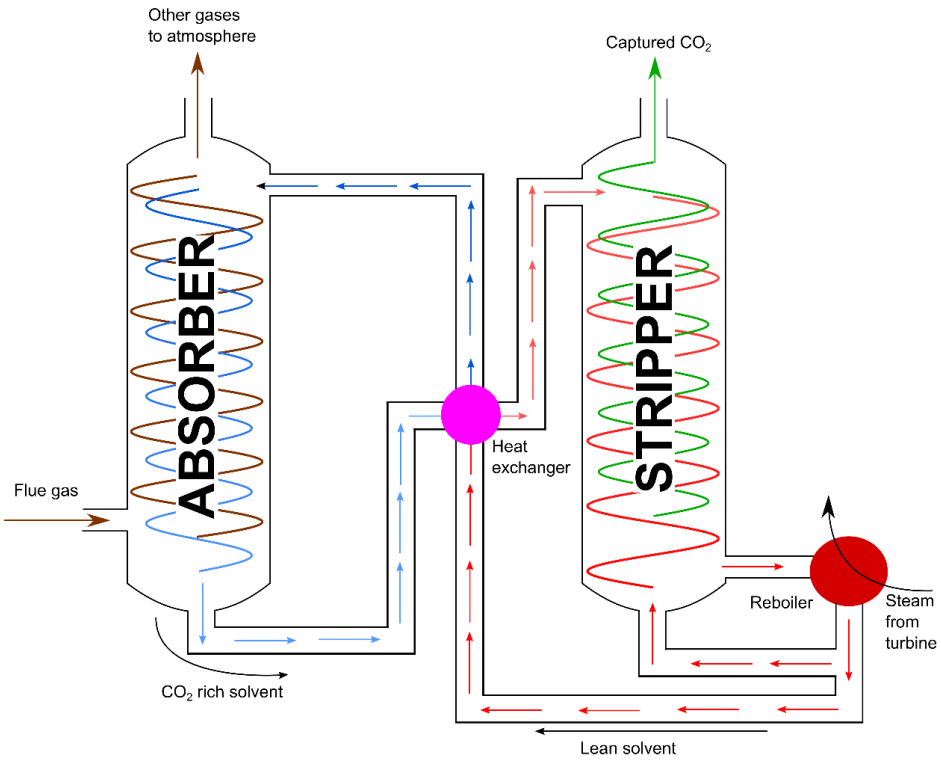

Figure 1.6: Schematic showing post-combustion CO_2 capture with amine solvents.

The main energy costs of the process arise from the heat required on the desorption side. In power station deployment, this heat would be provided by steam diverted from the turbines through a reboiler. Thus the energy requirements of CCS constitute a direct "parasitic load" reducing the output from power generation.

The total energy cost of desorption is a combination of three factors. The first is the energy required to reverse the heat of CO_2 absorption. Absorption of CO_2 into MEA solution is highly exothermic (*ca.*85 kJ mol^{-1} at 40 °C)[29] and therefore this component is very important, comprising about 50-60% of the total heat duty. The second is the energy required to overcome the heat capacity of the capture solvent (termed the "sensible heat") and raise its temperature to 120 °C. Since amine capture solvents are usually aqueous, this tends to be considerable. The third component is the heat of evaporation of the water lost as vapour at this temperature.[30,31]

The overall energy cost of the capture process using MEA is very high. It is estimated that its implementation in post-combustion capture and storage would require approximately 20-30% of the energy output from a typical coal-fired power station.[15] Efforts to reduce this cost are twofold: use of better solvents, particularly mixtures of amines in order to reduce the heat requirement of

desorption (see 2.3); and improved heat integration in order to improve the efficiency of capture with a given solvent. This particularly focuses upon recovery of the exotherm from the absorber column in order to aid desorption.

The great advantage of using a chemical reaction for CO_2 capture is the selectivity involved, as in the case of amine solutions only acid gases are absorbed, and the remaining components are of little direct concern. However, impurities in the gas stream remain a vulnerability of the lifespan of the solvent. Sulfur compounds are absorbed similarly to CO_2, but form heat-stable salts which cannot be directly recovered.[32] Oxidation of the amine by oxygen in the flue gas is also a concern. Such degradation is not a concern for gas sweetening purposes (as frequent replacement of the solvent is a comparatively minimal issue for that process) but is a major issue for CCS. Hence, development of amine solvents must bear in mind stability as well as performance.

1.4.2 Physical absorption methods

CO_2 capture into solvents does not necessarily require a chemical reaction to take place, but can also be accomplished using simple physical solubility. Solubility of gases is governed by Henry's law, wherein the concentration c of a gas in liquid solution is given as $c = \frac{p}{k_H}$ wherein p is the partial pressure of the solute above the solution, and k_H is the Henry's law coefficient for the relevant solvent/solute combination (k_H is also temperature dependent). Hence in order to dissolve a substantial amount of gas, in this case CO_2, the solvent must have a high k_H for CO_2 solvation. Since CO_2 capture entails reversible solvation and desolvation of the gas, this process can be accomplished either via manipulation of p or of the temperature (and thus k_H). Selectivity is perhaps the most difficult challenge to overcome, as the solvent must distinguish between CO_2 and the other gases in the mixture.

A variety of physical solvents have been developed and used for natural gas sweetening, including the Rectisol process (refrigerated methanol),[33,34] the Fluor Solvent process (propylene carbonate),[35] the Selexol process (dimethyl ether of polyethylene glycol)[35] and the Purisol process (N-methyl-2-pyrrolidinone).[33] However, due to the pressure dependency of Henry's law solubility, physical solvents perform well only at relatively high partial pressures of CO_2, as

opposed to those solvents which rely on chemical reactions that are mainly dependent on the stoichiometry of the compounds involved. Hence, the application of such solvents to post-combustion CO_2 capture and storage remains infeasible unless significant advances are made.

1.4.3 Frontier technologies

A number of alternatives to the conventional solvent approach have attracted study. These alternatives share several common features: they make use of advanced materials for carbon dioxide capture with the potential for extremely high performance. However, practical issues arising from this complexity have thus far precluded their use on a large scale.

1.4.3.1 Ionic liquids

A particularly popular subject of chemical research is the use of ionic liquids (ILs).[36,37] An ionic liquid is a compound consisting entirely of ions, with a melting point below 100°C. ILs are distinguished by their low vapour pressure and high intrinsic conductivity. While many small molecule gases such as N_2, O_2 and H_2 are generally poorly soluble in ionic liquids, much better solubility of CO_2 in ionic liquids can be achieved, either by simple physical solvation,[38] or by reactive absorption into amine-functionalised ionic liquids.[39,40]

The advantage of using ionic liquids for CO_2 separation is their very large degree of customisability, as an enormous variety of possible anion and cation choices is available, and hence the solvent properties can, with sufficient knowledge of underlying trends, be carefully tuned to the desired application.[41] Since the physicochemical properties of ILs are poorly represented in the literature however, many of these trends are yet to be studied in sufficient depth.[38,42]

Despite the attraction of ionic liquids in laboratory studies, at present they remain deeply unattractive for use on an industrial scale. Ionic liquids are orders of magnitude more costly than simple solvents,[43] are very viscous,[44] are sensitive to contaminants, especially water,[45] and are difficult to purify or recycle due to their low volatility.[46] Ecotoxicological studies also indicate that ILs, especially those containing imidazolium cations, may be comparably or much more toxic than methanol or benzene in the environment,[47] undermining their claim to be “green” solvents.

1.4.3.2 Adsorption methods

Adsorption onto a wide range of solid media, including metal-organic frameworks (MOFs), zeolites and activated carbon, has been extensively studied for the separation of gases.[48] These are porous solids with a large surface area, and adsorb gases based upon pore size and structure. Regeneration can be accomplished either under reduced pressure (pressure swing adsorption) or increased temperature (temperature swing adsorption).[49]

Current adsorbents cannot, however, handle large concentrations (1.5 vol% or more)[50] of CO_2, something of an obstacle for their application in flue gas scrubbing. Furthermore, adsorption is slow and selectivity relatively poor, with co-adsorption of N_2 and especially water (which would necessitate predrying of the gas stream) a serious issue. Lastly, synthesis of many of these materials, particularly MOFs, is currently prohibitively expensive for the scale required.[28,51,52]

1.5 Summary

Climate change caused by CO_2 emissions is an emergency which cannot be solved only by long-term development of technologically advanced solutions, but requires an immediate solution. Application of carbon dioxide capture and storage (CCS) is an essential part of this solution, hastening the transition away from CO_2-emitting power while smoothing the economic challenges of replacing fossil fuels. A number of differing technical approaches to CCS have been proposed. Of these, post-combustion CO_2 capture offers the most straightforward approach to implementation, but this requires CO_2 capture at relatively low partial pressures for which existing capture technology is impractical.

Hence, a dramatic improvement in CO_2 capture performance in these conditions is urgently needed. Of the techniques currently in existence, those based on physical processes (solvation or adsorption) are fundamentally unsuited for the task due to the large pressure differentials required between the flue gas and outlet CO_2 streams, in addition to major concerns over selectivity and tolerance of impurities, especially water. On the other hand, absorption based on chemical

reactions may offer a greater potential for improvement due to the high selectivity and tolerance for low pressures inherent to the system.

2 Chemistry of Amine-based CO_2 Capture

2.1 Hydration equilibria of carbon dioxide

2.1.1 Properties of carbon dioxide in water

Carbon dioxide is considered an acid gas, since aqueous solutions of carbon dioxide are acidic. In such solutions, CO_2 undergoes hydration into carbonic acid, which may then be successively deprotonated to produce bicarbonate or carbonate salts at sufficiently high pH (Scheme 2.1). Carbonic acid is generally considered a transient species, comprising less than 1% of dissolved CO_2 in such a solution, and isolation of the free acid is extremely difficult, though not impossible,[53] as it rapidly decarboxylates in the presence of water, producing additional water in the process.

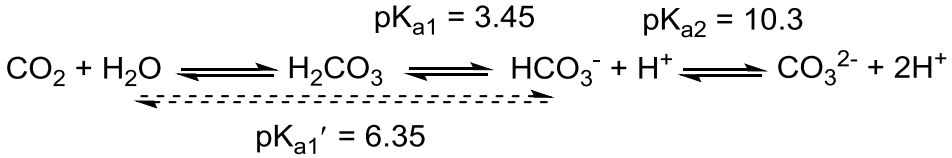

Scheme 2.1: Hydration equilibria of CO_2 in the presence of water with relevant pK_a values.

Due to the small amount of carbonic acid present in solution, the experimentally observable pK_a of dissolved CO_2, though routinely described as the "pK_a of carbonic acid" is not in fact the first dissociation constant of H_2CO_3 (pK_{a1} above) but an apparent dissociation constant dominated by the hydration of CO_2, denoted pK_{a1}'. This equilibrium carries considerable biological importance, as it is used as a pH buffer by many living things.

The solubility of bicarbonate and carbonate salts, especially of inorganic cations, is typically low in both water and organic solvents, and therefore carbonates are primarily encountered as minerals. Many common minerals in the Earth's crust are carbonates, including calcite ($CaCO_3$), siderite ($FeCO_3$), dolomite ($CaMg(CO_3)_2$), malachite ($Cu_2CO_3(OH)_2$) and azurite ($Cu_3(CO_3)_2(OH)_2$). On the other hand, solid bicarbonates are rare, as dissolved bicarbonates tend to disproportionate upon precipitation, producing the carbonate salt and CO_2.[54]

Alkali metals are a notable exception to this trend. Alkali metal carbonates are highly water-soluble, while the bicarbonates are moderately soluble, with solubility increasing in line with cation size. Bicarbonates of alkali metals are among the few stable solid bicarbonates. For these reasons, solution-phase carbonate chemistry is dominated by the alkali metal salts, along with other cations that permit similar behaviour, such as ammonium.

2.1.2 Application to carbon dioxide capture

Due to the acidic behaviour of CO_2, the gas is spontaneously absorbed into any sufficiently basic solution, as described in Scheme 2.1. This is a straightforward acid-base reaction between the base and carbonic acid, defined by the pK_a of the base in question and pK_{a1}' of carbonic acid. This process is relatively slow and is limited by the slow rate at which CO_2 is hydrated into carbonic acid.

A second absorption pathway is available for relatively strong bases, via formation of hydroxide. Hydroxide attacks dissolved CO_2 directly in a nucleophilic addition to produce bicarbonate, with no carbonic acid intermediate (Scheme 2.2).

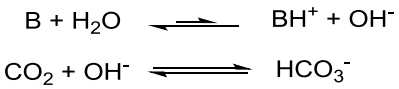

Scheme 2.2: Hydroxide-mediated absorption of CO_2 by an aqueous base, B.

Due to this latter pathway, the rate of absorption is highest at high pH, where the concentration of OH^- is most significant. Hydroxide bases, such as potassium hydroxide, are excellent CO_2 absorbers and are useful in applications where carbon dioxide must be irreversibly removed, such as diving and anaesthesia rebreathers, in CO_2 scrubbers aboard manned spacecraft or submarines, and controlled atmosphere storage. The most common CO_2 absorbent in these applications is soda lime, a solid mixture of calcium, potassium and sodium hydroxides.[55]

For applications where CO_2 capture must be reversible, including CCS, hydroxides are unsuitable as regenerating such a strong base from bicarbonate requires a prohibitively large amount of energy (for example, the enthalpy of absorption of CO_2 into NaOH is -109.4 kJ mol^{-1}).[56] On the other hand, CO_2 absorption with weaker bases proceeds at an unacceptably slow rate since the

hydroxide pathway is less available. Hence, an effective capture solvent must represent a compromise between these kinetic and thermodynamic considerations.

2.2 Formation of carbamates from amines

Contrary to the behaviour observed in other bases of similar basicity, CO_2 absorption into solutions of many amines is relatively fast. This is due to the formation of carbamate (Scheme 2.3) in addition to the bicarbonate formed by traditional acid-base chemistry. Carbamates are formed by a direct interaction of amine and CO_2 analogous to the nucleophilic attack of hydroxide shown earlier (Scheme 2.2) and hence the rate of absorption is not restricted by slow formation of an intermediate species.

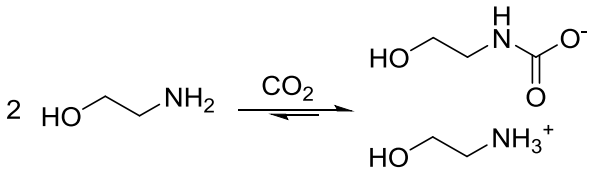

Scheme 2.3: Formation of carbamate from monoethanolamine.

Carbamate formation consists of replacing a labile N-H proton with CO_2. Hence, only primary and secondary amines may take part in this reaction, as tertiary amines lack such a proton. Furthermore, carbamate formation is disfavoured by steric hindrance near the nitrogen atom due to the spatial requirements of the comparatively bulky carbamate group.

2.2.1 Proposed mechanisms for carbamate formation

The mechanism for the reaction of amines with CO_2 is not fully understood, however experimental results are generally accepted to be consistent with two proposed routes. The so-called zwitterionic route was first proposed by Caplow in 1968. Under this interpretation, the formation of carbamate is a two-step process. Nucleophilic attack upon CO_2 by the amine occurs first, to produce a zwitterionic carbamate that is protonated at the nitrogen atom. This proton is then quickly transferred to a base (typically, but not necessarily, another molecule of the amine) to give the carbamate salt (Scheme 2.4).[57,58]

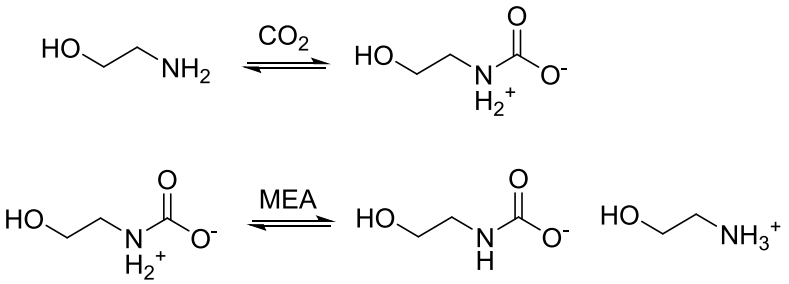

Scheme 2.4: Proposed zwitterionic mechanism for carbamate formation from monoethanolamine.

The alternative interpretation involves a formally termolecular reaction. A loosely bound encounter complex is formed, wherein the amine, CO_2 and proton acceptor are closely associated. CO_2 addition and proton transfer then take place simultaneously (Scheme 2.5).[59]

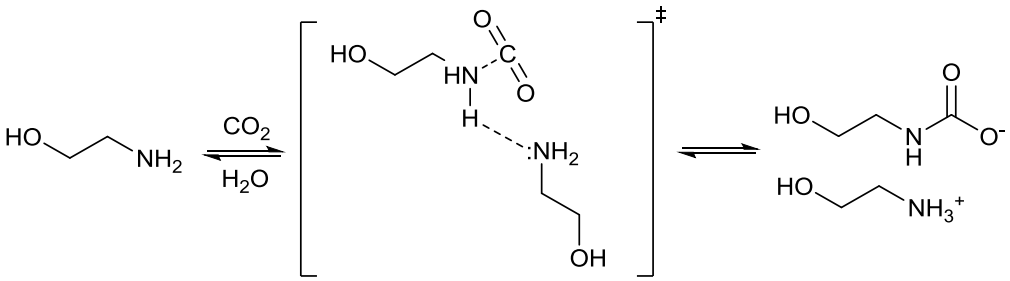

Scheme 2.5: Proposed termolecular mechanism for carbamate formation from monoethanolamine.

Hence, the two proposed mechanisms differ only in whether deprotonation of the nitrogen centre occurs concerted with that of carboxylation, or if the mechanism is stepwise with addition to CO_2 preceding deprotonation.

These are somewhat rigid interpretations as they lack an appreciation of the aqueous solvation sphere surrounding the molecules involved, and the role that this plays in the reaction. Direct experimental information is lacking due to the transience of the proposed intermediates. Computational studies of this reaction suggest that proton transfer does not occur directly to the base, but to a hydrogen-bonded water molecule, from which it is transmitted to the base via the Grotthuss mechanism.[60–62]

Other theoretical studies have also shown that solvation behaviour is of key importance to this reaction,[63] and in some cases can even prevent it entirely.[64] The example given in the latter case is that of 2-amino-2-methyl-1-propanol (AMP). Carbamate formation from this amine is disfavoured, for reasons generally credited to steric hindrance from its two α-methyl groups that

prevents the approach of CO_2.[65] However, the work of Stowe et al. suggests that the reason for its poor reactivity is not directly due to hindrance from these methyl groups, but their effect on the solvation shell of the amine. It is proposed that this hydrogen-bonded network of water molecules is forced to cluster in front of the amine by the presence of the methyl groups, and this cluster of solvent molecules then inhibits the approach of CO_2 to the nitrogen centre.[64]

2.2.2 Application of amines to CO_2 capture

When compared to other bases, carbamate-forming amines appear to be excellent agents for CO_2 capture. Amine solutions absorb CO_2 with exceptional speed comparable to that of hydroxides, but the thermodynamic barrier to regeneration is reduced due to their lower pK_a (*ca.* 9-11). For this reason, amine solutions have been studied and used extensively for CO_2 capture applications.

The major disadvantage of carbamate formation lies in the stoichiometry of its formation. Capture of one mole of CO_2 as carbamate requires two moles of amine, as compared to one mole of base if CO_2 is captured as bicarbonate. Furthermore, the heat of desorption from carbamates, though lower than that of hydroxides, is still relatively high. The operating cost of the solvent regeneration process is determined by three factors (detailed above in 1.4.1.1): the heat of desorption; the sensible heat; and the energy lost to evaporation. The latter two factors are strongly affected by the concentration of CO_2 which can be *reversibly* absorbed into solution, since less water must be heated per unit CO_2 captured. This concentration is reduced by the 2:1 stoichiometry of carbamate formation, and it is reduced further by the high stability of carbamate, from which recovery of CO_2 tends to be incomplete.

Practical CO_2 capture systems that incorporate carbamate formation tend to have a relatively low cyclic capacity, i.e. the amount of CO_2 that can be captured into the solution is much lower after regeneration than when using freshly prepared capture solvent. This is because not all carbamate is destroyed, but continues to cycle between the absorber and desorber.

2.2.3 Carbamate/bicarbonate speciation in amine solutions

2.2.3.1 Nature of speciation and interconversion of species

At this point it is important to recollect that amines are not only carbamate precursors but also Brønsted-Lowry bases. Hence, CO_2 may be absorbed into aqueous amine solutions by either or both of the pathways described thus far, to produce a balance of carbamate and bicarbonate absorption products. These two products exist in equilibrium with one another, certainly via desorption and reabsorption of CO_2, but kinetic studies also suggest that a direct pathway exists for interconversion via hydrolysis of carbamate (Scheme 2.6).[66]

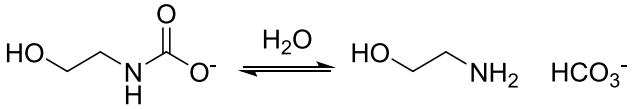

Scheme 2.6: Proposed interconversion between carbamate (of MEA in this case) and bicarbonate.

Little consideration has been given to a possible mechanism for this interconversion. A single *ab initio* study was published by Matsuzaki et al. proposing that this process proceeds via proton transfer from protonated MEA to form carbamic acid, followed by nucleophilic attack of hydroxide to give a tetrahedral intermediate. The intermediate subsequently decomposes to bicarbonate and amine (Scheme 2.7).[67]

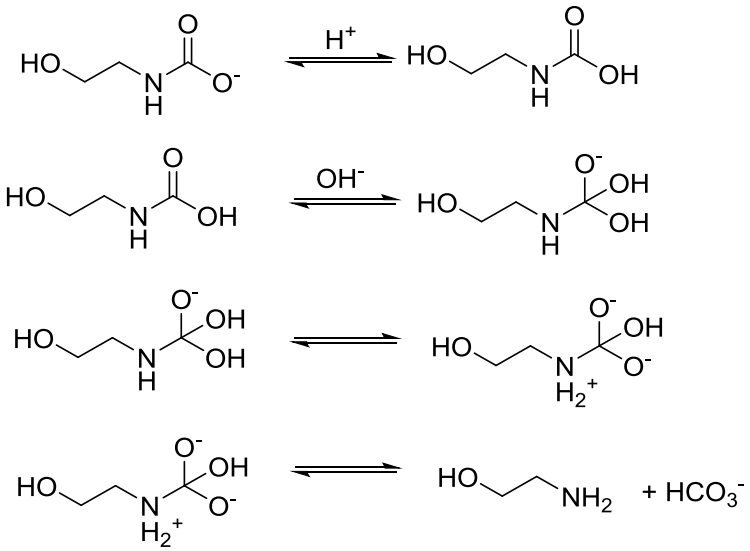

Scheme 2.7: Mechanism proposed by Matsuzaki et al. for interconversion of carbamate (of MEA in this case) and bicarbonate.[67]

This mechanism is somewhat questionable due to the unusual feature of both acid and base involvement in the same process. Protonation of carbamate is believed to be a necessary part of

the mechanism, as carbamate would make a very poor electrophile for the dissociation step. A possible alternative to the involvement of hydroxide would be nucleophilic attack on carbamic acid by neutral water, producing a mechanism along the lines of that shown in Scheme 2.8 (below).

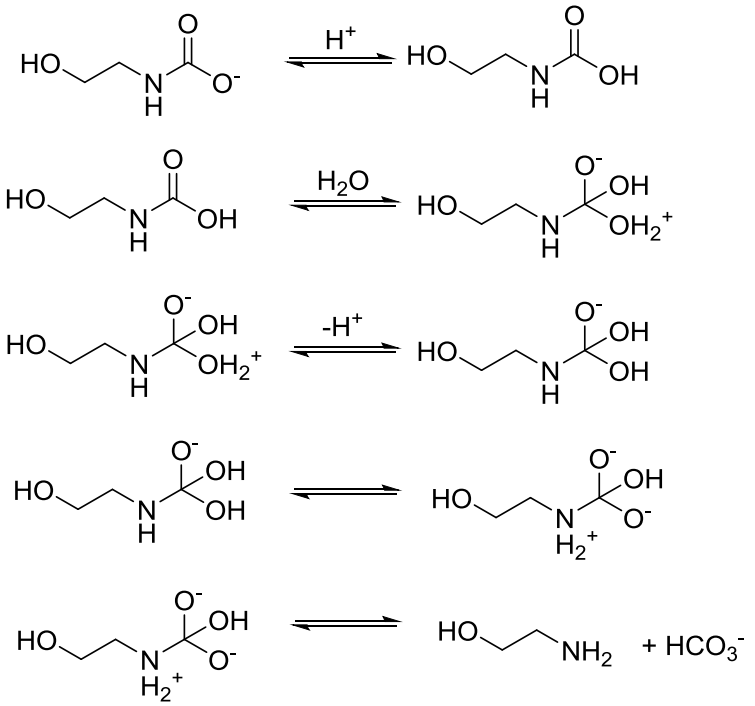

Scheme 2.8: Alternative mechanism, not involving hydroxide, for interconversion of carbamate and bicarbonate.

Capture of CO_2 as bicarbonate is much more efficient than as carbamate due to the 1:1 stoichiometry of this process. This would translate to reductions in the energy cost of desorption, since a smaller volume of solvent must be heated per unit CO_2 captured.

Hence, it would be desirable for an amine-based capture solvent to favour bicarbonate over carbamate as an absorption product in order to minimise the energy and capital requirements of the capture process, provided that the kinetic advantage of carbamate formation, namely its extremely fast rate of absorption, is retained. In order to achieve this, a simple means of measuring the concentrations of bicarbonate and carbamate in such capture solvents is necessary. A wide variety of methods for this purpose have been developed, with varying degrees of success.

2.2.3.2 Studies using classical chemistry

Much early work relied on the separation and quantification of each component using preparative chemistry. A typical approach involved the addition of barium chloride, which provokes the precipitation of carbonate and bicarbonate as the extremely insoluble $BaCO_3$, while leaving carbamate in solution. This was developed by Faurholt in 1924 for the purpose of studying CO_2 hydration,[68] and has found some use in more recent times.[69,70]

A more advanced technique was employed by Caplow in work published in 1968.[57] Radiolabeled $^{14}CO_2$ was absorbed into amine solutions, then bicarbonate precipitated using $Ba(OH)_2$. The concentration of carbamate was then assayed by measuring the radioactivity of the filtered solution.

The disadvantages of these techniques are that they require relatively large sample sizes in order to achieve an accurate result, are time-consuming and prone to experimental error. For these reasons they are rarely used in modern work. However, where large amounts of analyte are available and/or where spectroscopic facilities are not, such preparative approaches may still be useful and should not be dismissed out of hand.

2.2.3.3 Spectroscopic studies

The development of modern spectroscopy has permitted the study of this speciation with far smaller sample sizes and greater accuracy. Some work has been carried out using infrared spectroscopy[71,72] as well as Raman spectroscopy.[73] These methods are not naturally adaptable to quantitative analysis, and their application in such a task requires appropriate calibration curves to be prepared for every system under study. This would present a fairly onerous requirement for a comparative study across many solvent compositions and hence none has yet been reported.

Nuclear magnetic resonance (NMR) spectroscopy, particularly ^1H NMR, is much better suited to such applications, as the area of a peak in the spectrum is directly proportional to the number of nuclei contributing to that peak and therefore quantitative analysis is straightforward.[74] NMR spectroscopy is a non-invasive technique which is highly adaptable to a wide variety of different systems.

^{1}H and ^{13}C are the nuclei of greatest interest to the study of amine speciation during CO_2 capture. ^{13}C NMR allows the study of all species present in solution, but quantitative ^{13}C NMR requires acquisition times on the order of many hours or even days in order to overcome the long spin-lattice relaxation times (T_1) of ^{13}C nuclei.[75] Accurate quantitative ^{13}C NMR spectra require a relaxation delay of 4-5 times the value of T_1, approximately 50 seconds in the case of bicarbonate, between each scan, which for a typical 2000-scan spectrum would add over 27 hours to the experiment time. A full discussion of the conditions required was published by Ciftja et al.[76]

A number of studies into CO_2 capture have been carried out using ^{13}C NMR. Chakraborty et al[77] performed early investigations with ^{13}C NMR of the absorption of CO_2 into 2-amino-2-methyl-1-propanol (AMP), showing that very little carbamate is formed by this amine, and that it captures CO_2 as bicarbonate. Svendsen and coworkers employed quantitative ^{13}C NMR to monitor the absorption of CO_2 into aqueous MEA, butylethanolamine, and *N*-methyldiethanolamine.[78] This study incorporated analysis across a range of temperatures, concluding that accurate quantitative analysis at high temperatures (≥70 °C) was infeasible due to the fast rate of chemical exchange in hot solutions. The same research group has also published a number of other studies employing ^{13}C NMR to probe CO_2 capture.[79–82] In common with other studies using this technique,[83] results tend to be relatively inconsistent and not necessarily effective for more than qualitative information, especially since the long experimental times required limit the number of data points that can feasibly be collected.

Quantitative ^{1}H NMR, on the other hand, is substantially more accessible, with required acquisition times on the order of minutes,[74] permitting many experiments to be conducted with ease. However, several species that are important to study of CO_2 capture are not directly observable via ^{1}H NMR due to their lack of a non-exchanging proton. These comprise CO_2 itself, HCO_3^- (bicarbonate), and CO_3^{2-} (carbonate). Concentration of these species must either be inferred indirectly or determined by a complementary measurement.

Suda et al.[84] succeeded in quantifying all major species present in carboxylation of MEA and other primary amines using ^{1}H NMR. The positions of protonation equilibria were calculated from literature pK_a values, allowing bicarbonate and related species to be accounted for indirectly. This

gave results that agreed well with previous modelling.[84,85] Maeder and coworkers have made use of ^{1}H NMR in numerous studies into the kinetics and thermodynamics of CO_2 absorption into solutions of MEA and similar amines. Their approach combined aliquots of aqueous MEA with potassium bicarbonate and hydrochloric acid solutions, generating carbamate in situ whose concentration relative to that of MEA was measured using NMR.[66] Böttinger et al. made use of ^{1}H NMR for *in situ* measurements of CO_2 capture into MEA and diethanolamine.[86] A comprehensive review of recent studies employing NMR spectroscopy to study CO_2 capture was published by Perinu et al.[87]

2.2.3.4 Carbamate/bicarbonate speciation in MEA and relation to CO_2 capture performance

The speciation that occurs during carboxylation of 5 mol L^{-1} MEA is significantly better understood than that of other amines due to the common use of this mixture in gas sweetening and as the prototypical amine capture solvent. Multiple studies using ^{1}H and ^{13}C NMR, as well as vapour-liquid equilibrium modelling, have shown that absorption of CO_2 into MEA produces almost entirely carbamate, bicarbonate only becoming a significant component of the solution if exposure to CO_2 is particularly long and the concentration of absorbed CO_2 approaches half that of the amine concentration (i.e. the maximum possible amount that could be absorbed solely as carbamate). A graphical example of this behaviour is shown in Figure 2.1 and is typical of the published literature.

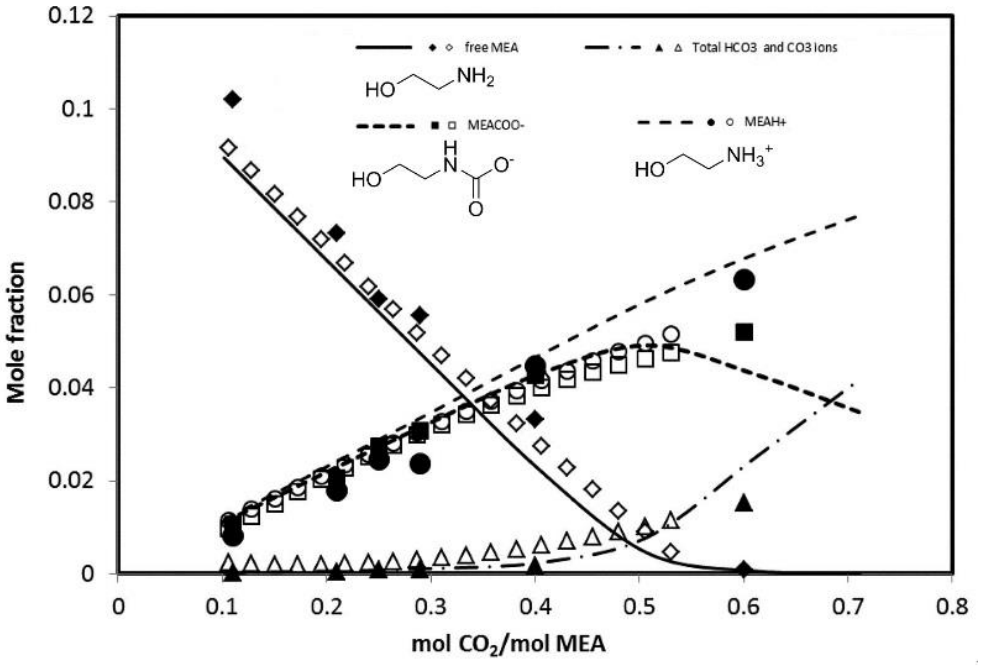

Figure 2.1: Species formed during carboxylation of 5 mol L^{-1} MEA. Data from: ^{13}C NMR study by Jakobsen et al. (filled symbols); combined titration/CO_2 gas analysis study by Matin et al. (hollow symbols); and Aspen Plus electrolyte-NRTL modelling following parameters developed by Zhang et al (lines).[78,88,89] *Adapted with permission from N. S. Matin, J. E. Remias, J. K. Neathery and K. Liu, Ind. Eng. Chem. Res., 2012,* ***51****, 6613–6618. Copyright 2012, American Chemical Society.*

This is relatively undesirable behaviour for a CO_2 capture solvent due to the difficulty of recovering CO_2 absorbed as carbamate. A combined absorption-desorption study of MEA carried out by Yang et al. found that attempted thermal regeneration of CO_2-loaded solvent caused the concentration of carbamate to *increase*, as CO_2 released from decomposition of bicarbonate was simply recaptured as carbamate.[83] This demonstrates the effect of the high thermodynamic stability of carbamate, which the temperature attainable by thermal regeneration (*ca.* 120 °C) is insufficient to fully overcome.

2.2.3.5 Speciation and CO_2 capture performance of other single-amine solvents

Capture solvent screening studies have explored a vast range of primary aliphatic amines,[†] of which examples are shown in Figure 2.2.[90] The performance of these tends to be relatively similar to MEA, displaying fast absorption rates along with a poor (*ca.* 50 mol%) overall capacity for

[†] Aromatic amines, including both anilines and pyridines, are unsuitable for carbon dioxide capture as their low basicity (e.g. the anilinium ion has a pK_a of only 4.6, comparable with acetic acid) is inadequate to carry out the necessary neutralisation reaction with carbonic acid.

CO_2, due once again to predominance of carbamate as the absorption product. Such amines tend to produce highly stable carbamate derivatives, which may be attributed to the minimal steric hindrance from substituents around the nitrogen atom. Efforts to understand carbamate stability (and thus capture performance) based on the properties of the amine have produced mixed results. No correlation between capture capacity and amine pK_a was found, though pK_a is positively correlated with the *rate* of absorption, likely due to the increased nucleophilicity of more basic amines. On the other hand studies of aliphatic amines suggest a strong link between carbamate stability and the ^{15}N NMR chemical shift.[90,91]

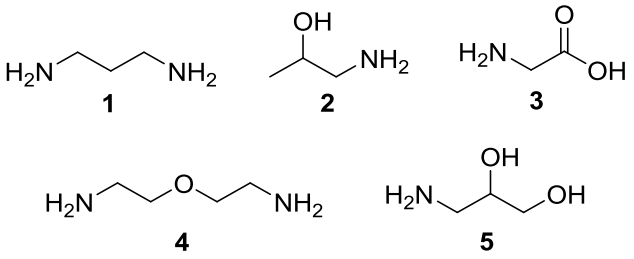

*Figure 2.2: Examples of primary amines studied for CO_2 capture performance: 1,3-diaminopropane (**1**); 1-amino-2-propanol (**2**); glycine (**3**); 2-(2-aminoethoxy)ethylamine (**4**); and 3-aminopropan-1,2-diol (**5**).*

Hence, interest in development of improved capture solvents turned to more sterically hindered primary and secondary amines, such as 2-amino-2-methyl-1-propanol (AMP) or 2-piperidineethanol (PE), shown in Figure 2.3. Carbamates derived from these amines are significantly less stable due to the effects of this steric hindrance, resulting in enhanced bicarbonate production while the carbamate is observed only in minimal quantities.[92] This allows much more CO_2 to be absorbed, up to 1 molar equivalent, with commensurate reduction in regeneration heat duty since less water must be heated per unit amount of CO_2 recovered. Unfortunately, the rate of CO_2 absorption into solutions of these amines is significantly slower than that for MEA, as the kinetic advantage of fast carbamate formation is lost.[65,77,93,94]

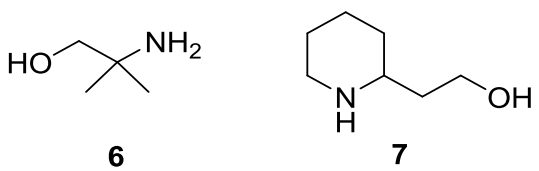

*Figure 2.3: Sterically hindered amines studied in CO_2 capture research: 2-amino-2-methyl-1-propanol (AMP, **6**) and 2-piperidineethanol (PE, **7**).*

The behaviour of secondary amines tends to vary between those detailed above, depending upon the stability of carbamates formed from these compounds. Piperazine is a particularly common subject of carbon dioxide research,[95–97] but many others have also received study (Figure 2.4).[82,98]

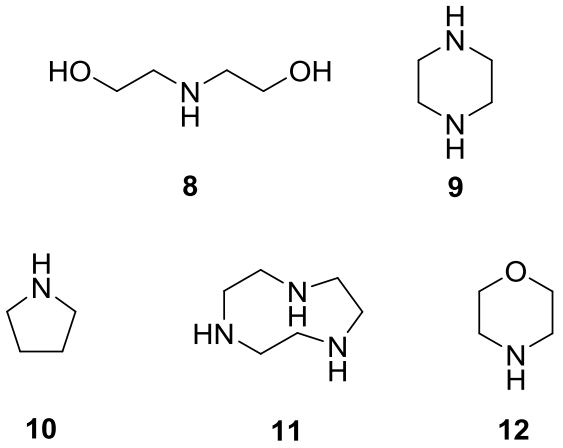

*Figure 2.4: Secondary amines studied in CO_2 capture research: diethanolamine (DEA, **8**); piperazine (PZ, **9**); pyrrolidine (**10**); 1,4,7-triazacyclononane (**11**); and morpholine (**12**).*

Lastly, a large number of tertiary amines have also been studied for CO_2 absorption (Figure 2.5). These do not take part in carbamate formation due to the lack of a labile proton, and therefore CO_2 is captured into tertiary amines exclusively as bicarbonate, with the usual implications of a high capture capacity and a poor absorption rate. Of the tertiary amines, *N*-methyldiethanolamine (MDEA) is the most heavily studied and often considered a "representative" tertiary amine in CO_2 capture studies. There are variations in performance among tertiary amines; for example, carbon dioxide absorption into tetraethyldiaminomethane (TEDAM) has been reported to be almost five times as fast as into MDEA, though this is still significantly slower than can be achieved with a carbamate-forming amine. The increase in absorption rate is possibly due to a cooperative interaction between the two nitrogen centres, but no further investigations have been reported.[92,99–101]

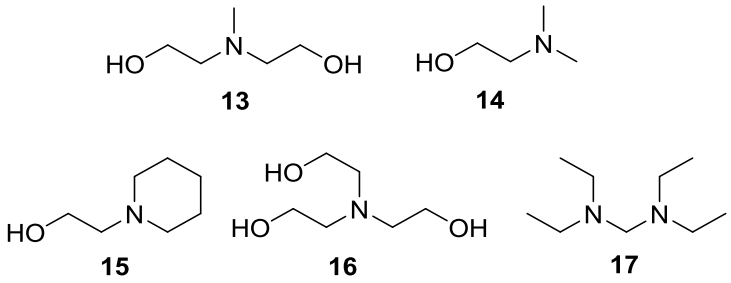

*Figure 2.5: Tertiary amines studied in CO_2 capture research: N-methyldiethanolamine (MDEA, **13**); 2-(dimethylamino)ethanol (**14**); 1-(2-hydroxyethyl)piperidine (**15**); triethanolamine (TEA, **16**); tetraethyldiaminomethane (TEDAM, **17**);.*

Hence, CO_2 capture performance by single-amine solutions may be approximately described as a continuum between the two extremes of bicarbonate and carbamate formation, dependent upon the degree of substitution of the nitrogen atom and neighbouring carbon atoms. Each of these extremes has its advantages, but neither is acceptable for a scaleable capture system. Bicarbonate-forming solutions exhibit a high capture capacity and comparatively cheap regeneration, but absorb CO_2 slowly. Carbamate-forming solutions absorb CO_2 very quickly, but have a low capture capacity and are difficult to regenerate.

An ideal capture solvent would combine the advantages of both modes of capture. This cannot easily be done with a single amine, as the centre of the continuum described above is more of a combination of the *disadvantages* of both modes of capture – a mixture of carbamate and bicarbonate which both forms slowly and is difficult to recover. A better capture solvent would need to improve the proportion of bicarbonate formed, without prejudicing the rate of absorption.

2.3 Blended-amine capture systems

Capture solvents composed from a mixture of amines have been found to yield significantly superior performance to either individual amine.[102–104] Such blended solutions typically take the form of a binary mixture of a carbamate-forming (i.e. primary or secondary) amine and a non-carbamate-forming (i.e. tertiary or sterically hindered) amine, in order to combine the beneficial properties of each. Absorption is fast due to capture as carbamate, and the absorption capacity is increased due to the formation of bicarbonate.

Numerous such blends have been studied and many more are doubtless under examination. Earlier work tended to focus on blends incorporating monoethanolamine as the carbamate-forming amine, combined with such non-carbamate forming amines as MDEA,[105] AMP,[106,107] *N*,*N*-dimethylethanolamine[108] and triethanolamine.[109] Compounds closely related to MEA are especially preferred, since these can be manufactured from ethylene oxide and ammonia as part of the same chemical process. Perhaps for this reason, the blend with MDEA is especially heavily studied, and has been tested up to pilot scale at the Boundary Dam CCS demonstration facility in Canada. A huge reduction in heat duty was reported from using this blend instead of MEA alone, but this gain is contingent upon maintaining the chemical stability of the capture solvent.[110]

Since monoethanolamine and related compounds are particularly prone to oxidative degradation, more recent studies have sought to introduce more stable alternatives. Piperazine, which also offers significantly faster absorption kinetics than MEA, has proven particularly attractive,[97,111] prompting study of blends of piperazine with AMP,[112–114] MDEA,[113] and many other amines for their carbon capture performance.

Introduction of blended amines has brought about a considerable reduction in the cost of CO_2 capture with chemical solvents. The energy cost of capture (excluding CO_2 compression costs) using MEA is typically estimated at approximately 4 GJ per tonne of CO_2 captured. More modern state-of-the-art solvents, on the other hand, have reduced this cost to about 2.5 GJ/tonne. It is estimated that the thermodynamic minimum energy requirement for CO_2 separation using this process is about 1 GJ/tonne.[15] Attainment of perfect thermodynamic efficiency is unlikely – well-established, comparable unit operations such as distillation and desalination have achieved an efficiency of only 20-30% - and therefore it is considered that further improvements in the efficiency of amine-based CO_2 capture are likely to be increasingly difficult to achieve.[111] It is nevertheless imperative that such improvements be found, since current energy requirements remain very onerous when CO_2 capture and storage produces no financially viable product.

2.4 Limitations of amine capture systems

Large-scale deployment of amine solvents for CCS presents many technical challenges which have yet to be dealt with. Understanding of the scale that CCS demands is key to dealing with such challenges, as compromises that would be acceptable for smaller applications are not necessarily viable in this case. Similarly, laboratory tests using pure reagents and materials may fail to predict complications that arise from using comparatively impure reagents and harsh conditions in an industrial process.

2.4.1 Corrosivity

Aqueous MEA and related solutions are highly corrosive to steels and stainless steels.[115,116] This may be exacerbated by certain impurities in the flue gas, of which O_2 and H_2S are a particular concern.[117] Left unchecked, such corrosion would do considerable damage to the fabric of the capture plant and require heavy expenditure on replacement materials. Corrosion-resistant steels are a possible solution, but these are extremely costly and would therefore impose heavy capital costs. Existing large-scale pilot projects, such as that at Boundary Dam, Canada, make use of ceramic-lined concrete, which offers a low-cost but somewhat inflexible solution.

Some research has investigated the possibility of including anti-corrosion additives in the capture solvent, or of protecting vulnerable steels with a corrosion-resistant barrier, but with mixed results. For example, Srinivasan et al. found sodium thiosulfate to be an effective anti-corrosion coating for short-term exposure, but ineffective over a longer term due to the instability of the coating.[118] Sodium metavanadate ($NaVO_3$) is a very effective soluble corrosion inhibitor, but has been found to promote degradation of the amine solvent.[119]

2.4.2 Solvent stability

Stability of the capture solvent is a significant concern. Alkanolamine solvents are highly prone to degradation, which shortens the lifetime of the solvent and creates a problem of large-scale disposal. The chemistry of amine degradation is highly complex. Numerous degradation products and mechanisms have been identified or proposed in published literature (Scheme 2.9), of which a full review has been published by Gouedard et al. which highlights how poorly supported many

of these proposals are.[120] For example, the carbamate of MEA undergoes a slow cyclisation to 2-oxazolidinone, which may then react with additional molecules of MEA to produce a variety of possible compounds.[121]

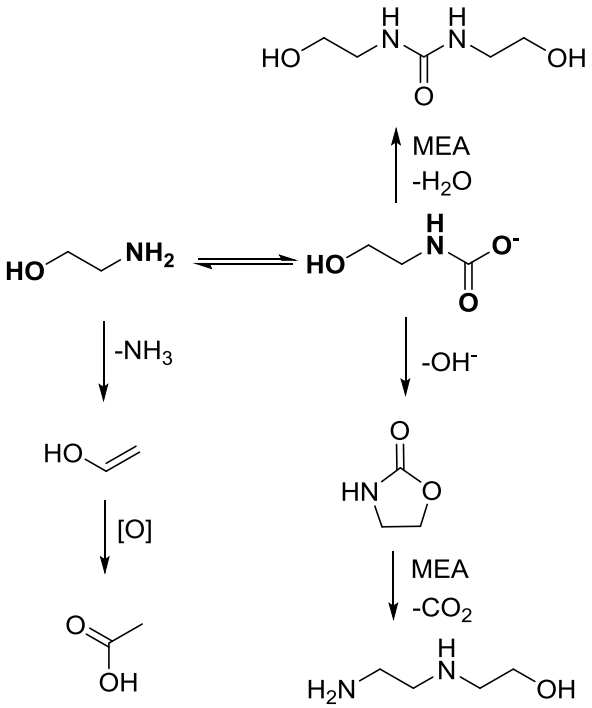

Scheme 2.9: Some major proposed pathways and decomposition products for degradation of carboxylated MEA, based on analysis of degradation products. Many more have been reported.

The situation becomes even more complex when blended amines are considered. Blending has been observed to enhance or reduce the stability of a given amine, and opens up further degradation pathways if reactions between the different amines in the mixture are possible.[107,108,122]

2.4.3 Volatility and environmental release

Release of amine capture solvents and their degradation products to the atmosphere is a significant environmental concern given the large scale that CCS deployment would require. The main pathway for such a release in the course of normal operation would be through exchange with gases passing through the absorber column and thence to the atmosphere, though the consequences of inadvertent solvent leakage and spillage must also be considered. Many proposals for CO_2 capture include a water wash in order to minimise release of volatile amines, but this does not wholly prevent such release.[123]

Assessments focused upon MEA have indicated that release of the amine to the atmosphere presents a significant environmental hazard to areas surrounding a CO_2 capture plant, especially to freshwater ecosystems.[124] On the other hand, the same assessment did not find any significant contribution from degradation products of MEA (formaldehyde, ammonia, acetaldehyde).

There are significant concerns that use of amine capture solvents may lead to the release of nitrosamines and nitramines (Figure 2.6) as possible degradation products. These compounds are highly carcinogenic, with very low permitted thresholds. Secondary amines such as piperazine are especially susceptible to oxidation in this manner.[125,126]

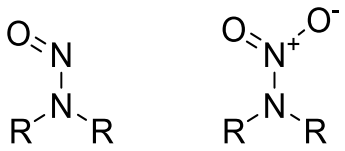

Figure 2.6: Structures of the nitrosamine (left) and nitramine (right) functional groups.

Degradation within the capture solvent has already been considered, but the further reactivity of amines released to the environment must also be considered as this may lead to products not observed in closed-system studies. For example, Onel et al. have shown that under certain atmospheric conditions, MEA and its derivatives are prone to photo-oxidation, potentially leading to high levels of nitramine production.[127,128]

2.5 Conclusions

Despite significant technical improvements, the cost of CO_2 capture with amine solvents remains high, and this is further complicated by the low stability, high corrosivity and environmental hazard of these compounds. Nevertheless, full-scale deployment of CCS is required as soon as possible and since such chemical solvent techniques remain the most industrially developed capture process for this application, it is likely that initial deployment will still make use of amines. Hence, whether CO_2 deployment occurs in the near term at all is likely to hinge upon the costs and environmental impacts of the amine capture technology available.

3 A ^{1}H NMR Approach to Speciation in Amine-based CO_2 Capture

3.1 Introduction

As discussed in the previous chapter, the CO_2 capture performance of amine solutions is strongly dependent on the distribution of species formed in solution. The most desirable outcome would be to maximise the proportion of bicarbonate formed, while retaining the fast absorption rate associated with carbamate formation. This would allow a higher concentration of CO_2 to be absorbed, and minimise the energy required for its thermal recovery.

Experimental studies on speciation have tended to focus on individual capture solvents, in particular that of MEA. While this provides insight into the mechanics of the solvent in question, there is a need for the more general understanding that would arise from broader studies. Such understanding would make it easier to identify promising candidates for capture agent research, and provide more information to aid the development of models for amine behaviour.

In order to carry out such broad studies, a fast and generalisable approach to studying this speciation is necessary. This chapter will focus on the development of such a method. Among the tools available, ^{1}H NMR spectroscopy was deemed the most suitable for the task, as this technique offers fast acquisition times, high accuracy and broad applicability, all of which are essential for a generalisable study to be undertaken. While a number of other techniques have been employed by prior studies (see 2.2.3) none of these meet all three of the criteria listed above.

The most widely used alternative to ^{1}H NMR in this field is ^{13}C NMR. The key advantage of using this nucleus is that it allows direct quantification of species without a non-exchanging proton, notably bicarbonate. However, properly applied quantitative ^{13}C NMR is non-trivial to set up and requires impractically long acquisition times, a fact reflected in the relatively small number of

data points reported in published studies. Such a disadvantage renders ^{13}C NMR inapplicable for the generalisable approach sought herein.

Inability to quantify certain species is a key challenge that must be solved when using ^{1}H NMR. Prior approaches - either to ignore such species entirely, or to estimate their concentration using published pK_a values (in essence, a modelling approach) provide insufficient detail for the goals of this work. Hence, a new approach is needed which would enable measurement of all major species in solution with minimal instrument and operator time.

3.2 Development of ^{1}H NMR analysis for monoethanolamine carboxylation

The existing scientific literature overwhelmingly focuses on the speciation found using 5 M MEA, and therefore the same solution was used to establish the methodology for this work, enabling corroboration with prior work. Successful reproduction of literature values of MEA speciation is a precondition for credible application of the methods developed herein to other, less well understood capture solvents.

Initial carboxylation experiments were performed on a small scale in an NMR tube, using a single stock solution of aqueous 5 M MEA. The solution was prepared from water containing 10 vol% D_2O in order to provide a lock frequency for the NMR spectrometer. Such an approach is readily scalable to carboxylation in larger quantities, as solutions could be prepared by spiking with a small amount D_2O, whereas the conventional technique of using 100% D_2O is not so adaptable. Since the chemical shift of the H_2O solvent peak is highly sensitive to pH, this cannot be used as a reference, and therefore addition of an internal chemical shift standard was necessary. Sodium 4,4-dimethyl-4-silapentane-1-sulfonate (DSS, Figure 3.1) was employed as this is a routinely used ^{1}H and ^{13}C NMR chemical shift standard for aqueous solutions.[74,129] As a sulfonate, DSS has a very low pK_a, and therefore provides a very stable reference except at extremely acidic pH values ($<< 1$).[130]

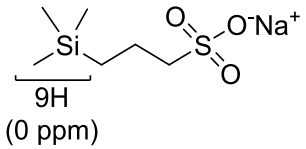

Figure 3.1: Chemical structure of sodium 4,4-dimethyl-4-silapentane-1-sulfonate (DSS), indicating protons used for ^1H NMR chemical shift referencing.

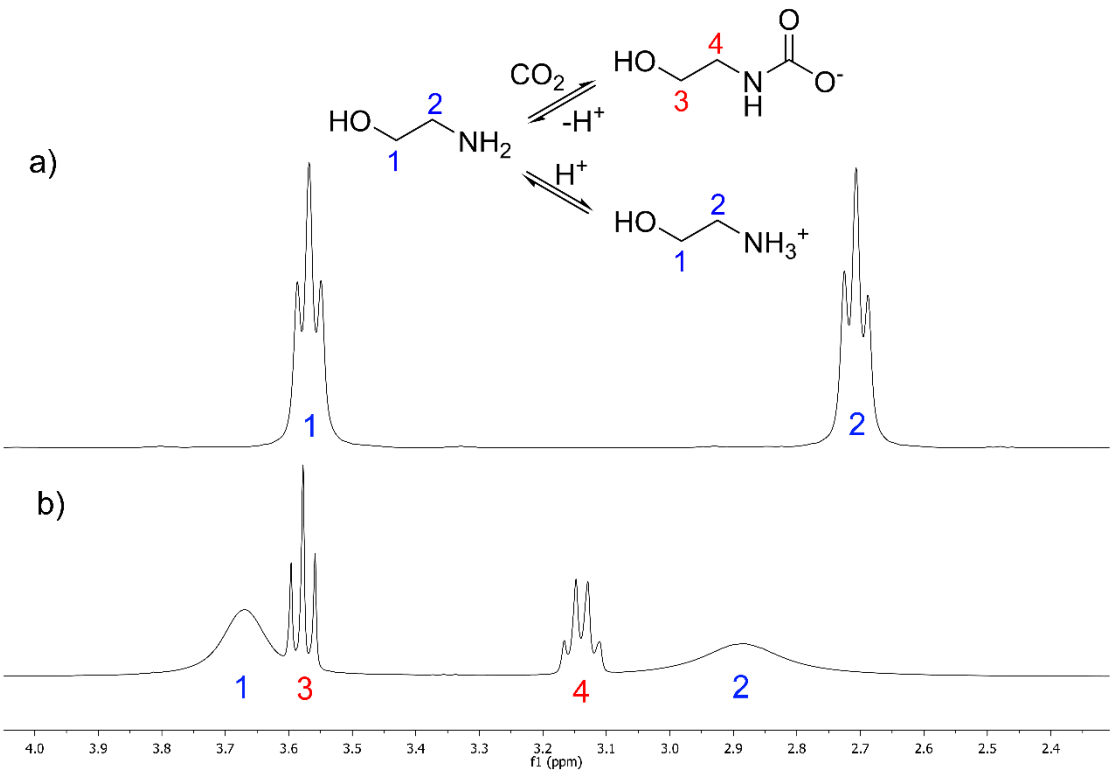

Figure 3.2: a) ^1H NMR spectrum of aqueous 5 mol L^{-1} MEA; b) Typical ^1H NMR of the same solution following exposure to CO_2. Assignment of visible species and the equilibria by which these are linked.

The ^1H NMR spectrum of carboxylated MEA is shown in Figure 3.2 and compared with that of MEA alone. The carbamate peaks manifest as a triplet at 3.58 ppm, and an apparent quartet at 3.14 ppm. The latter is in fact a doublet of triplets, arising from coupling of the CH_2-N protons not only to the other CH_2, but to the carbamate N-H. MEA itself gives two broad peaks at 3.67 and 2.88 ppm. These chemical shifts are somewhat further downfield than the accepted chemical shifts for MEA in water (3.57 ppm and 2.71 ppm) and arise due to the protonation equilibrium of MEA which is significantly faster than the timescale of ^1H NMR measurement (on the order of milliseconds).[131] Due to the fast rate of exchange, the free base and protonated forms are not separately observed, but instead a single, combined set of peaks is seen. The chemical shift of these combined peaks is a simple average of those of the two forms, weighted by their relative

concentrations, and is therefore pH-dependent in line with the pH-dependence of the equilibrium in question.

If the chemical shifts of the free base and protonated forms are known, then the proportions of each may be determined directly from the chemical shift. The chemical shift of the free base is available in published literature, and was reconfirmed by NMR of the MEA solution. The chemical shift of the protonated form was simply determined by addition of a small excess of HCl to this solution.

A 0.5 ml aliquot of 5 M aqueous MEA was added to an NMR tube, and CO_2 passed through the tube *via* a long syringe needle extending to the base of the tube at a constant flow rate of 0.3 L min^{-1} (measured using a rotameter built into the CO_2 supply) for a set period of time, an ^1H NMR spectrum then gathered, and the pH measured *in situ* using a miniaturised pH electrode. By repeating this protocol with fresh samples of MEA solution carboxylated over longer periods of time, a series of NMR spectra were obtained, each representing a single experiment observing the speciation of the MEA solution correlated against the pH of the solution.

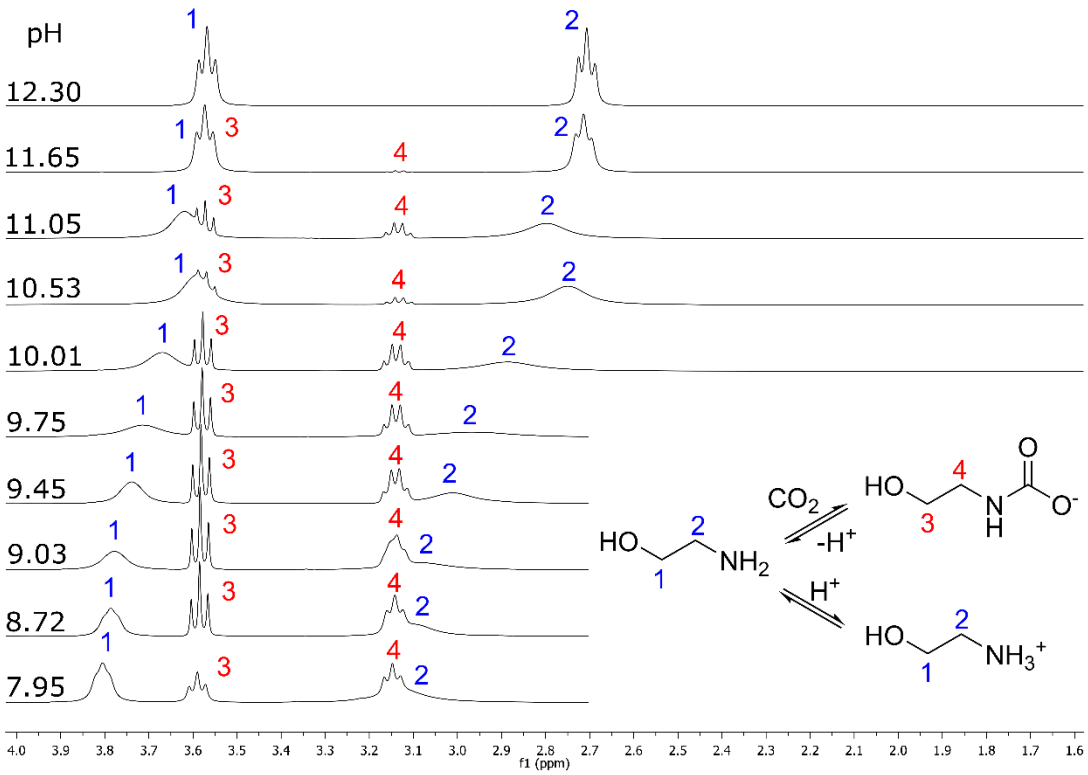

Figure 3.3: ^1H NMR stacked plot following carboxylation of 5 mol L^{-1} MEA. Assignment of visible species and the equilibria by which these are linked.

Figure 3.3 shows the ^{1}H NMR stacked plot arising from carboxylation of 5 M MEA. The pH-dependency of the MEA peaks is clearly evident, with these species moving downfield as more CO_2 is absorbed. No such movement is observed in the case of the carbamate, indicating that the formation of carbamic acid by the corresponding protonation equilibrium does not occur in this case. The reported pK_a of hydroxyethylcarbamic acid is sufficiently low (7.49)[66] that this equilibrium is unlikely to be significantly observable in this work, with the acid forming less than 10% of carbamic species at the lowest pH values measured. Hydroxyethylcarbamic acid is often considered to exist mainly as an intermediate in carbamate decarboxylation, a belief which is borne out by the observations herein.[67]

From the ^{1}H NMR spectra in Figure 3.3, the concentrations of carbamate and MEA (both free base and protonated form) were calculated from the integral ratio of the respective peaks. This is a direct correlation – e.g. if the integral of a given carbamate proton is twice that of a given MEA proton (both forms) this is an integral ratio of 2:1 and therefore the concentration of carbamate is 67% of the total (set at 5 M, hence in this case the concentration of carbamate would be 3.35 M). This relies on accurate integration and on the assumption that the overall concentration of MEA-derived species is constant, i.e. there are no mass losses of MEA or solvent through evaporation.

The free base and protonated forms were differentiated from one another by calculating back from the apparent chemical shift of their combined peak, since this chemical shift is simply a concentration-weighted average of that of the individual species present (e.g. if the chemical shift is equidistant from that of each species, then the two are present in equal concentration). Of the two available peaks for this use, the C*H*$_2$-N peak is preferable, since the chemical shift of these protons is more sensitive to protonation of the nearby nitrogen centre, but due to overlap with carbamate in some spectra, it is sometimes necessary to use the C*H*$_2$-O peaks instead. This chemical shift analysis has been reported for a study of MEA speciation using ^{13}C NMR by Jakobsen et al. but their use in a ^{1}H NMR study is novel and, as we shall see below permits access to the full speciation without the long instrument times required of quantitative ^{13}C NMR.[78] These calculations give the speciation shown in Figure 3.4, plotted against pH.

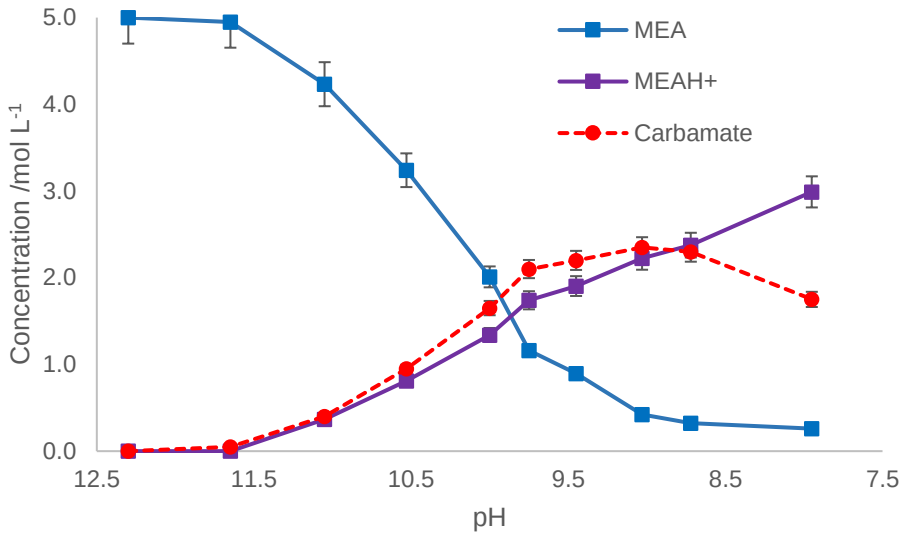

Figure 3.4: Species formed in carboxylation of 5 mol L^{-1} MEA, as observed by ^{1}H NMR. Observed species: MEA free base (blue); protonated MEA (purple); carbamate (red). Bicarbonate is also present but not directly observable.

Since these data represent a series of single experiments without replication, direct measurement of their consistency is not possible, but the accuracy of this approach may be estimated based on existing understanding of the uncertainty associated with ^{1}H NMR spectroscopy. The uncertainty of proton NMR integration was estimated at ~5%, and that of the chemical shift measurement at ~1%, based on commonly used values.[132] This gives an error of ±5% in the carbamate concentration measurements, and ±6% for the other two species. However, this does not account for the behaviour of individual spectra, and line broadening and overlap may lead to increased uncertainty in some cases.

The steady loss of free base is consistent with CO_2 absorption as a neutralisation reaction. However, since the stoichiometry of absorption differs across the two available pathways, the amount of CO_2 absorbed cannot be calculated from the free base concentration alone.

This amount was derived using the observed charge balance in solution. If only carbamate is formed by absorption, then an equimolar amount of protonated MEA should be formed. Additional protonated MEA would indicate the formation of a further anion, which must be bicarbonate. Once the concentration of bicarbonate and carbamate in solution are known, then determining the total concentration of CO_2 absorbed is a trivial sum.

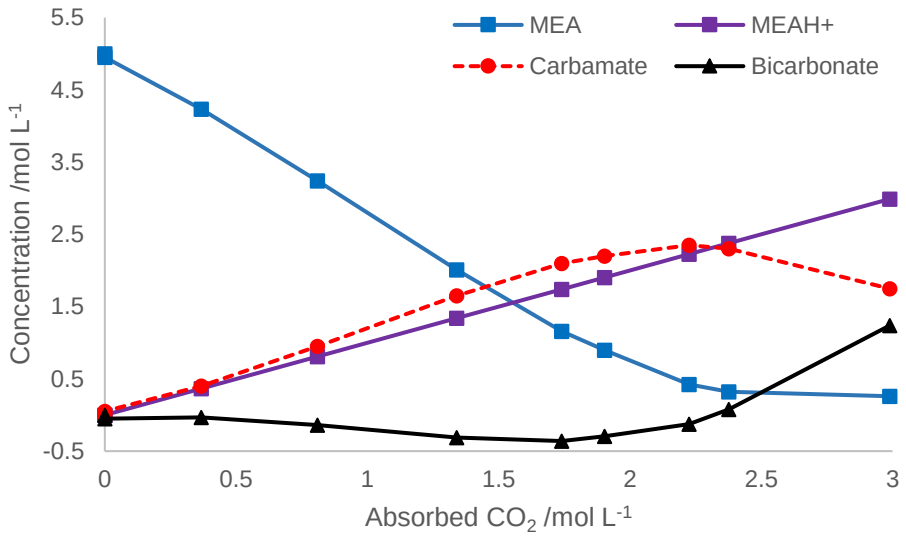

Figure 3.5: Species formed in carboxylation of 5 mol L^{-1} MEA at NMR scale, as observed by ^{1}H NMR. Observed species: MEA free base (blue); protonated MEA (purple); carbamate (red). Concentration of bicarbonate (black) estimated based on the charge balance of observed species.

Figure 3.5 shows the speciation once bicarbonate is taken into account, and plotted against the calculated concentration of CO_2 absorbed. An obvious issue with this approach emerges in the centre of the graph, wherein a negative value for the concentration of bicarbonate is returned. This arises from the ^{1}H NMR spectra (Figure 3.3) where broadening of the MEA peaks leads to a noticeable overlap with the carbamate peaks, causing the concentration of carbamate to be overestimated relative to that of MEA and thence distorts every calculated value.

While the speciation in Figure 3.5 nevertheless fits qualitatively with published speciation for 5 mol L^{-1} MEA,[88] the need for higher-quality spectra is evident. Such line-broadening as observed here is often the result of inhomogeneity in the sample under study. Achieving proper mixing is particularly difficult in narrow NMR tubes and is exacerbated by the comparatively high viscosity of the carboxylated MEA solution. Hence, it was deemed necessary to increase the experimental scale, to a quantity which could be easily mixed by traditional means.

To this end, the scale upon which carboxylation was carried out was increased from 0.5 ml to 30 ml, from which a sample was then taken for NMR analysis. CO_2 was supplied at a constant rate through a needle in a fixed position, providing reproducible conditions suitable for estimation of the rate of absorption. ^{1}H NMR spectra from these conditions exhibited sharp peaks with none of

the line broadening seen above, as shown in Figure 3.6. This enables significantly more accurate integration as peak overlap is minimised.

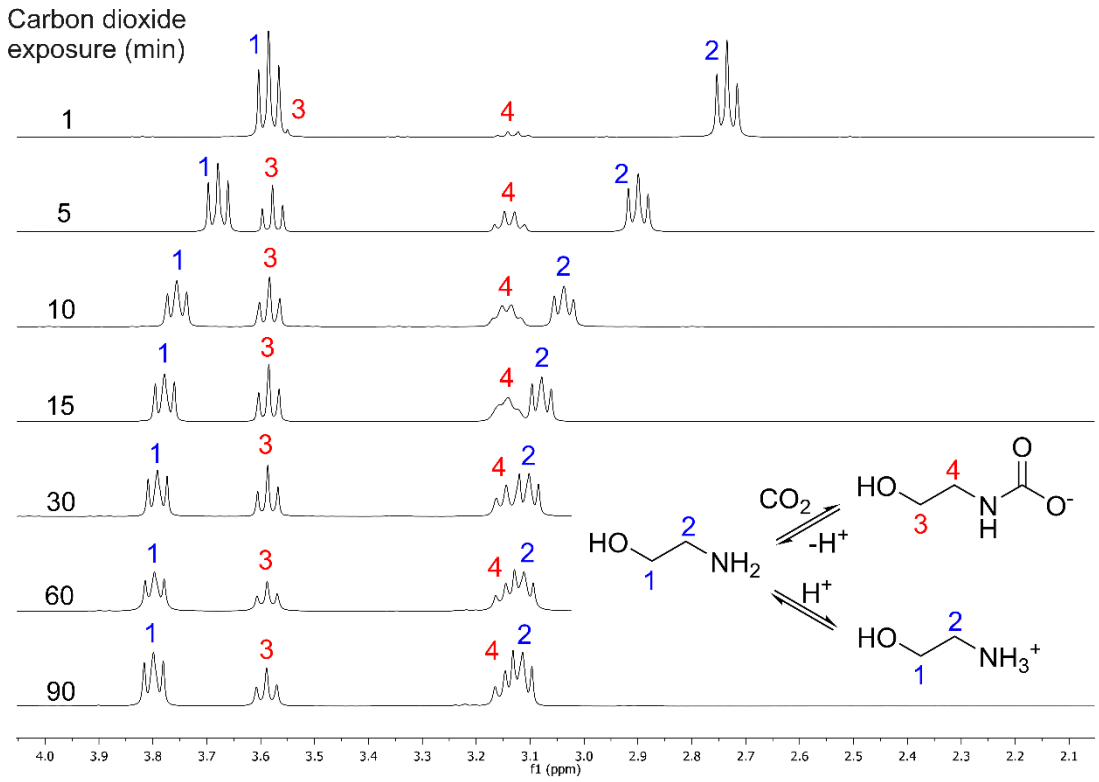

Figure 3.6: ^{1}H NMR stacked plot following carboxylation of 5 mol L^{-1} MEA on 30 ml scale.

Species concentrations were calculated in the same manner as described previously. The speciation measured by this approach is shown in Figure 3.7, and compared with published speciation. The data show good agreement, as concentration of carbamate is no longer overestimated, with consequent improvement in accuracy.

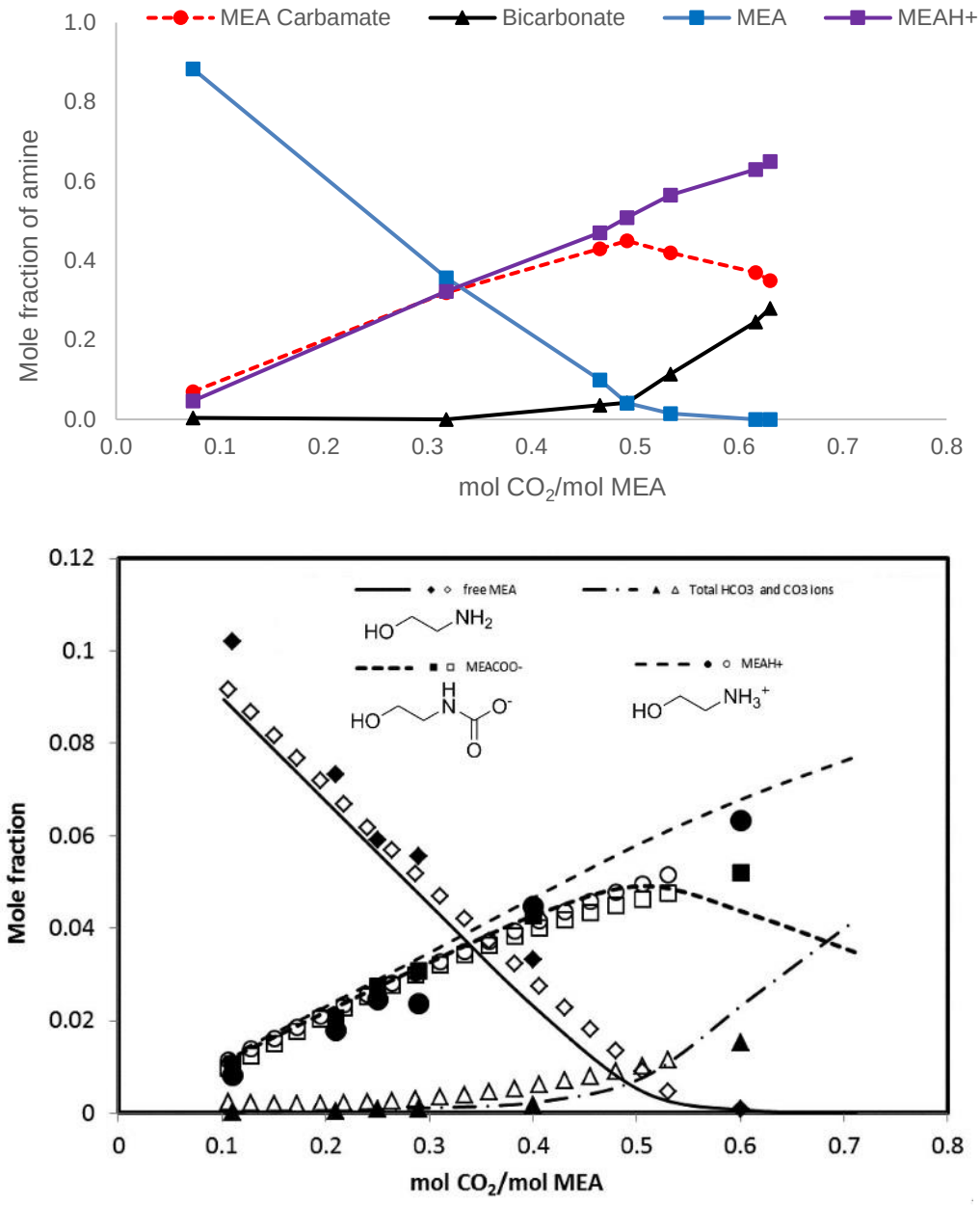

Figure 3.7: Above: species formed in carboxylation of 5 mol L^{-1} MEA on 30 ml scale. Observed species: MEA free base (blue); protonated MEA (purple); carbamate (red). Concentration of bicarbonate (black) calculated from charge balance of observed species. Below: Published literature data on speciation of this solution. Data from: ^{13}C NMR study by Jakobsen et al. (filled symbols); combined titration/CO_2 gas analysis study by Matin et al. (hollow symbols); and Aspen Plus electrolyte-NRTL modelling following parameters developed by Zhang et al (lines).[78,88,89]

Though the calculated values for bicarbonate concentration agree well with previously published measurements, these constitute an estimate rather than a direct measurement. In order to corroborate the values, the concentration of absorbed CO_2 was also measured directly with a gasometric approach, using a vapour-liquid equilibrium cell. This consisted of a stainless steel cell of known volume, sealed with the exception of a rubber septum through which solutions could be injected by syringe. Magnetic stirring was provided throughout experiments, while

pressure and temperature were monitored using built-in sensors. A full description of the cell is presented in section 8.1.2.1.

Within the cell was injected a known-volume sample of carboxylated solution, to which an excess of acetic acid was added. The straightforward neutralisation of carbonates and carbamates with acid releases an equimolar amount of CO_2, and this was quantified by measuring the pressure increase in the cell using a built-in pressure transducer, from which the number of moles of CO_2 was calculated using the ideal gas approximation. Typically a 2 ml sample was used together with 1 ml acetic acid, though in cases of low absorbed CO_2 concentration it was necessary to repeat the measurement with larger quantities (up to 5 ml) of carboxylated solvent in order to obtain a reasonably measurable pressure differential.

To use a representative example, 2 ml of MEA from a solution that had been exposed to CO_2 for 90 minutes (according to the protocol described on p43-44) produced a pressure increase from 1.00 bar to 1.38 bar when combined with 1 ml acetic acid within the cell. From the ideal gas approximation, $pV = nRT$, we rearrange for the expression $n = \frac{pV}{RT}$, and using the measured value for the temperature (20 °C) and the known volume of the cell (757 ml, after accounting for the *ca.* 3 ml of solution added) it can be calculated that 0.0063 moles of CO_2 were released, which for the 2 ml sample corresponds to an absorbed CO_2 concentration of 3.15 mol L^{-1}.

This method is well-established for measurement of the concentration of dissolved carbonates and is accurate so long as the vessel is properly sealed.[133] Hence, the rubber septum was regularly replaced after every four measurements in order to prevent the seal from being compromised by wear.

Measuring the concentration of CO_2 absorbed allows the concentration of bicarbonate to be calculated more directly in each experiment, by subtracting the concentration of carbamate from the total absorbed CO_2. Figure 3.8 shows a comparison between this method and the NMR-only method already described, and appears to produce more consistent results by eliminating the uncertainty associated with relying on NMR chemical shifts. In particular, the gasometric

approach does not return negative values for the concentration of bicarbonate at low concentrations, due to the improvement in accuracy of this method.

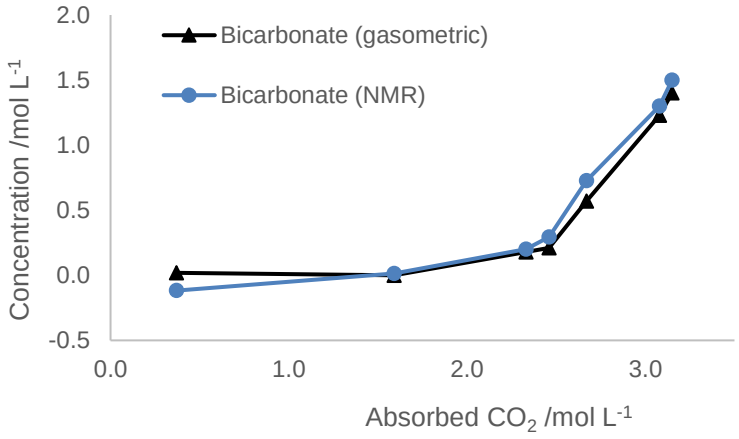

Figure 3.8: Comparison of values for bicarbonate concentration in carboxylation of 5 mol L^{-1} MEA, determined by two different means: from the residual charge balance of species measured solely by ^{1}H NMR (blue); and from the gasometrically determined absorbed CO_2 concentration, from the which the ^{1}H NMR-derived carbamate concentration is subtracted (black).

3.3 CO_2 absorption by amine blends

Following validation of the ^{1}H NMR-based approach with MEA, this section seeks to demonstrate its efficacy for study of blended amine solutions thanks to the broad applicability of ^{1}H NMR. The methods described for the study of MEA were deemed to be suitable without modification. The principal difficulty of applying this method to blended solutions was the possible presence of overlapping peaks from different species which may render it difficult to obtain accurate chemical shift values for some species. Since the chemical shift of the various amine species is pH-dependent, possible overlaps cannot easily be predicted ahead of time using the literature values available.

A wide variety of amine blends have received study for their capture performance. Perhaps the most well-known of these is the blend of MEA with *N*-methyldiethanolamine (MDEA), which has been subjected to testing up to pilot scale at the Boundary Dam CO_2 demonstration plant in Canada, showing promising reductions in heat duty when compared to a single MEA solution.[110,134,135]

Sterically hindered amines, exemplified by 2-amino-2-methyl-1-propanol (AMP) have attracted significant interest as non-carbamate-forming CO_2 capture agents, and their blends with other amines have received relatively detailed study. Initial work on AMP blends investigated the blend with MEA, finding superior performance compared to MEA/DEA blends.[106,135,136]

Cutting-edge research into carbon capture has tended to move away from MEA as a carbamate-forming capture agent owing to its poor stability, and toward piperazine (PZ) instead.[111] The same holds true for research on amine blends. In particular, the properties of the blend of AMP with piperazine have been closely examined by a number of research groups, reporting a very high capacity for CO_2 and faster CO_2 absorption than comparable MEA solutions.[112,137,138]

The three blended solutions described – MEA/MDEA, MEA/AMP, and AMP/PZ – were examined for their speciation using the ^{1}H NMR techniques described earlier. The question of which composition(s) should be employed is a complex one, as no standard composition exists and particularly successful blend compositions are considered proprietary by their developers. Hence, an extremely wide variety of blend compositions, often without any apparent compositional screening, has been used in published research.

For this work a uniform composition of 3 mol L^{-1} non-carbamate forming amine and 1 mol L^{-1} carbamate-forming amine was adopted. A full compositional screening is beyond the scope of this work, which at this juncture is to establish the feasibility of the ^{1}H NMR approach for mixed amine solutions.

3.3.1 CO_2 absorption by a blend of MEA and MDEA

Carbon dioxide was passed through a series of solutions containing 1 mol L^{-1} MEA and 3 mol L^{-1} MDEA and analysed by ^{1}H NMR in precisely the same manner as described for MEA alone. Despite the presence of two very similar amines, peak overlap was negligible and did not interfere with determination of species concentration by integration (Figure 3.9).

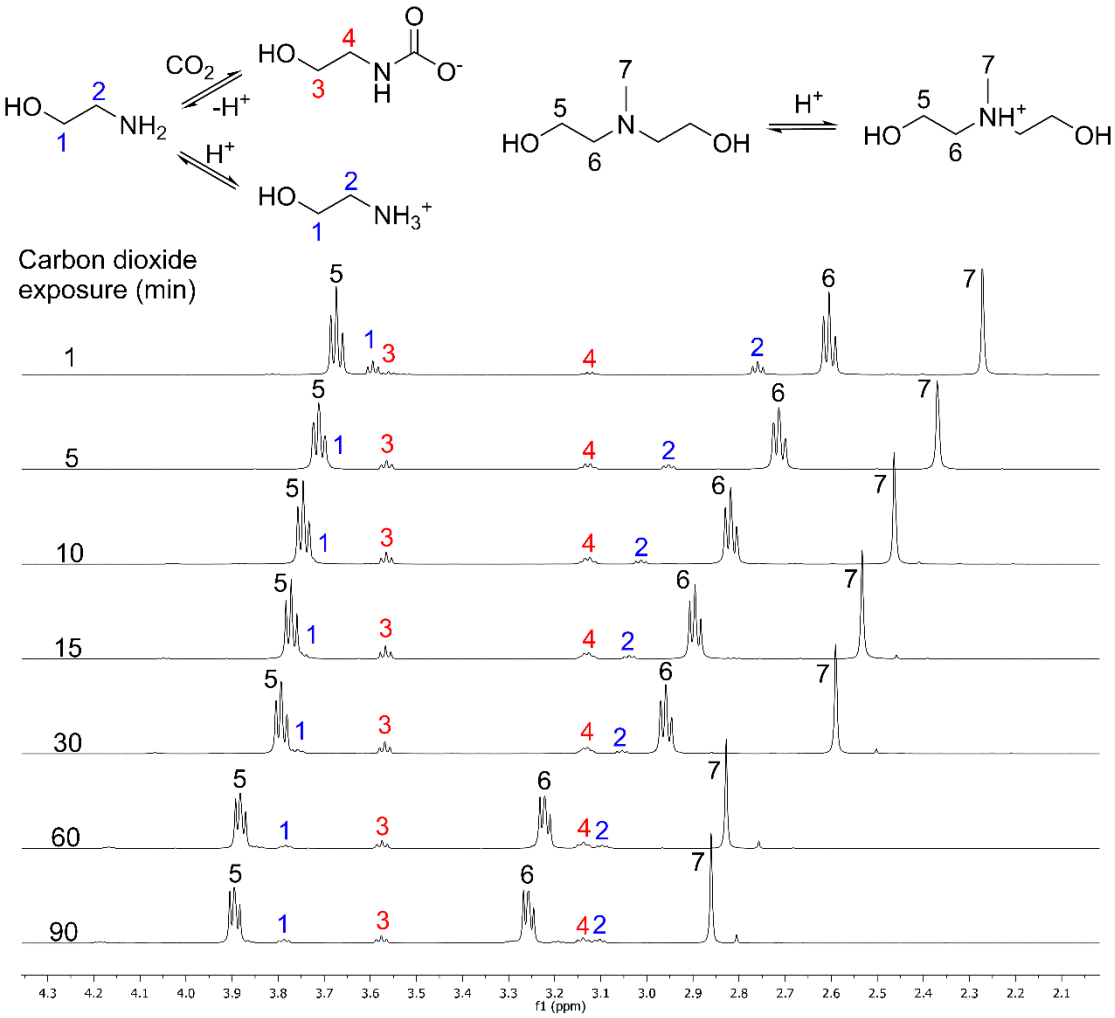

Figure 3.9: ^{1}H NMR stacked plot showing absorption of CO_2 into an aqueous solution of 1 mol L^{-1} MEA and 3 mol L^{-1} MDEA, with carboxylation products labelled.

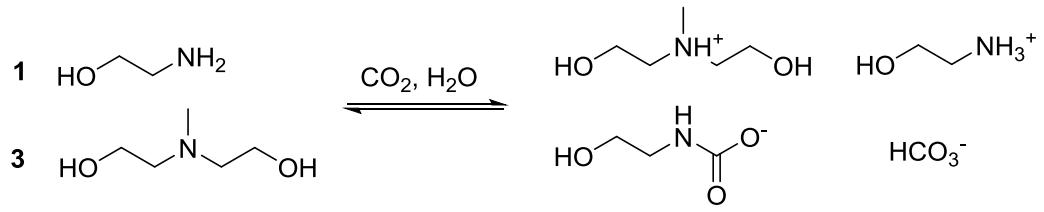

Scheme 3.1: CO_2 absorption products from a solution of MDEA and MEA.

The protonation of both amine species was observed based on the downfield shift of their respective peaks in response to carboxylation. Formation of the carbamate of MEA was also observed. This is consistent with the products expected from this reaction (Scheme 3.1). Of particular interest is the formation of at least one additional species, with significant peaks at 2.81 (s, 3H), 3.19 (t, 2H, $^{3}J_{HH}$ = 3.3 Hz), 4.19 (t, 2H, $^{3}J_{HH}$ = 3.1 Hz) in the final spectrum. Since these values are observed to shift downfield in response to carboxylation, it is likely that this species retains an amine moiety and is a derivative of MDEA.

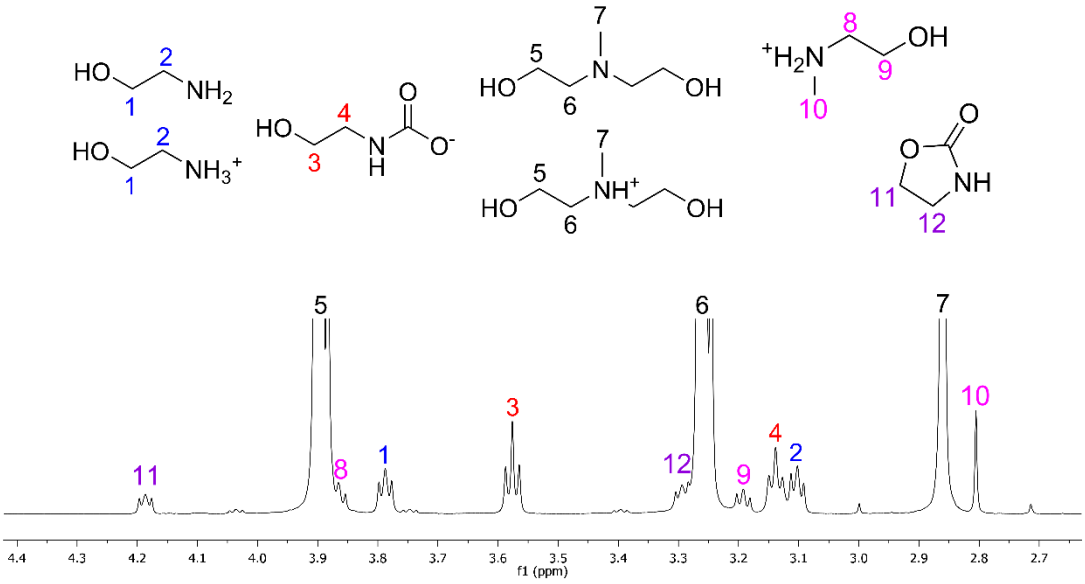

Figure 3.10: Assigned ^{1}H NMR spectrum of solution containing 1 M MEA and 3 M MDEA exposed to CO_2 for 90 minutes, showing minor absorption products.

Integral analysis confirms this as a derivative of MDEA, most likely 2-(methylamino)ethanol, a known product of the oxidative decomposition of MDEA.[139] This decomposition pathway is believed to produce formic acid as a byproduct, though neither formic acid nor formate are observed in this solution. 2-(methylamino)ethanol is present in comparatively large concentrations (up to 6 mol% of MDEA concentration), suggesting a high rate of degradation given the relatively mild experimental conditions of this work.

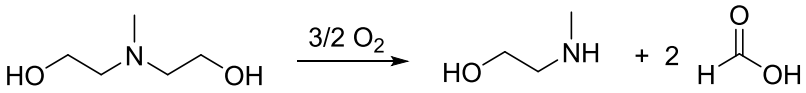

Scheme 3.2: Proposed formation of 2-(methylamino)ethanol from MDEA.

The carboxylated species formed in this solution are shown in Figure 3.11. As with MEA alone, carbamate is the major product when little CO_2 is absorbed, and bicarbonate predominates at higher CO_2 loadings. However, this is far less clear-cut than in the MEA solution – a notable concentration of bicarbonate is present even at low CO_2 loading of 1 mol L^{-1} or less.

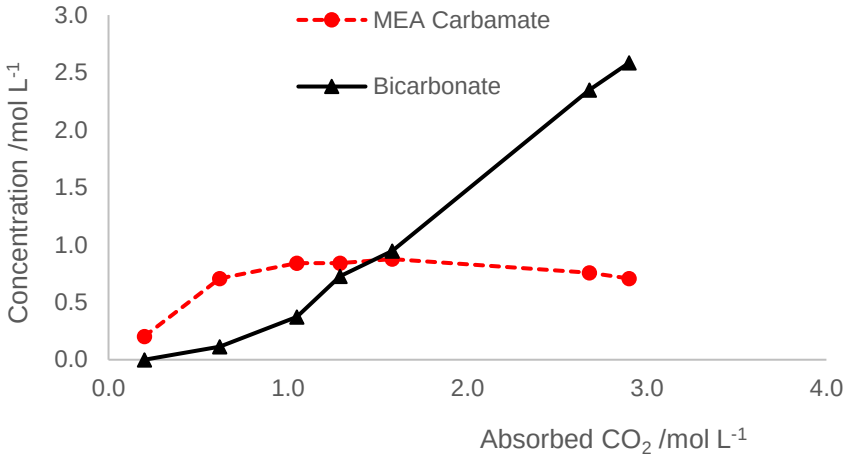

Figure 3.11: CO_2-containing species formed in solution of 1 mol L^{-1} MEA and 3 mol L^{-1}MDEA, showing bicarbonate and the carbamate of MEA.

It is notable that the concentration of carbamate does not significantly decline from its maximum of *ca.* 1 mol L^{-1}, suggesting that almost all MEA is converted to carbamate, the most stable capture product. The amount of carbamate that may be formed is still limited to 50 mol% of amine in the system, but now an additional limit is imposed because the MDEA which makes up the majority of the solution does not take part in carbamate formation. Thus, all MEA is consumed in carbamate formation combined with an equimolar amount of MDEA (as $MDEAH^+$), and remaining MDEA is left free to participate in bicarbonate formation.

In terms of this solution's performance in post combustion CCS, the increased concentration of bicarbonate would translate to a lower enthalpy of absorption and an improved absorption capacity. The latter is already evident, with a maximum CO_2 capacity of 2.9 mol L^{-1} being approximately comparable to that of 5 M MEA (3.15 mol L^{-1}) despite the notably higher concentration of the single-component MEA solution.

An increased concentration of bicarbonate at low CO_2 loadings is likely to be particularly beneficial, since this provides for a significant amount of easily-recoverable CO_2 with minimal contact time. Minimisation of gas/liquid contact time is especially important for implementation of CCS on an industrial scale as this is strongly related to the capital costs of the process, which are a dominant concern for initial investments.[23]

3.3.2 CO_2 absorption by a blend of MEA and AMP

CO_2 capture with a mixed solution of 1 M MEA and 3 M AMP proceeded in much the same manner as for the MEA/MDEA solution (Scheme 3.3). No degradation products were observed, but a very small amount (< 1 mol%) of a carbamate of AMP was observed in addition to the carbamate of MEA (Figure 3.12).

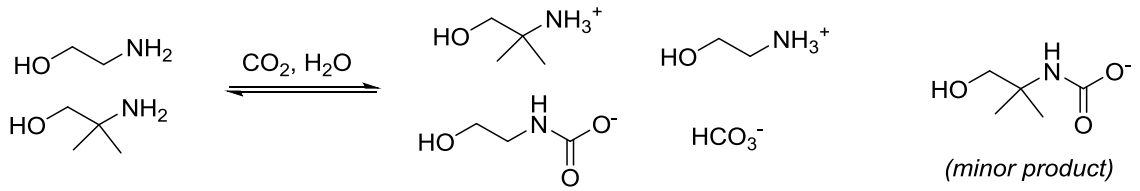

Scheme 3.3: CO_2 absorption into a solution of AMP and MEA.

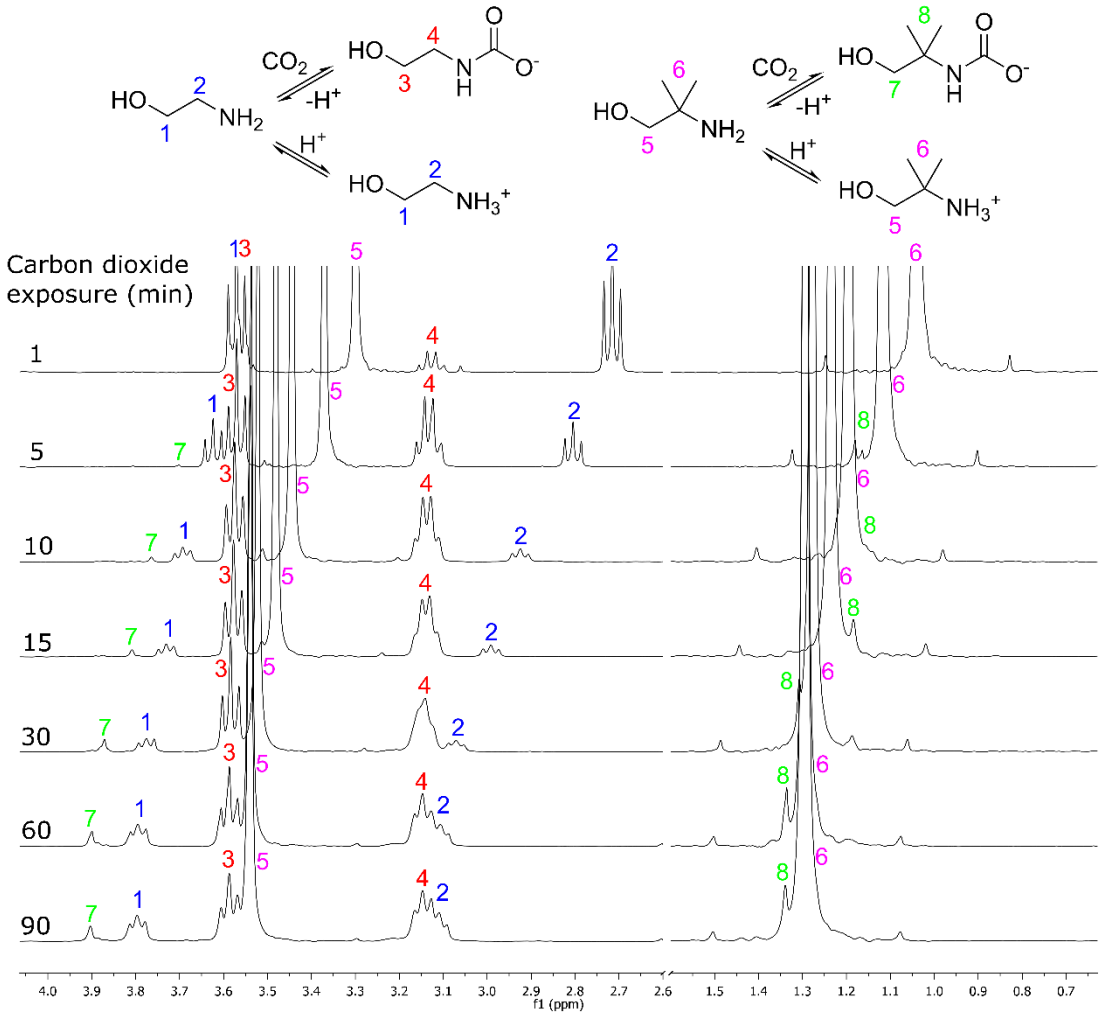

Figure 3.12: ^1H NMR stacked plot following carboxylation of a solution containing 1 mol L^{-1} MEA and 3 mol L^{-1} AMP.

Speciation analysis shows results broadly similar to that of the MEA/MDEA blend (Figure 3.13). In solutions with a low (< 1.75 M) CO_2 loading, the solution contains a mix of bicarbonate and

carbamate with carbamate being most dominant, while above 1.75 M CO_2 loading the situation reverses. It is notable, however, that the rate of absorption is significantly improved over the MEA/MDEA blend. For example, given 30 minutes of gas/liquid contact time, 2.35 mol L^{-1} CO_2 (59 mol%) is absorbed into the MEA/AMP blend, compared with only 1.58 mol L^{-1} (40 mol%) for the MEA/MDEA blend.

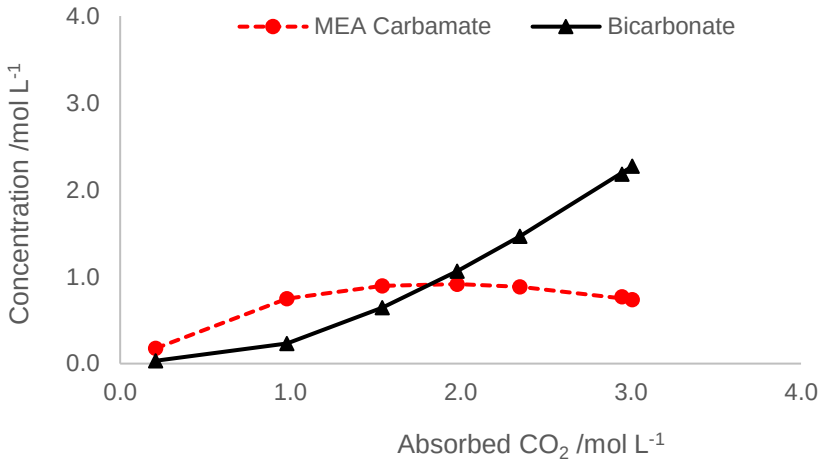

Figure 3.13: CO_2-containing species formed in solution of 1 mol L^{-1} MEA and 3 mol L^{-1}MDEA, showing bicarbonate (black) and the carbamate of MEA (red).

In addition to improved kinetics, no degradation products are observable in the solution using AMP, implying a significant improvement in stability over MDEA. Together, these factors justify the replacement of MDEA with AMP in CO_2 capture solvents.

3.3.3 CO_2 absorption by a blend of PZ and AMP

Piperazine presents a particularly difficult challenge for ^{1}H NMR speciation analysis since, as a diamine, a number of different species are possible, some of which are distinguishable by NMR and some engaging in fast chemical exchange. Following formation of a carbamate, the second amine of that molecule may be protonated (producing a zwitterion) or carboxylated a second time to produce a bis(carbamate). Possible species known to be formed by CO_2 absorption into piperazine are shown in Figure 3.14.[140] Note that while protonation of piperazine occurs during absorption, the second pK_a of this molecule (5.3) is too low for the dicationic form of this molecule to become significant in this case.[141]

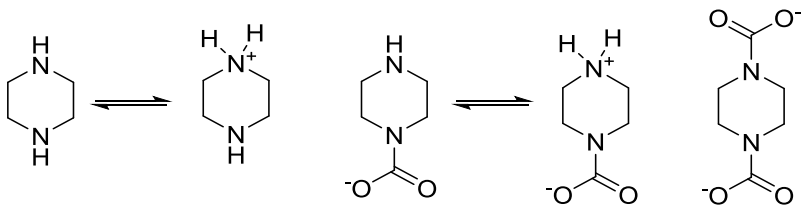

Figure 3.14: Possible species present in carboxylated aqueous solutions of piperazine. Species linked by equilibrium arrows undergo rapid exchange and are not distinguishable from one another by NMR at room temperature.

Carboxylation of a mixed AMP/PZ solution therefore produces a very diverse mixture of numerous similar species, many of which have overlapping NMR peaks. Furthermore, this solution is particularly viscous and becomes even more so upon CO_2 absorption, which leads to line broadening in the NMR spectrum and further overlap. Thus, the AMP/PZ solution might be considered a particularly challenging test for the NMR approach to speciation.

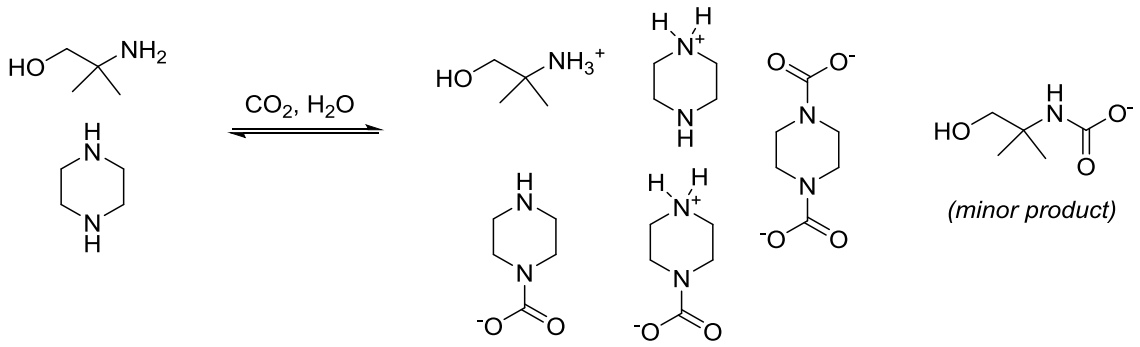

Scheme 3.4: Absorption of CO_2 into a mixed solution of AMP and PZ.

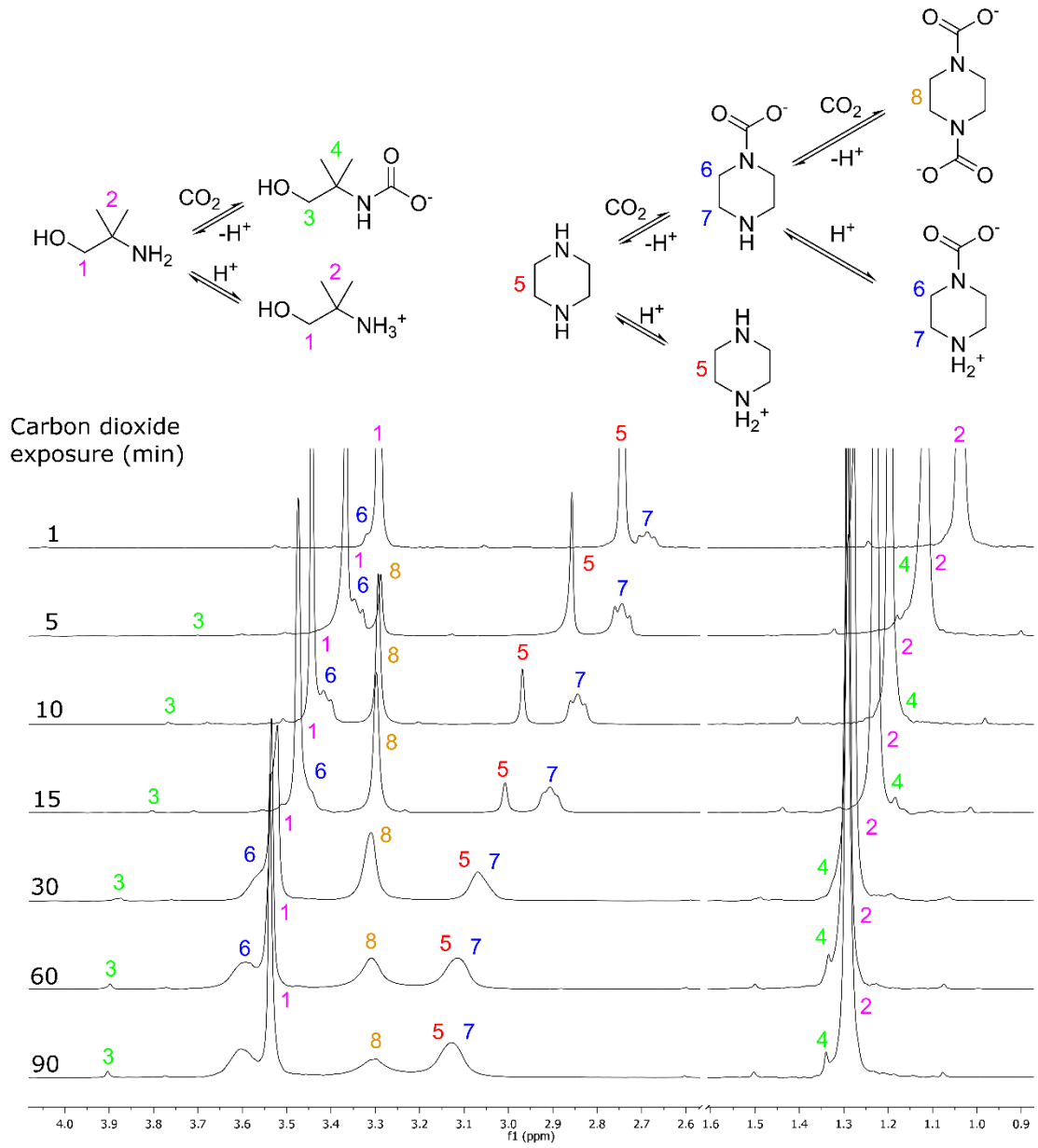

Figure 3.15: ^{1}H NMR stacked plot following carboxylation of an aqueous solution containing 1 mol L^{-1} piperazine and 3 mol L^{-1} AMP.

Overlaps and broadening notwithstanding, species determination for this solution remains possible, taking advantage of the fact that the 6H peak of AMP is clearly separated from the various piperazine derivatives and therefore provides a reliable integral reference from which the integration of other peaks could be successively deduced. The only significant difficulty is differentiation of the two piperazine monocarbamate species (the anion and zwitterion) since the chemical shifts associated with either of these species are not known, and cannot be reliably estimated *in situ*.

The information available from ^{1}H NMR is sufficient for measurement of carbamate species concentrations, but is therefore insufficient for calculation of bicarbonate concentration. Hence, we must rely on the vapour-liquid equilibrium approach described in 3.2 in order to obtain a proper estimate of bicarbonate concentration.

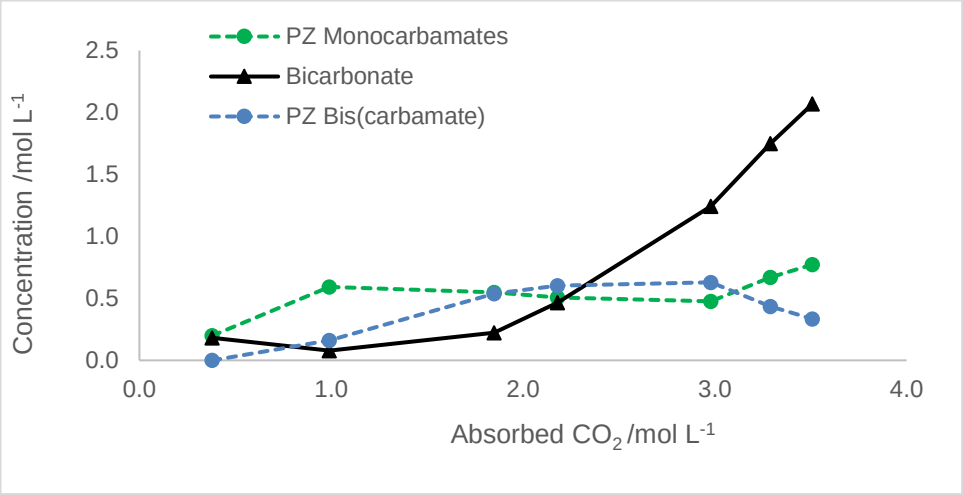

Figure 3.16: Carboxylated species formed in carboxylation of solution containing 1 mol L^{-1} piperazine and 3 mol L^{-1} AMP, showing piperazine monocarbamates (green), piperazine bis(carbamate) (blue) and bicarbonate (black).

The species formed in solution are shown in Figure 3.16. It is evident that both mono- and dicarboxylated piperazine are formed, together with significant amounts of bicarbonate at higher concentrations.

3.4 Conclusions

This chapter has illustrated the development of a method of analysing CO_2 absorption into amine capture solvents both by ^{1}H NMR alone, and by ^{1}H NMR supported with gasometric analysis. Such methods have been shown to reproduce literature measurements of the speciation in 5 M MEA, and their application to a variety of blended capture solvents supports the observations of improved performance of these solvents that had been reported based on more superficial studies.

The methods of analysis developed herein are straightforward, quick and adaptable to new systems, even those displaying particular complexity (as seen with the solution of AMP and PZ). Thus, they would be ideal for a large-scope screening study, whether this be focused on the discovery of new amines for CO_2 capture, or on compositional screening of blended amine capture solvents.

4 Use of Phenoxide for Carbon Dioxide Capture

4.1 Introduction

Thus far, most research into blended CO_2 capture solvents has focused on the mixture of an amine which can form carbamates with an amine that cannot. Despite the improvements in capture performance that such solutions provide over single-amine solutions, the disadvantages associated with use of an amine-dominated capture solvent remain (as elaborated upon in section 2.4). Such capture solvents tend to be corrosive and prone to oxidative degradation. They present an environmental hazard which is exacerbated by the volatility of the free base and the toxicity and/or carcinogenicity of some amine degradation products.[142]

Since non-carbamate-forming amines function only as a Brønsted-Lowry base and no other particular reactivity appears to be necessary, in principle any other Brønsted-Lowry base whose conjugate acid falls within a moderately basic pK_a range (*ca.* 9-11) could fulfil the role of bicarbonate promotion in blended CO_2 capture solvents. Significant deviation from this range is less likely to produce a successful capture agent, as an excessively low pK_a would limit the ability of the capture agent to deprotonate carbonic acid ($pK_{a1}' = 6.35$) while an excessively high pK_a would introduce an additional thermodynamic barrier to regeneration of the capture solvent.

Among the few other classes of compounds with basicities in this range, by far the most numerous are the phenoxides, with phenol having a pK_a of 9.95.[143] That phenoxide salts can capture CO_2 was identified in previous work carried out within the Rayner research group, but a more detailed study is needed.[144,145]

In relatively early work, phenoxides were considered as possible competitors to amines as CO_2 capture agents for gas sweetening application, but they were discounted due to the superior performance of amines.[146] They have received relatively little attention since then, but being both

inexpensive and available in the large quantities that CCS would require, their use as capture agents would certainly be economically feasible provided capture performance is sufficient.

Phenoxides have also received attention in the context of CO_2 utilisation, as their potassium or sodium salts can be converted to aryl carboxylic acids in the Kolbe-Schmitt process (Figure 3). This classic reaction is a source of numerous important compounds in chemical industry, most notably salicylic acid.[147]

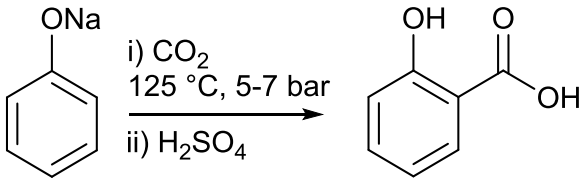

Scheme 4.1: Kolbe-Schmitt carboxylation of sodium phenoxide to produce salicylic acid.

Barbarossa *et al.*[148] recently reported reversible CO_2 capture into alkaline resorcinol solutions, employing a variant of this reaction to produce β-resorcylic acid as the capture product. Other past work on phenoxides in carbon capture has considered their potential as anions within an ionic liquid.[149,150] Since water is absent from such a system, bicarbonate cannot form and carboxylation reportedly produces phenyl carbonate anions. These reactions are illustrated in Scheme 4.2.

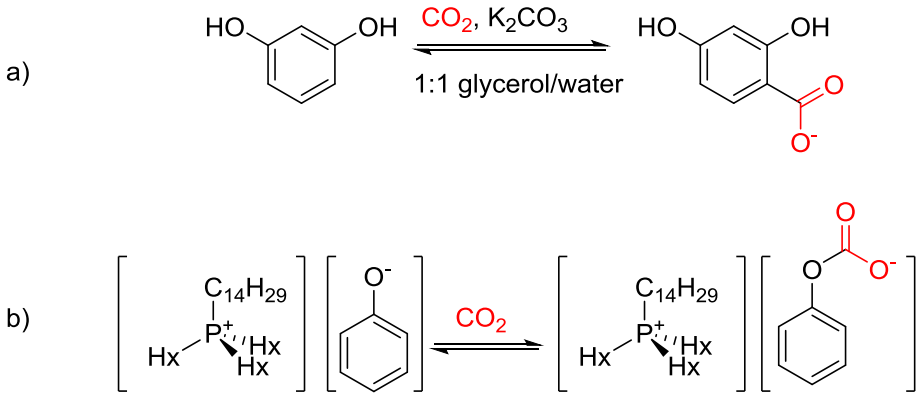

Scheme 4.2: Published approaches to CO_2 capture using phenoxide compounds: a) carboxylation of resorcinol by Barbarossa et al.[148] and b) carboxylation of phenolic ionic liquids by Wang, Dai et al.[149]

Herein, only the reactivity of phenoxide as a Brønsted-Lowry base is desired, in order to replicate the behaviour already observed in CO_2 capture by tertiary amines in blended solvents. Side reactions such as the Kolbe-Schmitt-type carboxylations described above would be detrimental to CO_2 capture performance as the decarboxylation of their reaction products is typically much

more difficult to accomplish than for bicarbonate, giving poor yields even under harsh conditions.[148,151]

This work will seek to develop a CO_2 capture solvent that proceeds along the lines shown in Scheme 4.3, using a phenoxide salt combined with an amine. Such a system would not completely eliminate amines from CO_2 capture, as carbamate formation from a primary amine is necessary in order to achieve acceptable kinetics of absorption. However, a phenoxide blend could greatly reduce the concentration of amine needed in the capture solvent, correspondingly reducing the corrosivity and environmental hazards posed by the amine itself.

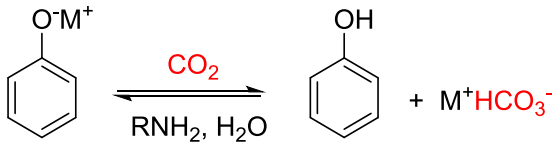

Scheme 4.3: Proposed approach to CO_2 capture using a phenoxide salt together with an amine. Ammonium and carbamate derivatives of the amine would also be expected as absorption products.

The speciation-focused methods of analysis developed in the previous chapter will be applied as necessary herein, in order to study the properties of the phenoxide-based capture solvent and to compare these with existing amine blend capture solvents.

4.2 CO_2 absorption by potassium phenoxide

As a starting point, a 1 M aqueous solution of potassium phenoxide was prepared *in situ* from phenol and potassium hydroxide. The potassium salt was chosen due to the particularly high aqueous solubility of potassium bicarbonate compared to other alkali metal bicarbonates, in order to avoid excessive precipitation. Pure CO_2 was passed through samples of this solution in a graduated cylinder for a set time span (1, 5, 10, 15, 30, 60 and 90 minutes respectively) at ambient pressure with the CO_2 flow rate being controlled at 0.3 L min^{-1} and the temperature at 25 °C. ^{13}C NMR spectra of the resulting solutions evidenced a peak corresponding with bicarbonate/carbonate (the rapid exchange of protons between these species producing a single peak that represents both species) and no other new compounds were observed in ^{1}H or ^{13}C NMR, confirming the absence of any measurable Kolbe-Schmitt-type carboxylation. This is not a

surprising result, as while resorcinol has been reported to undergo Kolbe-Schmitt carboxylation in similar conditions, it is more nucleophilic than phenol for which much harsher conditions and high CO_2 pressures are typically required.[148]

The amount of CO_2 absorbed into the solution was measured using a vapour-liquid equilibrium cell, following the gasometric method already described in Chapter 3.[133,152] Application of this method to 1 M aqueous KOPh showed CO_2 absorption approaching a maximum of 1 mol L^{-1} of absorbed CO_2, behaviour consistent with the stoichiometric neutralisation of phenoxide by CO_2 to produce phenol and potassium bicarbonate (Scheme 4.4).

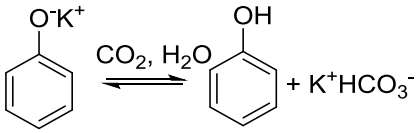

Scheme 4.4: Hydration of CO_2 by potassium phenoxide.

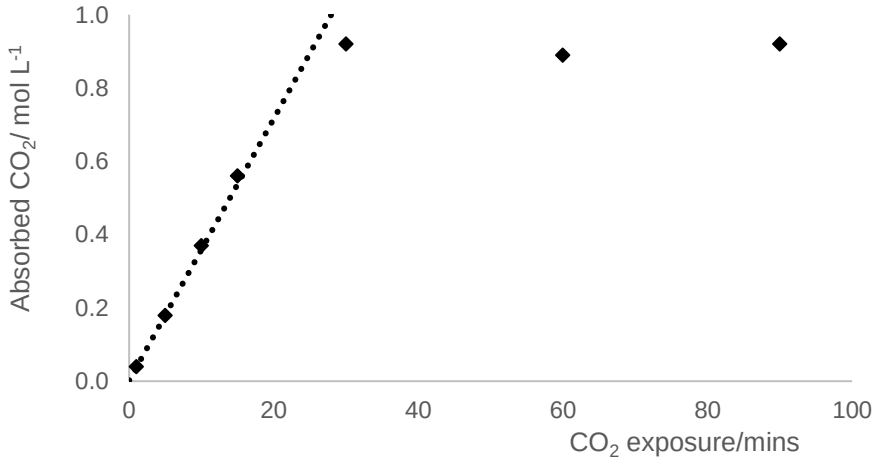

Figure 4.1: CO_2 absorption into 1 M aqueous KOPh, with linear trendline showing the initial rate of absorption. Concentration of absorbed CO_2 measured via gasometric method.

It is well known that the rate of bicarbonate formation mediated by amines is usually slow in comparison to carbamate formation.[153] Absorption rates are very important for CCS applications as a low absorption rate leads to excessive size requirements for absorption columns. Thus, approximate rate data was obtained in order to assess the impact of capture solvent composition on the rate of reaction, in addition to the capture capacity and speciation. The initial rate of absorption was estimated from a linear extrapolation of the initial data points in a plot of absorbed

CO_2 against contact time (Figure 4.1). Pure CO_2 was used for the carboxylation experiments in an effort to avoid mass transfer limitations on the absorption rate.

The observed rate of absorption for 1 M KOPh with 100% CO_2 was 0.036 mol CO_2 L^{-1} min^{-1}, which is indeed much slower than that reported in studies of amine solutions.[153] A similar experiment using aqueous 5 M MEA demonstrated an absorption rate almost an order of magnitude faster (0.32 mol CO_2 L^{-1} min^{-1}), a difference too great to be explained by the increased concentration of the latter. This confirms the necessity of including a carbamate-forming amine in order to achieve acceptable absorption kinetics.

4.3 CO_2 absorption by blends of potassium phenoxide and ethanolamine

Hence, the study turned to blends of KOPh with ethanolamine, with the aim of understanding the effects of phenoxide upon capture performance, particularly reaction rate, speciation and loading. To this end, the versatile ^{1}H NMR approach developed in the previous chapter was employed.

4.3.1 Multiphase behaviour

In order to determine the effect of KOPh upon CO_2 capture by aqueous MEA, a variety of possible combinations of the two capture agents was screened (Table 4.1, *vide infra*). In many cases a two-phase mixture was produced. ^{1}H NMR analysis of the two phases showed that the upper phase consisted mostly of phenol along with a small quantity of MEA and derivatives (from 2-8 mol% of total MEA depending upon composition), with an overwhelming majority (>95%) of carboxylated salts present in the aqueous lower phase (Scheme 4.5). The separation is likely due to the formation of phenol, which has low (*ca.* 1 mol L^{-1}) aqueous solubility.

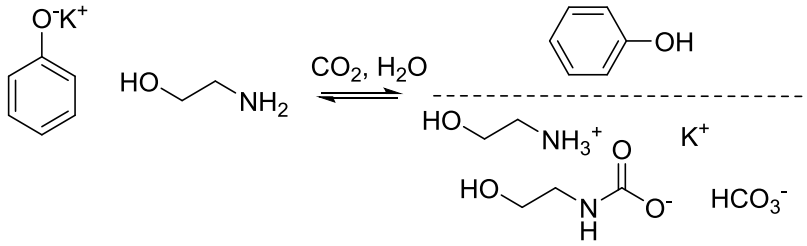

Scheme 4.5: CO_2 absorption products in aqueous blends of KOPh and ethanolamine, and approximate phase distribution.

Of the blended compositions listed below, only the most dilute (i.e. that containing 1 M MEA and 1 M KOPh) did not show any phase separation. In the other compositions, phase separation occurred at relatively high CO_2 loading. The volume balance of the two phases was approximately proportional to the concentration of KOPh in the starting solution, with more initial KOPh producing a larger organic phase as a greater amount of phenol was produced by carboxylation.

Table 4.1: Summary of the rate and capacity for CO_2 absorption into aqueous solutions containing varying concentrations of MEA and KOPh.

Entry	MEA (mol L^{-1})	KOPh (mol L^{-1})	Abs. %[a]	Initial rate[b]	Absorbed CO_2 (mol L^{-1})[c]
1	5	0	63	0.32	3.15
2	0	1	92	0.036	0.92
3	1	1	82	0.18	1.66
4	1	2	79	0.18	2.36
5	1	3	88	0.17	3.50
6	2	1	70	0.22	2.16
7	2	2	66	0.24	2.65

[a] *Maximum mol% CO_2 absorbed relative to concentration of base in solution.*
[b] *mol L^{-1} min^{-1}. Calculated from a linear extrapolation of initial slope of a plot of absorbed CO_2 against CO_2-liquid contact time.*
[c] *Maximum CO_2 concentration measured via gasometric method. Carboxylation conditions: 25 °C, 30 mL sample volume, CO_2 flow 0.3 L min^{-1} for 90 min.*

This biphasic behaviour complicated species determination somewhat, as a homogeneous sample is required in order to obtain ^{1}H NMR spectra of sufficient quality. Furthermore, chemical shift values of MEA derivatives were found to be variable by several tenths depending on the concentration of phenol in solution (with the point of phase separation having a particularly major effect due to removal of phenol from the aqueous phase). Due to this phenomenon, the chemical shift analysis used in the previous chapter to determine the positions of proton equilibria was not possible in this case.

Hence, a simplified method of analysis was adopted, focusing only on the carboxylated species involved. Concentration of carbamate was still determinable directly from the ^{1}H NMR spectra, while the concentration of bicarbonate was determined by deduction of carbamate from the total CO_2 loading as determined gasometrically, both methods already having been demonstrated in the previous chapter.

Furthermore, the multiphase behaviour of the solution needed to be taken into account. To this end, each phase was extracted and analysed separately, and their amounts relative to one another

calculated based on integration of the ethanolamine- and phenoxide-derived peaks in the NMR spectrum. The ratio of these in the total solution is known based on the initial composition (and does not significantly vary in the course of carboxylation due to the low volatility of these compounds) and is defined as the average of the same ratio in each phase, weighted by the amount (mole fraction) of each phase. Hence, measurement of this ratio in the organic and aqueous phases allows the determination of the mole fraction of each phase relative to the whole, and knowledge of this mole fraction then allows the proportions of each species to be related to the whole mixture.

Precipitation of $KHCO_3$ was observed in the two most concentrated solutions, containing respectively: 1 M MEA/3 M KOPh; and 2 M MEA/2 M KOPh after particularly long exposure to CO_2. The identity of this precipitate was implied by the lack of any significant organic species in a ^1H NMR spectrum (quantitatively referenced against sodium formate), and confirmed by both the ^{13}C NMR spectrum and use of the gasometric method (see previous chapter) to measure the mass fraction of acid-sensitive carbonates in a standard aqueous solution prepared from the precipitate. The concentration at which $KHCO_3$ began to precipitate (*ca.* 3 mol L^{-1}) is broadly consistent with its reported aqueous solubility.[154] This may present a problem in more concentrated solutions if the amount of precipitate produced becomes unmanageable.

4.3.2 Effects of composition on absorption rate and capacity

The amount of CO_2 that could be absorbed was shown to vary based on the concentration and composition of the capture solvent (Table 4.1). Increases in the concentration of capture agent generally resulted in diminishing returns. For example, comparison of the two equimolar mixtures containing respectively: 1 M MEA/1 M KOPh; and 2 M MEA/2 M KOPh of each base, respectively shows that although a higher concentration of CO_2 was absorbed when more capture agent was present, the amount of CO_2 absorbed in proportion to the amount of capture agent used (molar capture efficiency) was reduced from 82% to 66%.

Compositions in which the concentration of KOPh was greater than that of MEA, containing respectively: 1 M MEA/1 M KOPh; and 1 M MEA/3 M KOPh demonstrated a higher CO_2 capacity solutions containing the same total concentration of base but a higher proportion of MEA. For example, the solution of 1 M MEA/3 M KOPh absorbed up to 3.50 M of CO_2 (88%

absorption) compared to the solution of 2 M MEA/2 M KOPh which reached a maximum of only 2.65 M of CO_2 (66% absorption). This is likely due to promotion of bicarbonate formation by the additional phenoxide, leading to a higher maximum absorption of CO_2 due to the advantageous stoichiometry of this product.

The initial rate of CO_2 absorption was estimated from the gradient of CO_2 loading with time, using a linear extrapolation through the origin. This rate appears to be dependent mainly on the concentration of MEA, and is not measurably affected by changes in KOPh concentration. This is demonstrated by the fact that increases in MEA concentration led to a faster rate, but increases in phenoxide concentration did not, even if this greatly increased the total concentration of capture agent. Such behaviour is consistent with previously-published kinetic studies into CO_2 capture by MEA, which showed that the rate of carbamate formation, dependent upon MEA concentration, is the fastest pathway of CO_2 absorption by a wide margin.[155] The rate data collected in this work suggests that the addition of a bicarbonate-forming reagent such as potassium phenoxide does not supplement the initial rate of absorption, and therefore a substantial amount of MEA is still required in order to achieve a viable absorption rate, at least at low CO_2 concentrations.

4.3.3 Speciation analysis

Closer examination of the species formed by carboxylation of phenoxide/MEA blends shows a loosely similar speciation pattern to that already observed in 5 M MEA, but with a general increase in the concentration of bicarbonate. Generally speaking, carbamate was found to be the principal carboxylated species when relatively little CO_2 had been absorbed, but the concentration of bicarbonate became significant as more and more CO_2 was absorbed. Solutions containing concentrations of MEA equal to or less than the concentration of KOPh produced a marginally larger proportion of bicarbonate than 5 M MEA, but do not otherwise differ significantly from the speciation seen in that capture solvent – as exemplified in the performance of the 1 M MEA/1 M KOPh (Figure 4.2) and the 1 M MEA/2 M KOPh solutions (Figure 4.3).

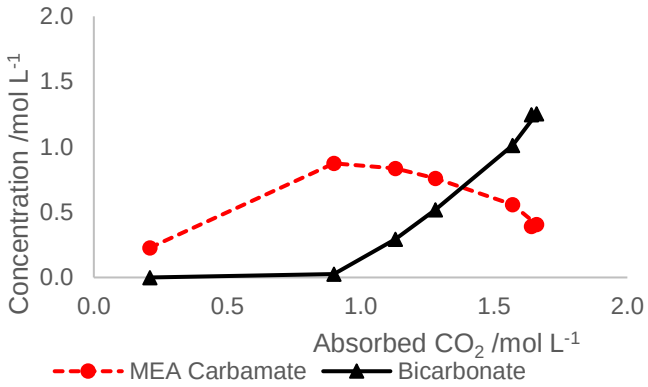

Figure 4.2: Carboxylated species formed by absorption of CO_2 into solutions containing 1 M MEA and 1 M KOPh.

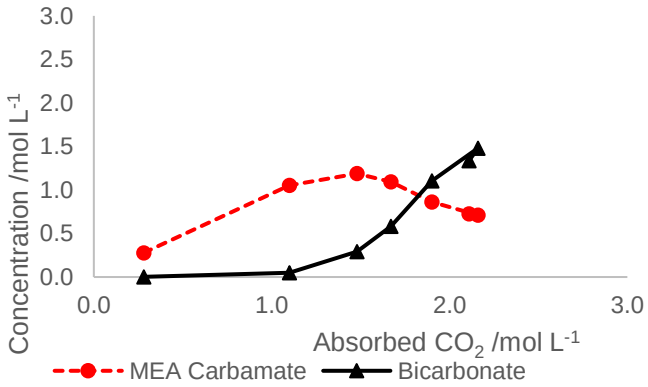

Figure 4.3: Carboxylated species formed by absorption of CO_2 into solutions containing 2 M MEA and 1 M KOPh.

Conversely, solutions prepared using an excess of KOPh over MEA exhibited much higher concentrations of bicarbonate in the early phases of the reaction, such that bicarbonate was a significant absorption product over the entire range of CO_2 concentrations. This behaviour is likely to be strongly advantageous for CCS applications, since the enthalpy of decarboxylation of bicarbonate is significantly lower than that of an equivalent carbamate. The presence of bicarbonate at low concentrations would therefore allow efficient CO_2 capture with only a limited contact time with the gas stream being required, reducing the capital costs that would otherwise be necessary for a sufficiently large absorption column.[50]

The high concentration of bicarbonate in solutions containing an excess of KOPh also accounts for the higher maximum CO_2 concentrations observed in these solutions, due to the advantage of the 1:1 stoichiometry of bicarbonate formation over the 2:1 stoichiometry associated with carbamate formation. This difference in stoichiometry may also underlie the divergent behaviour

of solutions containing an excess of phenoxide. Formation of carbamate requires 1 mole of carbamate-forming amine as well as 1 mole of base, whereas formation of bicarbonate requires only 1 mole of base. Hence, the maximum concentration of carbamate that can be obtained is equal to either the concentration of amine, or half the total concentration of base (whichever is lowest).

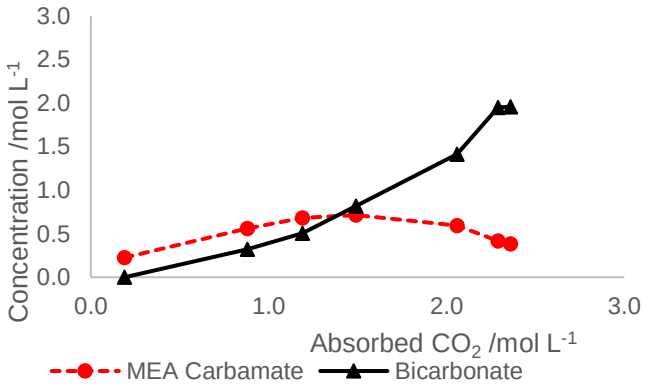

Figure 4.4: Carboxylated species formed by absorption of CO_2 into solutions containing 1 M MEA and 2 M KOPh.

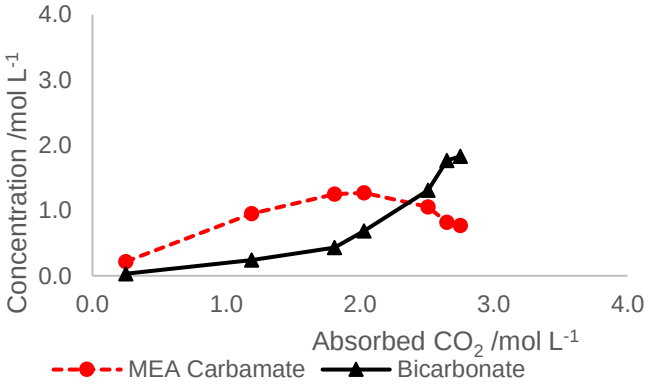

Figure 4.5: Carboxylated species formed by absorption of CO_2 into solutions containing 2 M MEA and 2 M KOPh.

In solutions where the amine comprises half or more of the total base, the limit on carbamate concentration is 50 mol% of the total, and changing the proportion of amine within this region does not affect that limit. However, when the proportion of amine is below 50% of total base, the maximum concentration of carbamate also falls below 50% as it is now constrained by the amount of amine available. Thus, from solution composed of 1 M MEA/2 M KOPh, the maximum amount of carbamate that can be formed is only 33 mol%, and this limit drops further to 25% in the

solution containing 1 M MEA/3 M KOPh. Examination of Figure 2.3 confirms that these limits are indeed approached and not exceeded.

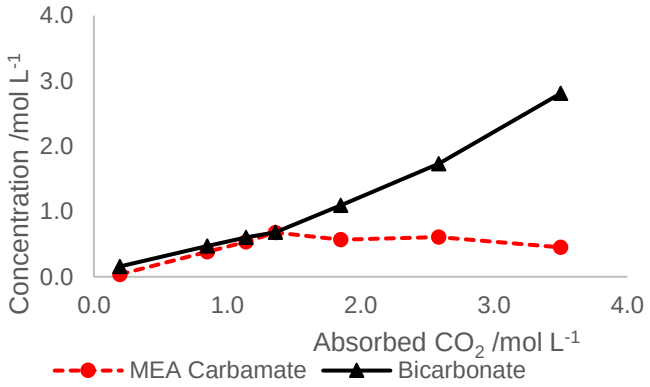

Figure 4.6: Carboxylated species formed by absorption of CO_2 into solutions containing 1 M MEA and 3 M KOPh.

Consideration of the stoichiometry therefore accounts for the relatively low proportions of carbamate that are formed, and the rapidity by which this maximum is reached. However, this alone is insufficient to explain the relatively high concentration of bicarbonate that is present *before* the limit on carbamate is reached. When CO_2 is absorbed into 5 M MEA, the concentration of bicarbonate remains very low until no more carbamate can be produced, but this is not the case for our solutions containing high proportions of phenoxide. Since the pK_a of phenol (9.95) is slightly higher than that of MEA (9.5) one possibility is that the increased basicity of the solution slightly favours bicarbonate formation over carbamate. This may occur either directly (phenoxide-promoted hydration of CO_2 being slightly more favourable than the equivalent reaction for MEA) or indirectly, by deprotonation of bicarbonate to form carbonate. This would remove bicarbonate from its equilibrium with carbamate,[66,67,155] thus pulling the equilibrium away from bicarbonate.

4.4 Comparison with amine blends

In order to test the hypothesis that the higher pK_a of phenoxide affects its CO_2 capture performance, a comparative study was undertaken using other amines commonly used in CO_2 capture studies. This also aimed to investigate whether the phase separation observed in the phenoxide-containing systems has a significant effect, as these amines do not exhibit such behaviour.

Table 4.2 shows a comparison of the CO_2 capture performance of blended-amine capture solvents studied in Chapter 3 with that of the MEA/phenoxide blend of the same concentration. The observed speciation throughout carboxylation of these solutions is shown in Figure 4.7 below.

Table 4.2: Summary of the rate and capacity for CO_2 absorption into aqueous solutions containing 1 mol L^{-1} of A and 3 mol L^{-1} of B.

Entry	A (1 mol L^{-1})	B (3 mol L^{-1})	Abs. %[a]	Initial rate[b]	Absorbed CO_2 (mol L^{-1})
1	MEA	MDEA	72	0.13	2.90
2	MEA	AMP	75	0.20	2.52
3	PZ	AMP	70	0.13	3.51
4	MEA	KOPh	88	0.17	3.50[c]

[a] *Maximum mol% CO_2 absorbed relative to capture agent used.*
[b] *mol L^{-1} min^{-1}. Calculated from a linear extrapolation of initial slope of a plot of absorbed CO_2 against CO_2-liquid contact time.*
[c] *Maximum CO_2 concentration measured via gasometric method. Carboxylation conditions: 25 °C, 30 mL sample volume, CO_2 flow 0.3 L min^{-1} for 90 min.*

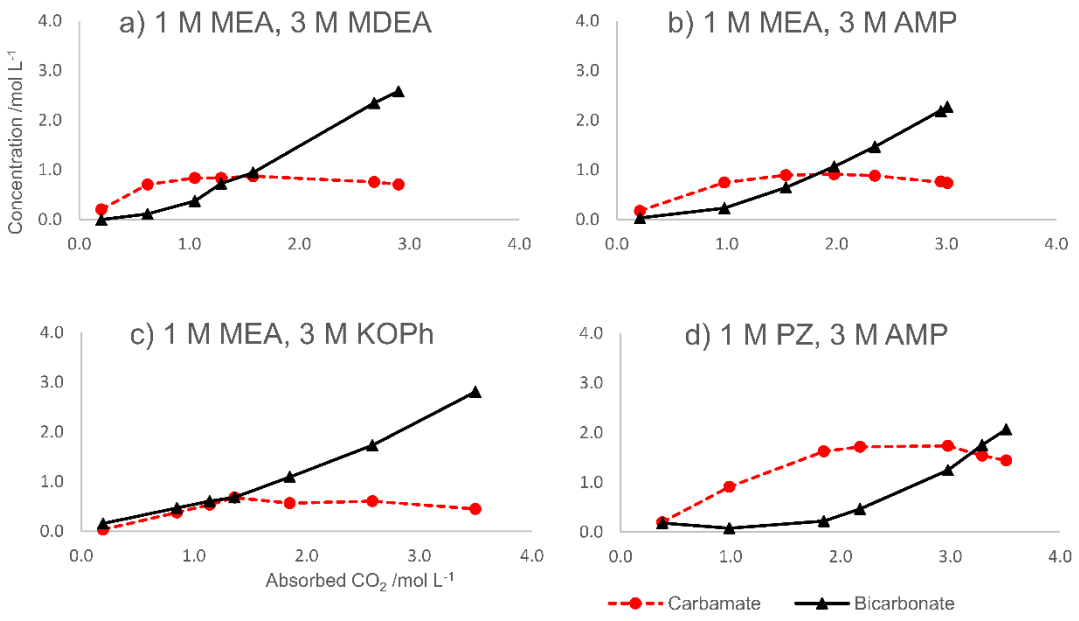

Figure 4.7: Carboxylated species formed by absorption of CO_2 into solutions containing 1 mol L^{-1} of A and 3 mol L^{-1} of B, where A and B are, respectively: a) MEA and MDEA; b) MEA and AMP; c) MEA and KOPh; d) PZ and AMP. All solutions studied at 25 °C and also contained 5 mmol L^{-1} DSS as an internal ^1H NMR standard. Note that in the case of the piperazine solution, "carbamate" considers the total amount of carbamate functional groups in solution, though there are several carbamate-containing species.

In comparison with the equivalent phenoxide-containing solution (Table 4.2, entry 5), two of the blended amine solutions (the MEA/MDEA and PZ/AMP blends) produced a noticeably slower initial rate of absorption, whereas that for the MEA/AMP blend (entry 2) was more comparable to the phenoxide blend. The CO_2 capture performance of the phenoxide solution was, however, significantly better than any of the amine solutions at higher CO_2 concentrations, resulting in a much higher molar capture efficiency (88% of total base concentration, compared to a maximum of 75% among the blended amines). No precipitation of bicarbonate was observed in the amine

blend solutions, whereas the phenoxide solution produced a biphasic liquid with substantial $KHCO_3$ precipitate as previously described.

The observed speciation in the phenoxide solution is also significantly more bicarbonate-focused than in any of the amine blends (Figure 4.7), demonstrating an initial absorption phase wherein approximately equal amounts of carbamate and bicarbonate are formed, followed by a latter phase (>1 mol L^{-1} CO_2 absorbed) wherein bicarbonate predominates.

Since the pK_a values of MDEA and AMP are quite different to phenoxide (Table 4.3), this would imply that the relatively high bicarbonate concentration at low CO_2 concentrations is not necessarily caused by the non-carbamate-forming base having a high pK_a. In particular, phenoxide and AMP have similar basicities, and yet observed speciation in the MEA/AMP blend is inferior to that of the MEA/KOPh blend with less bicarbonate produced.

Table 4.3: pK_a values (25 °C, aqueous) for conjugate acids of capture agents used.

Compound	pK_a
MEA	9.44[156]
Phenoxide	9.95
MDEA	8.57[157]
AMP	9.68[156]
PZ[a]	9.73[158]

[a]*First pK_a value.*

The origin of the very high maximum absorption of the phenoxide solution is intriguing. A possible explanation for this is its multiphasic behaviour; removal of the conjugate acid (phenol in this case) to a separate phase may provide sufficient driving force for CO_2 absorption to continue. Due to the slow rate of CO_2 absorption at high CO_2 concentrations, the maximum possible CO_2 concentration may not be industrially relevant, however, as reaching this would require excessively long gas-liquid contact times.

4.5 Conclusions

This work has shown that the CO_2 absorption performance of potassium phenoxide-MEA blends is comparable to that of other amine blends at the laboratory scale. Blends incorporating phenoxide demonstrated similar or better absorption rates, similar speciation, and higher maximal CO_2 loading than those incorporating other non-carbamate-forming amines. Phenoxides could therefore offer a viable alternative to tertiary amines in blended solutions. The two-phase behaviour which these compositions exhibit is interesting and may offer benefits when employed on a larger scale, where absorption kinetics are often mass-transfer limited. When employed on a packed column, the higher solubility of CO_2 in phenol than water may aid in gas-liquid transfer, as the CO_2 could dissolved first in phenol before crossing into the aqueous phase and reacting with capture agents.

However, phenoxide cannot fully replace amines in capture solvents, as a carbamate-forming amine is still required in order to achieve a viable rate of absorption. Hence, the problems of amine corrosion and degradation, nitrosamine emissions and high energy costs remain unsolved. A truly amine-free method of CO_2 capture is needed in order to solve these issues, but appears unlikely to be achieved using phenoxide.

5 CO_2 Capture using pK_a-Swing Absorption

5.1 Introduction

As has been illustrated across the preceding chapters, improvements to amine-based carbon dioxide capture technologies in recent times have tended to be incremental in nature. Heat duty requirements have not notably advanced since the beginning of the 21st century, and more recent research has produced a diverse array of amine solvents but few significant cost reductions.[15] Overcoming such cost pressures are of critical importance to the widespread adoption of post-combustion CO_2 capture, since the process adds significantly to the operating costs of power production without generating any significant financial return.

Hence, many researchers have sought out alternative approaches, some of which were outlined in Chapter 2. However, none of these has yet proven suitable for use in post-combustion capture, owing to their high complexity and/or poor tolerance of the conditions involved. While prolonged development may eventually overcome these issues, CCS technology is needed on an industrial scale as urgently as possible. IPCC forecasts suggest that without substantial implementation of CCS in the coming decades, climate change mitigation will be significantly more difficult and costly to achieve.[12]

5.1.1 Basicity-swing absorption

A new capture solvent-based technology that may provide an answer to these challenges has been described by C-Capture Ltd.[159] This approach proposes using mixed organic/aqueous solutions of carboxylate salts as a CO_2 absorbent. Such a solution would be completely amine-free, thereby eliminating the environmental and toxicological issues associated with the use of such chemicals, as carboxylates are comparatively benign. Since carboxylates are already highly oxidised species, they are not susceptible to oxidation in the manner of amines, which may provide a much more stable capture solvent than previously considered possible. Furthermore, simple carboxylic acids

are already bulk commodity chemicals; hence a carboxylate-based process would be inexpensive to scale up to the very large quantities that CCS would require.

5.1.1.1 Solvent dependence of pK_a

In aqueous solution, most carboxylates are insufficiently basic to facilitate the absorption of carbon dioxide. However, pK_a is a solvent-dependent quantity, and the pK_a of a carboxylic acid is especially sensitive to the nature of the solvent in which it is dissolved, becoming less acidic (and thus the carboxylate becoming more basic) in less polar environments.[160] As an illustration, Table 5.1 shows the pK_a of acetic acid in various solvents, showing that its acidity varies by many orders of magnitude depending upon its solvation environment.

Table 5.1: Acid dissociation constant (pK_a) of acetic acid in various solvents, as measured by Raamat et al. (H_2O, MeCN),[161] Rived et al. (MeOH),[162] and Bordwell et al. (DMSO)[163]

Solvent	pK_a of acetic acid
H_2O	4.76
MeOH	9.72
DMSO	12.3
MeCN	23.51

Ions are far more sensitive to their solvation environment than neutral molecules, as they are stabilised by interactions with polar solvents. Water in particular is an exceptionally good solvent for ions, and therefore a given ion is usually much more stable in water than another solvent. Thus, the balance of ions in the equilibrium is a major factor affecting the pK_a of an acid across different solvents. When discussing the dissociation equilibrium of a Brønsted-Lowry acid, by definition the dissociated (conjugate base) side of the equilibrium always contains a charge in the form of a proton. Therefore, whether an acid-base equilibrium changes the number of ionic species in solution depends on whether the acid form is neutral (as in a carboxylic acid or phenol) or charged (as in an ammonium salt).

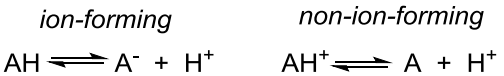

Scheme 5.1: Illustration of acid-base equilibria which form additional ions and those which do not.

The pK_a of a neutral acid is therefore far more sensitive to solvation properties than a charged acid, since the effect of poor ion solvation is to suppress dissociation. For this reason, acetic acid

is a much weaker acid in organic solvents than it is in water, with the difference being even more pronounced in less polar solvents (Table 5.1). Conversely, the pK_a of triethylammonium is relatively insensitive to the solvent in which it is dissolved (Table 5.2) since ionic species are present on both sides of its dissociation equilibrium and therefore any disfavouring effect on the formation of such species is largely cancelled out.

Table 5.2: Acid dissociation constant (pK_a) of triethylammonium (Et_3NH^+) in various solvents, as measured by Rived et al. (H_2O, MeOH),[162] *Kolthoff et al. (DMSO),*[164] *and Kaljurand et al. (MeCN).*[165]

Solvent	pK_a of triethylammonium
H_2O	10.67
MeOH	10.78
DMSO	9.0
MeCN	18.82

5.1.1.2 Control of pK_a using composition of mixed solvents

In mixed-solvent solutions, pK_a tends to be intermediate between the extremes of the pure solvents, but this is a complex relationship, governed by the solvation of every species involved in the equilibrium. For example, the pK_a of amines in water/alcohol mixtures has been observed to be lower than in either of the pure solvents, owing to preferential solvation of the free amine in alcohol combined with stabilisation of ionic species by water. Conversely, carboxylic acids are always less acidic in water-solvent mixtures than in water. These relationships are exemplified in Figure 5.1, contrasting the pK_a of acetic acid and the anilinium ion in differing mixtures of water and ethanol.

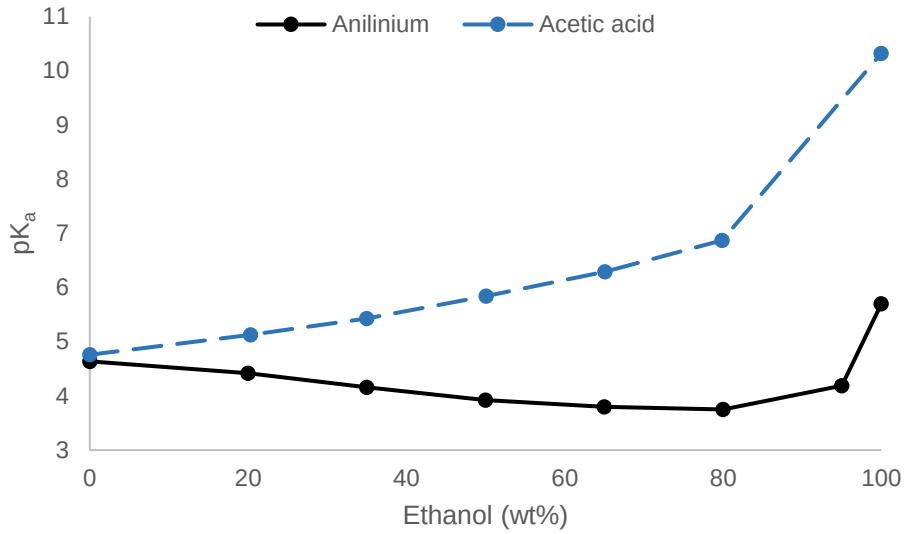

Figure 5.1: pK_a of anilinium and acetic acid in water/ethanol mixtures, as reported by Gutbezahl and Grunwald (anilinium);[166] *and Grunwald and Berkowitz (acetic acid).*[167]

Due to this behaviour, pK_a values in mixed solvents cannot be trivially predicted by interpolation, but must be directly measured. Perhaps due to the vast number of possible solvent/solvent/solute combinations, experimental data on such solutions is limited and tends to be specific to particular systems that were of interest to the authors of a given study.[160,168]

5.1.1.3 Hypothesised involvement of solvation-induced pK_a changes in CO_2 absorption by unconventionally weak bases

While the acid-base behaviour of carbon dioxide in aqueous solution is well-understood due to its role in numerous biological and inorganic systems, surprisingly little is known about the same in conjunction with organic solvents. In this case, mixed organic/aqueous solvent mixtures are of most interest, since the hydration of CO_2 to carbonic acid cannot occur in the absence of water.

Prior work by C-Capture Ltd. has shown that mixed organic/aqueous solutions of carboxylate salts absorb substantial amounts of carbon dioxide, in defiance of the carboxylates' low aqueous basicity. This phenomenon has been demonstrated across a wide range of carboxylates, organic solvents and concentrations.[159] Absorption produces the carboxylic acid and a bicarbonate salt (Scheme 5.2), indicating an acid-base reaction similar to that described for tertiary amines in Chapter 2.

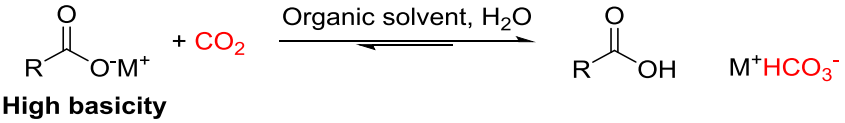

Scheme 5.2: Absorption of CO_2 by carboxylate salts in mixed organic/aqueous solution. The ratio of solvent to water may be 3:1 or greater.

This reactivity strongly implies that the pK_{a1}' of CO_2 is relatively insensitive to solvation in comparison to the conventionally expected behaviour of carboxylic acids, and thus in certain solvent mixtures, containing only limited amounts of water, the equilibrium between bicarbonate and the carboxylate can be reversed in order to induce gaseous absorption.

Similar reactivity has been known to exist in carboxylate-containing ionic liquids in the presence of water for some time, since the first report by Quinn et al. in 1995 (Scheme 5.3a).[169,170] Quinn et al. also observed the same reactivity in fluoride-containing ionic liquids (Scheme 5.3b), a fact which supports a pK_a-swing explanation since the pK_a of hydrogen fluoride is known to be extremely susceptible to solvation, more so even than carboxylic acids (for example, the pK_a of HF in DMSO is 15, compared with 3.17 in water).[171] A number of more recent studies have found stoichiometric CO_2 absorption into 1,3-alkylimidazolium carboxylate ionic liquids (Scheme 5.3c), though in this case the situation is complicated by the availability of a second absorption pathway in strictly water-free conditions, defined by carbene-like reactivity of the imidazole (Scheme 5.3d). Since acid-base absorption to form bicarbonate requires water, the two pathways do not coexist, but the same ionic liquid may absorb CO_2 in both the presence and absence of water. In both cases, however, the carboxylate anion plays a key role as a proton acceptor.[172–175]

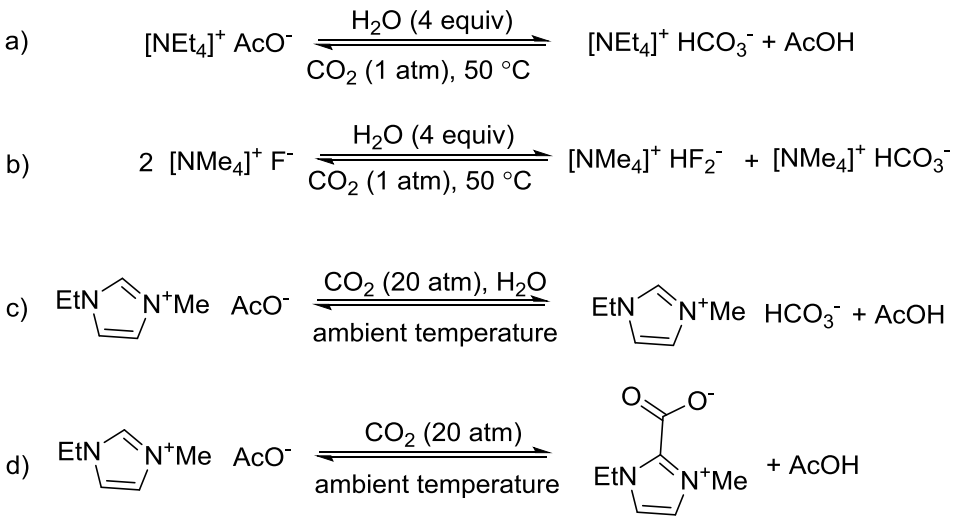

Scheme 5.3: Selected examples of CO_2 chemisorption by ionic liquids exploiting unconventional basicity of the anion: a) and b) reported by Quinn et al.,[169] *c) and d) reported by various authors in multiple similar ionic liquids, products elucidated by Gurau et al.*[174]

Besides the efforts of C-Capture Ltd., it appears that no published work has sought to extend this reactivity from the realm of ionic liquids to more orthodox solutions. Ionic liquids are relatively unproven on a large scale and suffer from many disadvantages if they are to be applied to CO_2 capture, in particular their expense, their viscosity and susceptibility of many of their properties to contaminants;[42] issues which may be completely avoided through the use of simple alkali metal salts dissolved in conventional organic solvents mixed with water.

5.1.1.4 Proposed pK_a-swing desorption by addition of water

Such a means of CO_2 capture may be followed by conventional thermal desorption, as discussed in previous chapters. However, it also allows for a most unusual means of desorption – the addition of water. This changes the solvent composition, consequently pushing the relevant pK_a values back toward aqueous values. CO_2 is then released *via* another acid-base reaction between the carboxylic acid and bicarbonate (Scheme 5.4).[174] This means that unlike other capture solvents, both CO_2 absorption *and* desorption are thermodynamically favoured, exothermic steps. Thermodynamically favoured desorption is a significant advantage over existing systems, since this permits desorption of CO_2 to be carried out at elevated pressure, minimising subsequent compression costs.[159]

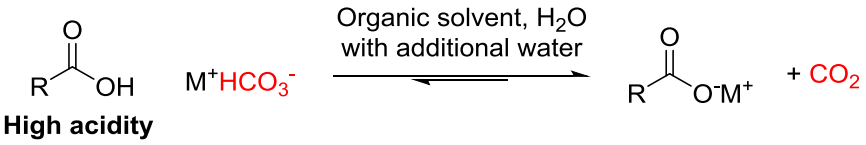

Scheme 5.4: Desorption of CO_2 from carboxylate-based capture solvent, provoked by the addition of water.

Desorption of CO_2 regenerates the carboxylate salt, but produces a solution containing more water than the initial capture solvent. In order to reuse the solvent, an additional regeneration step is therefore needed, consisting of the removal of this excess water. This is thermodynamically disfavoured and therefore it is likely that the main operating cost of the process will arise from this step.

The removal of water from solvents has been of great interest throughout the history of chemistry and numerous industrially mature means of doing so are available. Distillation is the more traditional approach, with newer membrane-based technologies offering lower energy costs. Whichever approach is used, it is important to minimise loss or degradation of the solvent components in order to reduce operating costs. A schematic of the whole capture process is shown in Figure 5.2, showing how the solvation-controlled variation of the pK_a of the carboxylic acid relative to that of CO_2 would control the processes of absorption and desorption.

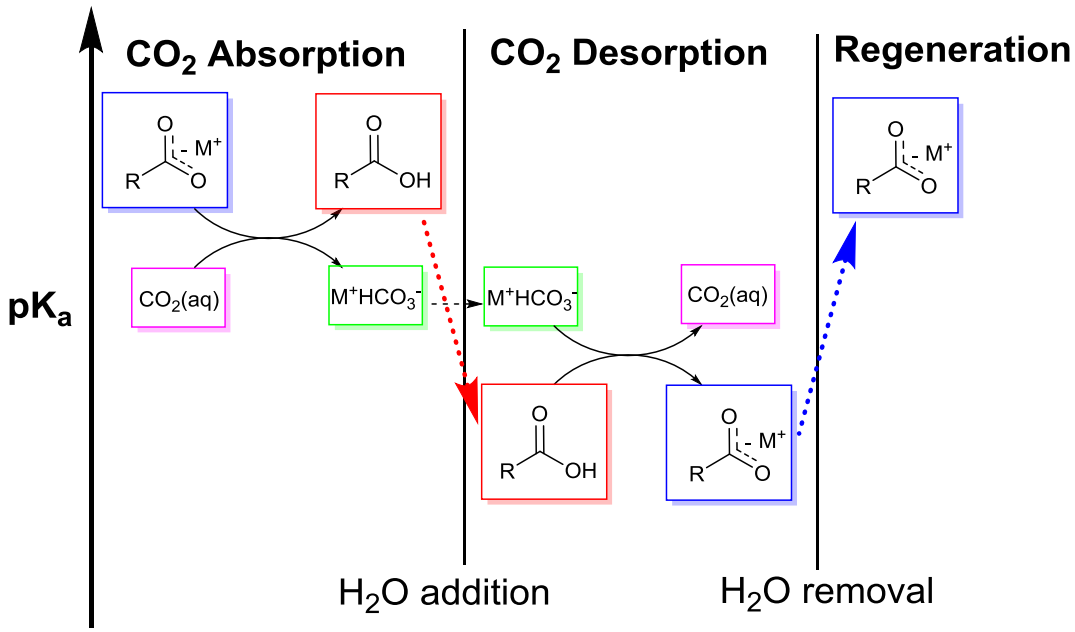

Figure 5.2: Diagram of the key steps involved in the C-Capture process for CO_2 capture, illustrating hypothesised shifts in pK_a as the composition of the solvent changes.

Though the relative insensitivity of the pK_a of CO_2 to its solvation environment is implied by the reports cited above, it must be emphasised that the acid-base chemistry of CO_2 outside aqueous solution is very poorly understood and no values for its pK_a in other solvent systems have been reported. A thorough understanding of this chemistry will be necessary in order to facilitate effective implementation of the pK_a-swing CO_2 capture approach described herein, across a range of different compositions. The solvent composition is likely to change throughout the process, not only due to intentional water addition and removal but also during the CO_2 absorption (which consumes an equimolar amount of water) and CO_2 desorption (which releases the same) steps, and tolerance of the capture solvent to such variations needs to be appreciated. Furthermore, due to the great diversity of available nonaqueous solvents, an understanding of the characteristics that enhance the effectiveness of pK_a-swing CO_2 capture would be a great aid to capture solvent development.

Hence there is a clear need for an experimental study of pK_a values relevant to CO_2 capture in mixed solvents. Even aside from the poor understanding of nonaqueous aCO_2 acidity, existing experimental data on carboxylic acid pK_a values in mixed solvents is lacking, due to the sheer number of possible combinations. Nor can this gap be adequately filled by computational methods, as calculated pK_a values have an associated error on the order of multiple pK_a units, which is unacceptably large for this purpose.[176,177]

5.1.2 Relevant carboxylate pK_a values in the scientific literature

Though the general lack of relevant experimental data on pK_a values in organic/aqueous solvent mixtures has already been noted, several studies have been carried out using simple carboxylic acids in various solvent mixtures. Alcohols, particularly methanol, are especially well-studied since they are comparatively easy to work with, being protic solvents with somewhat similar properties to water.

Figure 5.3 shows the pK_a of formic, acetic and propionic acids in various methanol/water mixtures, as determined potentiometrically by Grunwald and coworkers.[178] The same research group also measured the pK_a of butyric acid in the same solvents, but this is not shown in the

figure as the pK_a of butyric acid is extremely close (within 0.06 pKa units or less) to that of propionic acid.

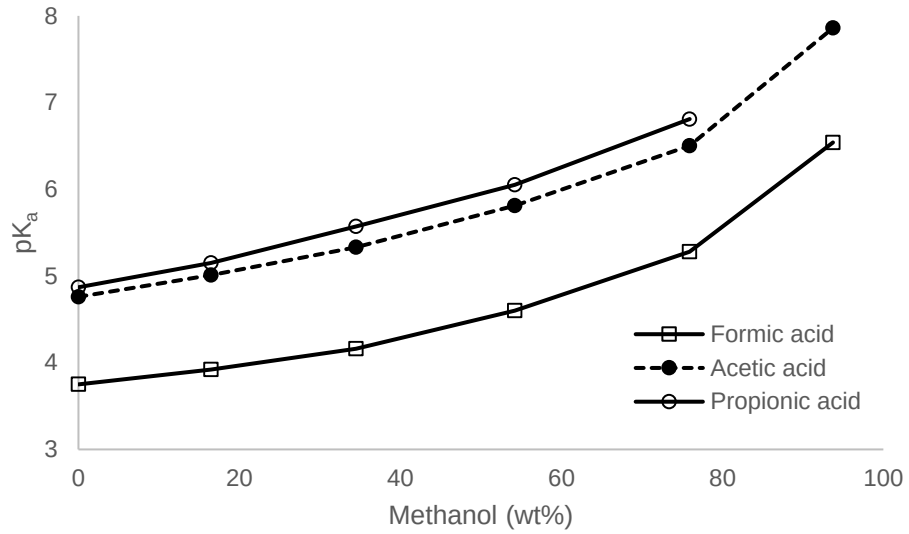

Figure 5.3: Acid dissociation constants of formic, acetic and propionic acids, measured in methanol/water mixtures at 25 °C by Grunwald and coworkers.[178]

It is notable that the pK_a of these acids is much more strongly affected by solvent composition at the predominantly organic end of the scale than the aqueous. This is the effect of preferential solvation of the carboxylate by water. Carboxylate is largely unaffected by solvent composition so long as there is sufficient water to form a solvation shell around it, and it is only when the proportion of methanol becomes sufficiently overwhelming to take part in carboxylate solvation that the pK_a begins to rise significantly.[168]

Figure 5.4 shows published values for the pK_a of acetic acid in aqueous/organic mixtures prepared from different organic solvents.[167,178,179] It shows the similarity between the alcoholic solvents, except in very dry compositions where direct alcohol-solute interactions are more likely. The pK_a values for dioxane are significantly higher. Dioxane cannot stabilise carboxylate by hydrogen-bond donation in the manner of protic solvents, which pushes the acid-base equilibrium toward the free acid.

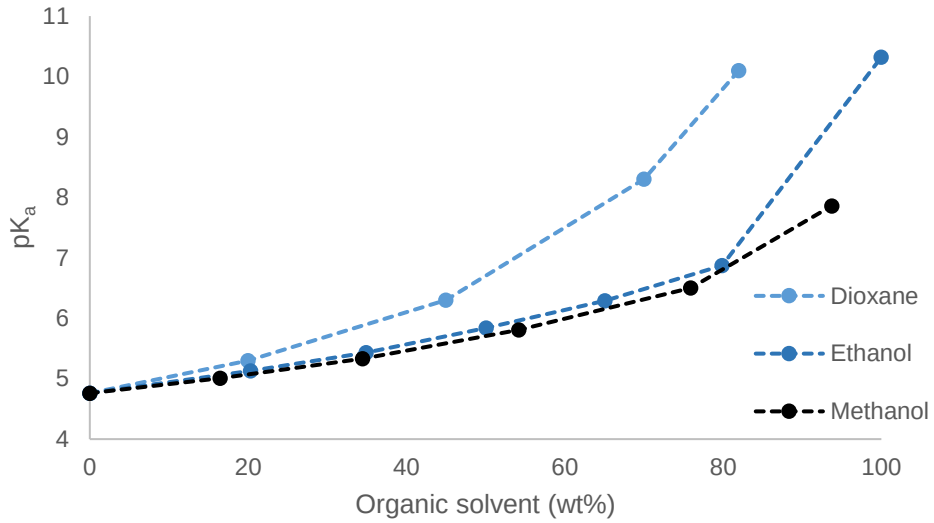

Figure 5.4: Acid dissociation constant of acetic acid, measured at 25 °C in mixtures of water and one of three different organic solvents – methanol,[178] *ethanol*[167] *and 1,4-dioxane.*[179]

The relative antiquity of these pK_a studies bears mentioning, despite their frequent citation,[160,168,180] with the oldest having been published in 1936 and the most recent in 1955. Following the advent of more modern instrumentation and theoretical understanding, their accuracy is somewhat open to question, thus providing further impetus for a new experimental study in this area.

5.2 Measurement of carboxylate pK_a in aqueous/organic solvent mixtures

Standard approaches to measurement of pK_a employ idealised conditions which diverge significantly from those that may be found in the actual operation of a CO_2 capture solvent. For pK_a measurement, high-purity reagents at relatively low concentration and a standard temperature of 298 K (25 °C) are routine, whereas true industrial conditions would involve high concentrations of low-purity reagents, operating at temperatures of 40 °C or higher. This apparent contradiction is due to the fact that a pK_a measurement is not an attempt to model an entire system, but the physical measurement of a single thermodynamic property, and such idealised conditions are intended to eliminate confounding variables which would render that measurement impossible, and to provide information that is generalisable rather than that which is specific to a particular concentration, impurity level, experimental protocol etc.

The issue of temperature deserves special mention. There is little intrinsic experimental advantage to carrying out measurements at 25 °C rather than 40 °C or some other temperature (the only benefit being a small improvement in ease of temperature control due to remaining close to ambient temperature). However, the vast bulk of pK_a and thermodynamic studies are carried out using 25 °C as a "standard temperature" even if other temperatures are also examined. Hence, the advantage of carrying out pK_a measurements at this temperature is that this facilitates comparison with existing scientific literature, which must be considered a priority in order to integrate new findings with pre-existing knowledge.

5.2.1 Methods

The classic means of measuring pK_a is *via* potentiometric titration of the acid in question against a strong base, or of the conjugate base against a strong acid (the results are equivalent). A diverse array of other methods exists, utilising conductometry, UV/Vis spectroscopy, HPLC, ^{1}H NMR, electrophoresis and many other techniques, but the principle underlying all of these approaches is the same: measuring the concentrations of acid and conjugate base as a function of pH.[181,182]

For this study, the potentiometric approach was deemed to be most suitable, as it is very well-understood and widely applied, and many of the other common approaches are unsuitable for measuring the pK_a of carbon dioxide. For example, carbonates lack a chromophore for UV/Vis analysis, nor (as dealt with extensively in the preceding chapters) do they have a non-exchanging proton for ^{1}H NMR analysis.

Aqueous potentiometric titrations are straightforward to devise, but the challenge inherent to this work was to adapt the method for use in systems which are mostly not aqueous, as many potential pitfalls present themselves. Most notably, a pH electrode calibrated in aqueous buffer solutions will not produce reliable measurements when placed in a different solvent, and therefore a different means of calibration is necessary. Furthermore, pH electrodes are less effective in solutions of low conductivity, and a glass electrode intended for aqueous titrations will not function at all in, for example, a dry DMSO solution with no electrolyte.[168]

Fortunately, completely dry organic solutions are of little interest to this work, as at least one equivalent of water is necessary in order to absorb CO_2 as bicarbonate. Thus, the complex and error-prone techniques devised to deal with pK_a measurements in such systems, such as the use of indicator series, are not necessary in this case. Published work on organic/aqueous mixtures shows that the methods and instruments developed for aqueous solutions can be used for these mixtures, provided the appropriate adjustments are made. The adjustments necessary are discussed in detail below. In short, solute-solute interactions (dependent on ionic strength and concentration) are much more pronounced outside aqueous solution and must be minimised. Additionally, the electrode must be calibrated for the solvent mixture in question, and increased ionic strength facilitates electrode function by improving the solution conductivity.[183–185] The conditions employed for the titrations in this work are summarised in Scheme 5.5.

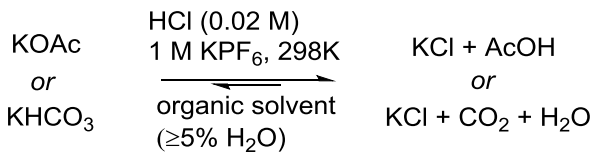

Scheme 5.5: Reaction scheme of potentiometric titrations for pK_a determinations of acetic acid and carbon dioxide in this work.

Experimental approaches to pK_a measurement in nonaqueous systems are discussed in more complete detail by B. G. Cox in *Acids and Bases: Solvent Effects on Acid-Base Strength*.[168]

5.2.1.1 Titrant and analyte composition

For this work, titration of the conjugate base against a strong acid is most appropriate. That approach is absolutely necessary for determining the pK_a of carbon dioxide, as a known solution of e.g. potassium bicarbonate can be prepared and titrated, but the same cannot easily be done for carbonic acid or CO_2 gas. Carboxylic acids could in principle be studied either way (and indeed titration of the free acid with strong base is most common in published literature),[178] but the carboxylate salt is titrated herein, with the aim of providing pK_a values that are as comparable as possible with those measured for bicarbonate.

Potassium salts were used throughout due to the high aqueous solubility of potassium bicarbonate, which would be an important feature for a CO_2 capture system where bicarbonate is the only

capture product, in order to minimise or avoid precipitation. HCl was used as the strong acid titrant, being routinely used for such measurements. Although the pK_a of HCl is known to increase in nonaqueous solutions, it remains sufficiently acidic for use as a strong acid in the solutions under study due to the presence of water.

It is critically important for the properties of the solution, other than pH, to remain approximately constant throughout the titration, in order to eliminate confounding variables. Ionic strength is of particular concern, as variations in ionic strength change the activity of the ions in solution and therefore the observable pK_a. Two approaches to this exist for aqueous titrations – either the titration is performed at low ionic strength, and the activity coefficients of the relevant species directly calculated using any of various models that have been constructed for the purpose (the classic being the Debye-Hückel equation, with much more complex and advanced models in use for modern work); or the ionic strength is maintained at a constant level by the addition of a comparatively high concentration of a simple salt to serve as a non-interacting "background electrolyte", the usual choice being 0.1 M KCl. It is important to note that while these approaches often yield similar results, they are not strictly comparable since measurement takes place in differing environments, using differing assumptions. Despite this fact, both approaches are common in the literature, and pK_a values are routinely quoted without clarification of which method by which they were obtained.[182,186]

Calculation of activity coefficients is an unsuitable approach for titrations in mixed solvents, as the calculation relies on solvent properties (such as their electrical permittivity) that are unknown for the mixture, or model parameters which are not appropriate outside the solvent(s) that the model was intended for. Additional measurement of such properties as the electrical permittivity presents an undesirable complication when dealing with numerous different solvent mixtures. Thus, the constant ionic strength approach was adapted for use in mixed solvents. While KCl is the most commonly used electrolyte for this purpose, it is an inappropriate choice in this work due to the poor (<0.1 M) solubility of KCl in the presence of large amounts of organic solvent.[187] Instead, the background electrolyte chosen for this work was 0.1 M KPF_6. This is both unreactive, stable and soluble in a wide variety of different solvents, while still being relatively small. Other

salts with similar properties, such as potassium tetrakis(3,5-bis(trifluoromethyl)phenyl)borate, possess very large anions which diverge significantly from the simple chloride in behaviour. Potassium hexafluorophosphate has seen use both as an electrolyte in nonaqueous electrochemistry,[188,189] and as a source of hexafluorophosphate, valued in inorganic chemistry as a weakly-interacting counteranion to highly reactive complexes such as Crabtree's hydrogenation catalyst.[190] Hence, this choice should provide the same simple increase in ionic strength as KCl while minimising confounding interactions with itself or other solutes.

It is necessary that titrant and analyte concentrations be as low as practically possible for two principal reasons. Firstly, this minimises the effect of the position of their equilibrium on the overall ionic strength of the solution (since any changes will be insignificant compared to the concentration of KPF_6). Secondly, solute-solute interactions are also minimised. Such interactions are usually of small concern in aqueous solution, as water is an excellent solvent for ions. However, they can become a serious issue when organic solvents are present, since this may provoke the association of dissolved ions into mutually interacting pairs or clusters which effectively "hide" free protons from the pH electrode, leading to misleading measurements. Carboxylates are known to be particularly prone to such clustering.[168] This behaviour is of course highly relevant to CO_2 capture solvents prepared at realistic concentrations (on the order of moles per litre) and will be further discussed in Chapter 6. For the purpose of measuring underlying pK_a values, it

Lower bounds on titrant and analyte concentration are set by the purity of the solvent and the ability to weigh out such amounts accurately. In practice it was found that millimolar concentrations were an acceptable compromise. Redistillation of the organic solvent in question from potassium hydroxide, together with recrystallization of the KPF_6 from water, was necessary in order to eliminate small concentrations of acidic impurities, which overwhelmed initial titrations.

Finally, the concentration of titrant was purposely chosen to be much higher than that of the analyte, in order that the added titrant volume was small in comparison to the total, and thus the

total volume (with attendant confounding effects relating to mixing, heat transfer and dilution/concentration) did not change excessively over the course of the titration.

5.2.1.2 Potentiometric measurements

A combination glass electrode filled with an aqueous solution was used for the measurement of pH. Previous studies have obtained good results with such an electrode in mixed organic/aqueous systems, provided that sufficient time is allowed for the electrode to reach equilibrium with the solution prior to titration.[191]

A potentiometric titration yields a series of electrode potential measurements, from which pH values are calculated from the Nernst equation (see equation (1) below) after calibration for the standard electrode potential of the system. In usual operation in aqueous solutions, these calculations are automatically performed by the instrument based on routine calibration with standard buffer solutions, and therefore a pH value is directly read off by the user. Electrode calibration for mixed solvent systems is not so trivial due to the lack of available standard buffer solutions.

For this work, the *in situ* calibration method of Grunwald was adapted.[178] Grunwald's method is based on the approximation that beyond the equivalence point of the titration,‡ the presence of excess strong acid suppresses dissociation of any weaker acids in the solution (this is untrue when very close to the equivalence point, but an excellent approximation otherwise). Thus, the solution can be treated as if it were neutral at the equivalence point and strong acid added thereafter.

In such strong acid-only solutions, direct calculation of the pH is straightforward, since the strong acid is considered to be completely dissociated and therefore the concentration of H^+ is equal to the concentration of acid. This calculated pH can then be related to the potential measured by the electrode using the Nernst equation:[168]

In general:
$$E = E_0 - \frac{RT}{F}\ln[H^+] \quad (1)$$

‡ This equivalence point was determined prior to (and independently of) electrode calibration using the Gran method described in section 5.2.2, since it is a function of the *shape* of the potential curve rather than its magnitude.

Hence, for the pH electrode:
$$E = E_0 - \frac{2.303RT}{F} pH \quad (2)$$

Rearranging:
$$pH = \frac{(E_0 - E)F}{2.303RT} \quad (3)$$

Wherein E is the measured electrode potential, E_0 is the standard potential of the cell, and F is the Faraday constant (96,485 C mol^{-1}). The figure of 2.303 is a logarithmic conversion factor necessitated by the switch from a natural logarithm to the base-10 used for pH. The purpose of electrode calibration is the determination of E_0, since this is the potential difference between the electrode and the external solvent, and is specific to each different solvent system.

Each titration produced a series of measured potentials beyond the equivalence point (i.e. values for E), together with the pH values calculated from the concentration of acid added beyond the equivalence point. Therefore, a curve of "measured" pH values, calculated from the measured E values using equation (3), could be fitted to the known, concentration-derived pH values by choosing the correct value of E_0 to use in the equation. This was done using simple least-squares fitting in the Microsoft Excel (2013) software package.

Given a value for E_0, pH across the entire titration curve was then computed from the measured E values using equation (3).

5.2.2 Determination of pK_a values of carboxylic acids in various solvent mixtures

The acid dissociation constants of acetic acid in dioxane/water and ethanol/water mixtures were determined by potentiometric titration of potassium acetate against HCl, making use of the protocols set out above. pK_a values were calculated from the titration curves using the Gran method.[192,193] The Gran method is a proven, robust approach that makes use of a series of functions originally derived by Gunnar Gran from the general equations describing titration. For example, the Gran function F_1 for the titration of a monoprotic base with a strong monoprotic acid is defined as:

$$F_1 = (V_0 + v)[H^+] = (v - v_{eq})t \quad (4)$$

Wherein V_0 is the initial volume of the analyte solution, v the volume of titrant added, v_{eq} the volume of titrant added at the equivalence point, and t the titrant concentration. Each Gran

function describes a particular region of the titration curve. F_1 above describes the titration once all base has been added, and in this region a plot of F_1 against titrant volume produces a linear curve which intercepts the x-axis at the equivalence point. Such a plot is therefore useful for the determination of the equivalence volume.

Two Gran functions arise for each equivalence point in the titration. The function that describes the region before complete neutralisation is particularly useful, since its gradient is dependent upon pK_a. For a monoprotic titration, this function is F_2, defined as:

$$F_2 = \frac{(v_{eq} - v)}{K_a} = \frac{v}{[H^+]} \tag{5}$$

Thus, a plot of F_2 against titrant volume will produce a linear curve from whose gradient the pK_a of the analyte can be determined.

The Gran method represents a significant improvement over earlier methods of titration analysis, since it does not rely on data points obtained at the equivalence point (which tend to be both few in number and highly prone to error due to the low buffer strength of the solution at this point). In general it is much more resistant to experimental error than common alternatives, a useful asset for nonaqueous titrations where electrode response may be slow or erratic due to the reduced conductivity of the solution.[182] A full description of the Gran method is provided in section 8.3.3.

Finally, the uncertainty associated with the pK_a measurements presented herein was calculated by error propagation. The accuracy of the pH electrode is somewhat system-specific, and various values have been quoted for this. For this work, a relatively low accuracy of ±0.1 pH units was assumed, based on the fact that the mixed-solvent systems are unfriendly to electrode operation. Hence, the uncertainty of pK_a measurements presented herein was calculated to be ±0.15 pK_a units.

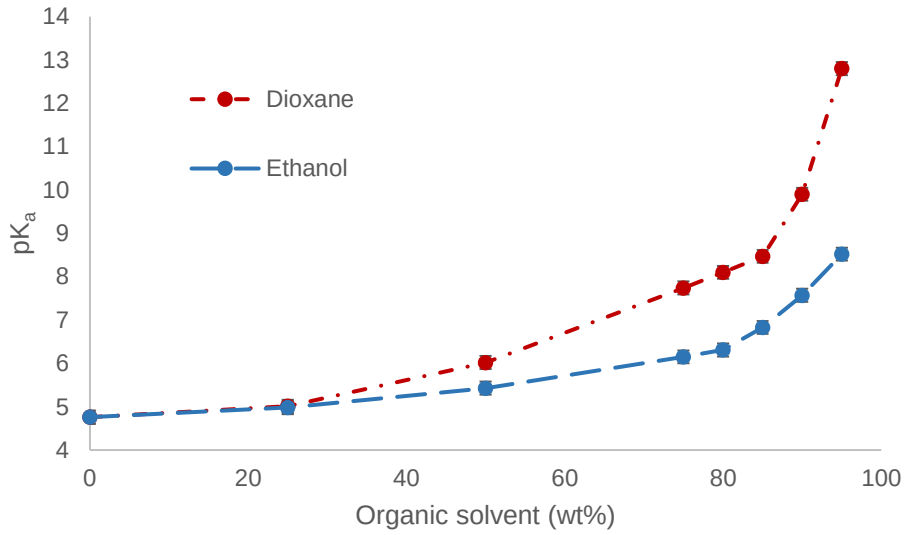

Figure 5.5: pK_a of acetic acid in ethanol/water mixtures and dioxane/water mixtures, as measured by potentiometric titration.

Figure 5.5 shows the measured pK_a of acetic acid in mixtures of ethanol and water at various proportions, alongside the same for dioxane/water mixtures. The preferential solvation effect described earlier is clearly in effect here. At low (<40%) organic proportions, the difference in pK_a value from pure aqueous solution is minimal. On the other hand, as the proportion of organic solvent in solution increases above 80%, the pK_a becomes increasingly sensitive to solvent composition.

The difference in pK_a between the two organic solvent systems is of interest and may be explained in terms of the ability of the organic solvents to stabilise the various species in this equilibrium. Ethanol has the ability to stabilise cations by electron donation from its oxygen centre (Figure 5.6a), and anions *via* hydrogen bond donation (Figure 5.6b). The latter is not possible in aprotic solvents such as dioxane, and thus anions are particularly poorly solvated in dioxane and its aqueous mixtures.

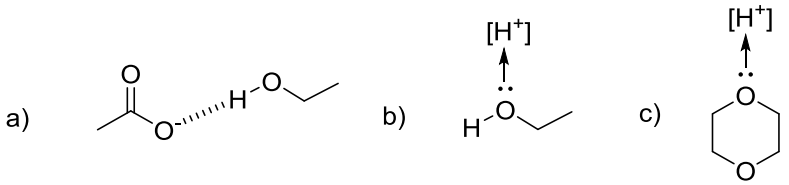

Figure 5.6: Solvent interactions between dissociated acetic acid and ethanol or dioxane solvents: a) hydrogen bonding of ethanol to acetate; b) electron donation from ethanol to solvated proton; c) electron donation from dioxane to solvated proton.

Owing to this effect, the pK_a of acetic acid in dioxane/water mixtures is considerably higher than in ethanol/water mixtures since the protonation equilibrium is driven to the left in order to avoid the unfavourable formation of acetate.

The same measurements were also carried out in mixtures of water with DMSO, ethylene glycol monobutyl ether (EGBE) and diglyme. Taken together, this provides a reasonable spread of high-boiling point solvents that are already in commercial use, as well as ethanol, which is better understood in these types of pK_a studies but too volatile for use in CO_2 capture.

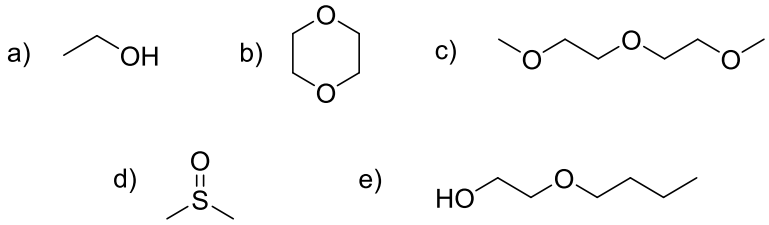

Figure 5.7: Organic solvents used in this investigation: a) ethanol; b) 1,4-dioxane; c) diglyme; d) dimethylsulfoxide (DMSO); e) ethylene glycol monobutyl ether (EGBE).

It is important to minimise solvent volatility, as a low boiling point would lead to considerable loss of solvent from the absorber, rendering it difficult to maintain a steady composition as well as posing a potential environmental hazard unless additional steps are taken to prevent release of solvent vapour.

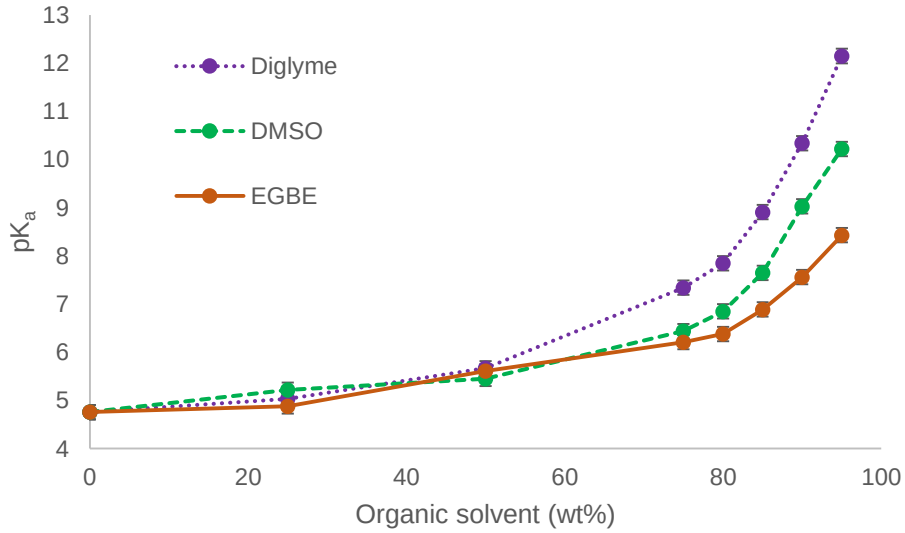

Figure 5.8: pK_a of acetic acid in diglyme/water mixtures, DMSO/water mixtures and EGBE/water mixtures, as measured by potentiometric titration.

The same preferential-solvation pattern is observed in these solvent mixtures (Figure 5.8) as with dioxane and ethanol above. It is noteworthy that the pK_a values measured in EGBE/water mixtures are almost identical to those observed in ethanol/water mixtures (Table 5.3), while being noticeably lower than in all other solvent mixtures studied. The key feature shared by these two solvents is that they are the only protic solvents used in the study. Thus, this supports the earlier suggestion that stabilisation of anions *via* hydrogen bond donation has a key effect on the protonation equilibrium of acetic acid, reducing the pK_a and dwarfing any other effects which may arise from the structural differences between EGBE and ethanol.

Table 5.3: Comparison of measured pK_a values of acetic acid in ethanol/water and EGBE/water mixtures.

Organic solvent (wt%)	pK_a (ethanol/H_2O) ±0.15	pK_a (EGBE/H_2O) ±0.15
0	4.76	4.76
25	4.98	4.88
50	5.43	5.61
75	6.15	6.21
80	6.31	6.38
85	6.71	6.89
90	7.63	7.56
95	8.52	8.43

In the aprotic solvents, significantly higher pK_a values are observed, consistent with the inability of these solvents to adequately stabilise acetate. However, there are clear differences between these three solvents, with acetic acid retaining greater acidity in DMSO than in diglyme and particularly 1,4-dioxane. The similarity of pK_a values observed in the latter two solvents is perhaps unsurprising given the structural similarity of these two ethereal compounds.

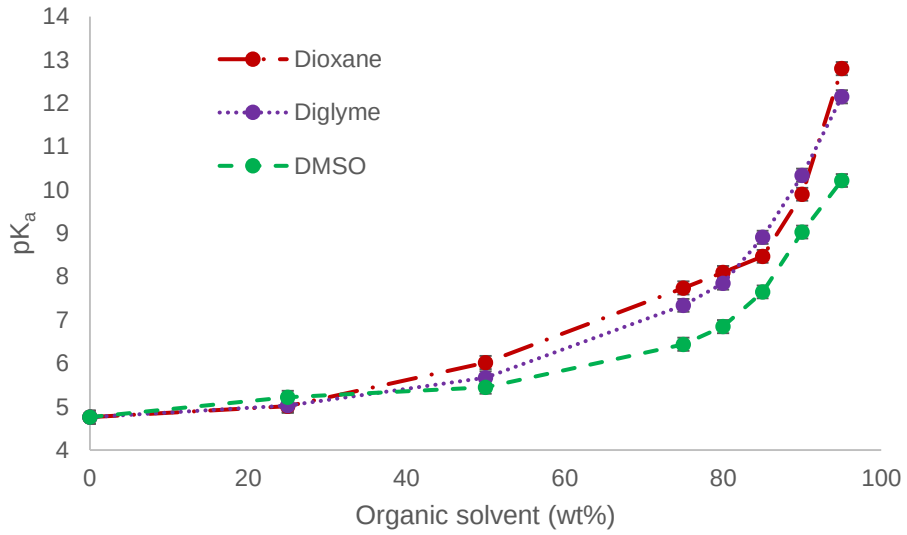

Figure 5.9: Comparison of measured pK_a of acetic acid in dioxane/water, diglyme/water and DMSO/water solvent mixtures.

The difference between DMSO and the ethereal solvents may be understood with reference to their differing ability to coordinate to cations. DMSO is well-known to be a relatively good solvent for cations due to its strong dipole, and thus is better at stabilising the solvated proton than are the ethereal solvents.[168]

5.2.3 Determination of first pK_a value of carbonic acid in various solvent mixtures

For consideration of CO_2 absorption, it is clear that the apparent first dissociation constant of carbonic acid is key (Chapter 2). This is measurable using the same techniques as already described for carboxylic acids, provided appropriate consideration is given to the properties of this particular system.

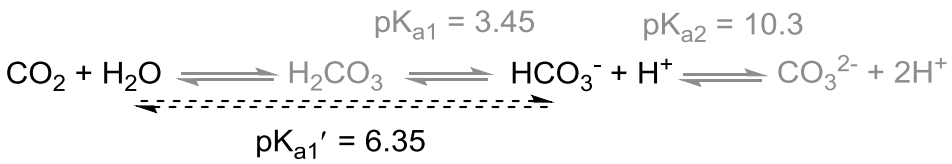

Scheme 5.6: Hydration equilibria of CO_2 in the presence of water, together with the relevant pK_a values in aqueous solution. The equilibrium describing CO_2 capture into solution is highlighted.

Most importantly, it must be recognised that this is a gas-liquid equilibrium and therefore quantification of the left side of the equilibrium is not necessarily straightforward due to possible loss of CO_2 gas from solution. This of course rules out any titration approach based on

deprotonating carbonic acid, since obtaining an accurate, dilute standard solution of CO_2 is not practical, and therefore pK_{a1}' is usually determined by titration of bicarbonate with acid.[68,186,194]

CO_2 exchange between the analyte and surrounding atmosphere during titration must be reduced as far as possible in order to avoid unexpected or misleading results. In practice, loss of CO_2 to the atmosphere is minimised by performing the titration at comparatively low concentrations, since in this case the amount of CO_2 produced is dwarfed by its (physical) solubility in the solvent, and release to the atmosphere is slow. It is of course also necessary to exclude atmospheric CO_2 from the analyte solution, which was accomplished in this work by flushing the analyte cell with nitrogen prior to each titration.

The pK_{a1}' of CO_2 was measured using the methods already described, in the following solvent mixtures at various proportions: ethanol/water; EGBE/water; DMSO/water; 1,4-dioxane/water; and diglyme/water. Results of this are shown in Figure 5.10.

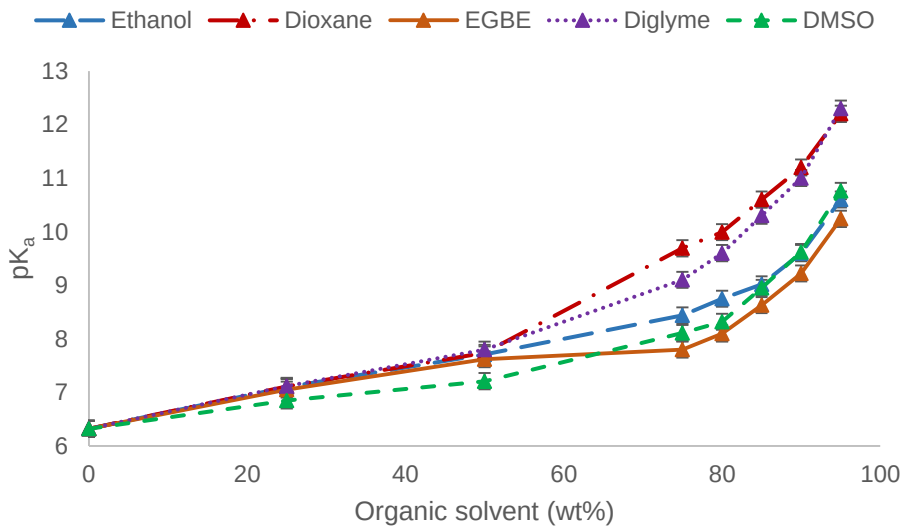

Figure 5.10: pK_{a1}' of carbon dioxide, measured in ethanol/water, dioxane/water, EGBE/water, diglyme/water and DMSO/water mixtures.

Broad trends are similar to those seen in the pK_a of acetic acid across the same solvents – preferential solvation limiting changes in acidity until the organic portion increases *ca*. 80 wt%, at which point the pK_a becomes noticeably more sensitive to further reductions in water content. pK_a values observed in mixtures containing either of the two ethereal solvents are noticeably higher than in other solvents.

Behaviour in the other three solvent mixtures – ethanol, EGBE and DMSO – is interesting as it seems to diverge from that seen in the case of acetic acid. The pK_a of CO_2 in DMSO-based mixtures is similar to that seen in mixtures prepared from either of the protic solvents, whereas the pK_a of acetic acid was noted to be higher in DMSO than in the protic solvents.

A small but significant divergence between the two protic solvents was also observed, with pK_a of carbon dioxide being up to 0.6 pK_a units higher in ethanol/water mixtures than in EGBE.

Most importantly for CO_2 capture purposes, the sensitivity of the pK_a of carbon dioxide to solvent composition is different to that of the pK_a of acetic acid. This can cause the two pK_a values to converge or diverge in drier compositions, with convergence being of particular interest since this would permit CO_2 capture by acetate-containing solutions to take place. The existence and degree of this separation appears to vary greatly depending on which solvent is used.

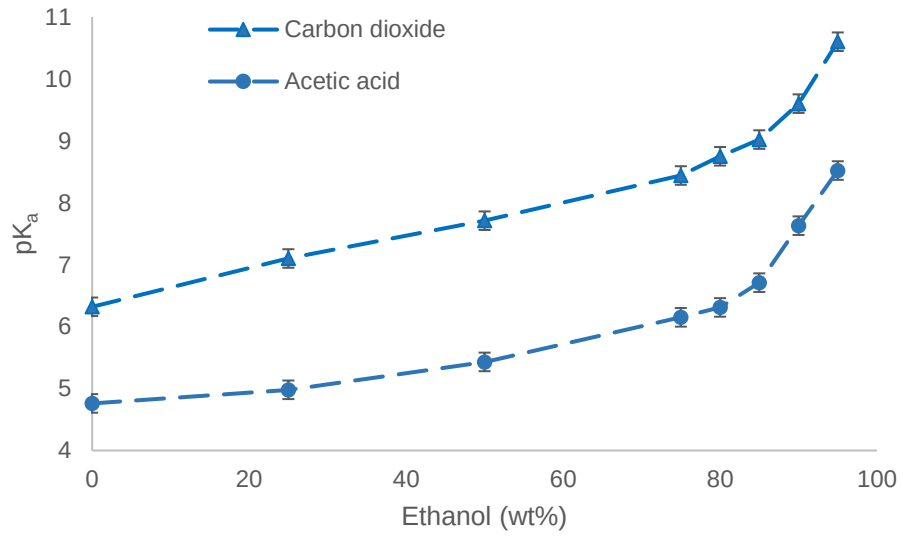

Figure 5.11: Comparison of measured pK_{a1}' of carbon dioxide with pK_a of acetic acid, measured in different ethanol/water mixtures.

In Figure 5.11, the acidity of CO_2 and acetic acid is compared across ethanol/water mixtures. A minor divergence is observed across the range of compositions studied. CO_2 is 1.56 orders of magnitude less acidic than acetic acid in pure water, and this is increased to a maximum of 2.4 in 80% ethanol, before a slight convergence in drier mixtures. Similar behaviour is seen in EGBE/water mixtures (Figure 5.12) though in this case the divergence is smaller and for the most part, the gap remains less than two orders of magnitude.

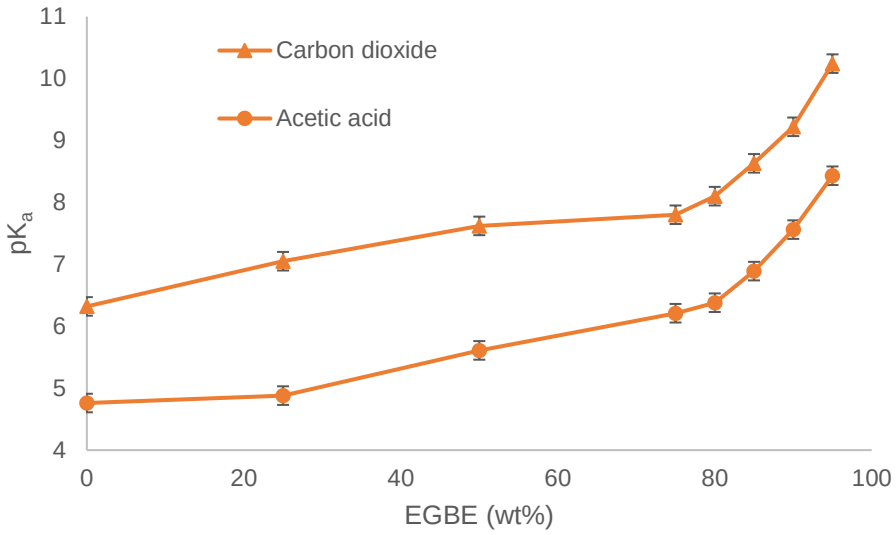

Figure 5.12: Comparison of measured pK_{a1}' of carbon dioxide with pK_a of acetic acid, measured in different EGBE/water mixtures.

The difference in pK_a between CO_2 and acetic acid in these two solvents are plotted below in Figure 5.13. Due to compounding of uncertainties, no clear trend is evident. However, it is interesting to note the divergence between ethanol and EGBE in relatively dry solvent mixtures, and particularly relatively large difference in pK_a values in mixtures containing a relatively low (25-50 wt%) proportion of EGBE. In such mixtures the stabilisation of ions, a central concern in drier solvents, ought not to be a significant concern as they are preferentially solvated by water.

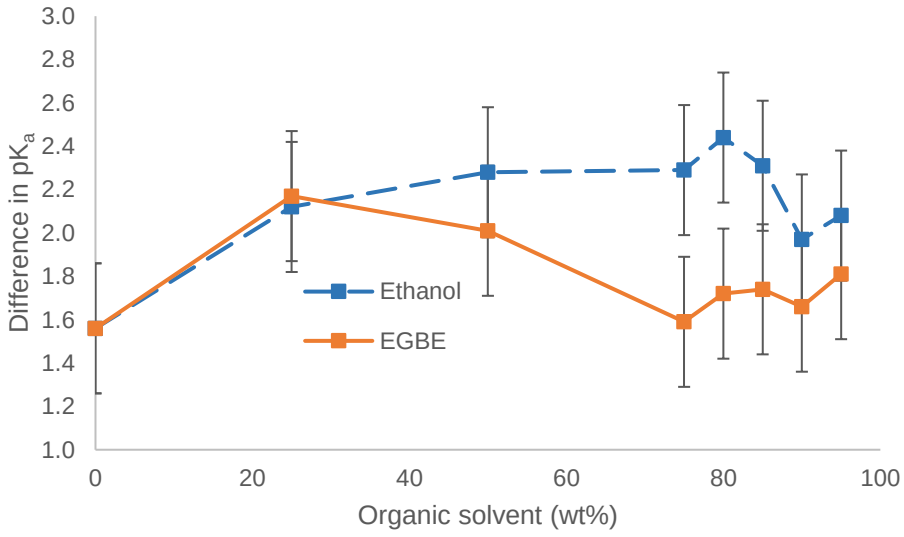

Figure 5.13: Solvent-dependent difference in pK_a between carbon dioxide and acetic acid. Comparison between ethanol/water and EGBE/water mixes.

Closer analysis of the data shows that the difference in this region arises from a comparatively rapid rise in the pK_a of carbon dioxide, while that of acetic acid is almost unchanged. A possible explanation for this behaviour may be found by considering the solvation of the neutral acid. In the case of amines, for example, the acidity of the ammonium cation is greater in mixed solutions than in either water or organic solution, because solvation of the free base is enhanced by the presence of an organic solvent and this drives the equilibrium toward dissociation.[195,196]

For carboxylic acids an analogous effect would be anticipated to reduce the acidity of the acid by favouring ion association. Neutral acid solvation would likely have a weaker effect on acetic acid than on carbonic acid, since the former is a relatively polar molecule, whereas the neutral form of the latter (CO_2) is much less so due to its lack of a dipole moment. Thus, the reason for the divergence in pK_a values at low wt% organic solvent may be attributed to the particular stabilisation of CO_2 in the presence of the organic solvent. When higher proportions of organic solvent are used, the effect is overwhelmed by the familiar issue of solvation of the ions in the equilibrium, and differences in acidity between the two acids are determined by which ions are least unfavourably solvated.

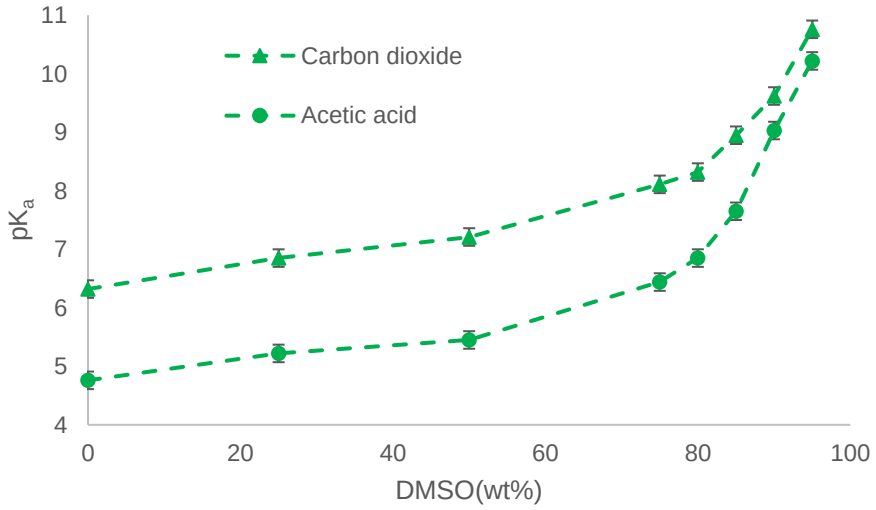

Figure 5.14: Comparison of measured pK_{a1}' of carbon dioxide with pK_a of acetic acid, measured in different DMSO/water mixtures.

In Figure 5.14, the acidity of carbon dioxide and acetic acid in DMSO/water mixtures is compared. Unlike in the protic solvent mixtures, a considerable convergence is seen above 80 wt% DMSO. In 95% DMSO the two acids are separated by only 0.5 pK_a units. This convergence is even closer in diglyme/water (Figure 5.15), and in dioxane/water solutions (Figure 5.16) a full crossover is observed.

This observed behaviour of CO_2 in this situation is distinctly unlike that of a typical carboxylic acid. For example, transfer of a carboxylic acid from water to pure DMSO is known to produce a typical increase in pK_a of approximately 6 units, with weaker acids producing a larger change.[168] In this case, however, carbon dioxide is a significantly weaker acid than acetic acid in water and yet is of comparable or lesser acidity in DMSO-predominant mixes.

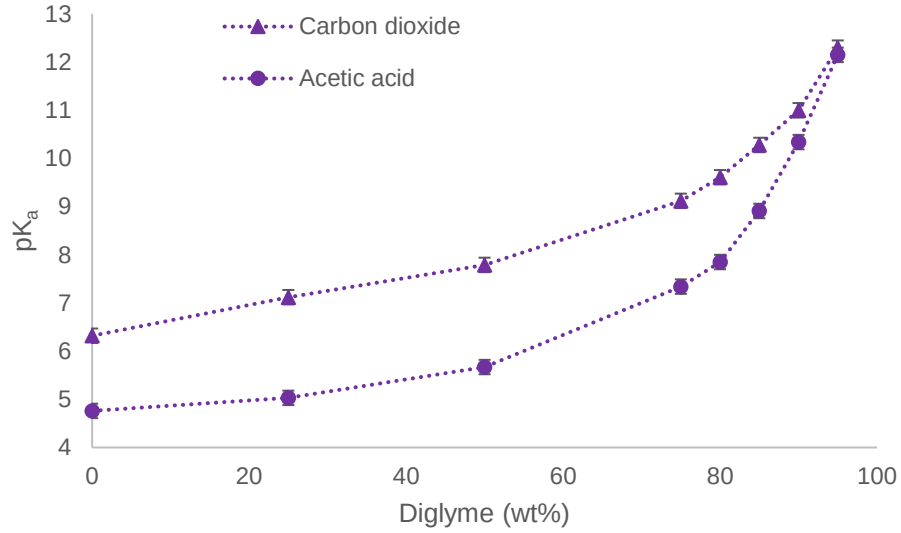

Figure 5.15: Comparison of measured pK_{a1}' of carbon dioxide with pK_a of acetic acid, measured in different diglyme/water mixtures.

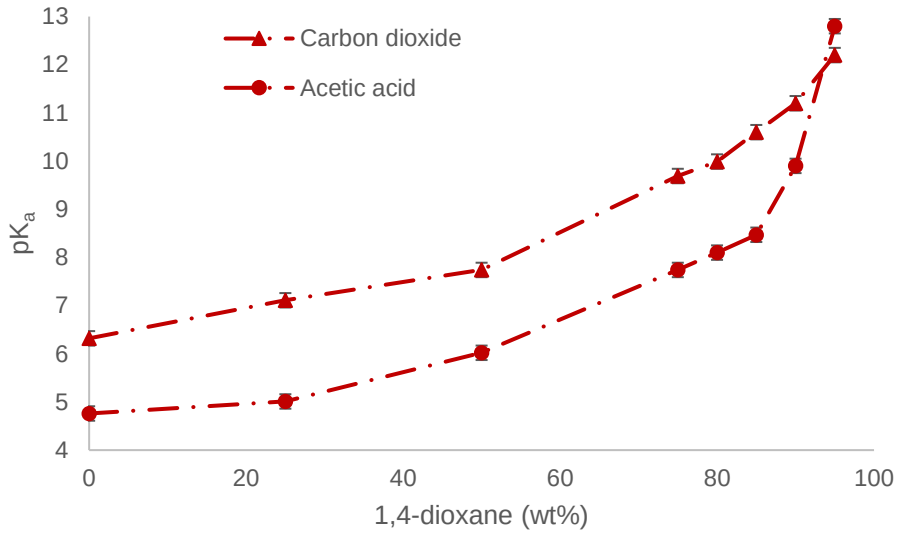

Figure 5.16: Comparison of measured pK_{a1}' of carbon dioxide with pK_a of acetic acid, measured in different 1,4-dioxane/water mixtures.

The cause of this convergence is unclear and becomes even more mysterious upon recollecting the definition of pK_{a1}' as an *apparent* equilibrium constant and not the true dissociation constant of carbonic acid, which is somewhat lower. This apparent equilibrium also contains the hydration equilibrium of CO_2 to carbonic acid, which requires water. In comparatively dry solvent mixtures, this should theoretically give carbonic acid a particularly *high* pK_{a1}', since dissociation of the acid removes more water from the solution, and so protonation and decomposition of bicarbonate ought to be favoured by Le Châtelier's principle. However, the experimental data shows quite clearly that this is not the case.

In summary, the measurements presented thus far have demonstrated a convergence in pK_a between acetic acid and carbon dioxide, but in most cases the crossover hypothesised at the beginning of this chapter has not been found. However, complete crossover is not necessary in order to achieve CO_2 capture. The closer the relevant pK_a values, the greater the equilibrium concentration of bicarbonate in solution, which provides a driving force for CO_2 absorption considering that the initial concentration of dissolved bicarbonate in a hypothetical capture solvent would be near-zero. The most definitive means of examining this proposal is to investigate the CO_2 capture ability of some of the mixtures presented here, and such a study is presented in the following section.

5.3 CO_2 absorption by carboxylate salts in DMSO/water solutions

In order to provide conclusive experimental proof of the pK_a convergence described above, it is necessary to test its most obvious application – as the basis for a CO_2 capture solvent, dispensing with idealised titration conditions in favour of molar salt concentrations. For this section it was decided to focus on DMSO/water mixtures, as promising pK_a convergence has already been observed in this solvent and acid-base chemistry in DMSO solution is far better understood than in the other aprotic solvents studied above. The CO_2 capture experiments were carried out in a vapour-equilibrium cell purpose-built for such experiments (see section 8.1.2.2). 150 mL of capture solvent (1 M potassium acetate in a DMSO/water mixture) was placed in the sealed cell and the headspace pressure reduced to 500 mbar and the system equilibrated at 25 °C. The pressure was increased to 650 mbar by introducing CO_2 through a regulator from a gas burette. Hence, the initial CO_2 partial pressure was 150 mbar, fundamentally the same as would be encountered in 15% CO_2 flue gas under real operation. Once the system had reached thermal equilibrium, the regulator pressure was successively increased in steps, equilibrating each time, to a maximum of 1500 mbar (and hence 1 atm pressure of CO_2). CO_2 absorption into solution was calculated from the changes in the gas burette pressure together with the known dimensions of the headspace inside the cell.

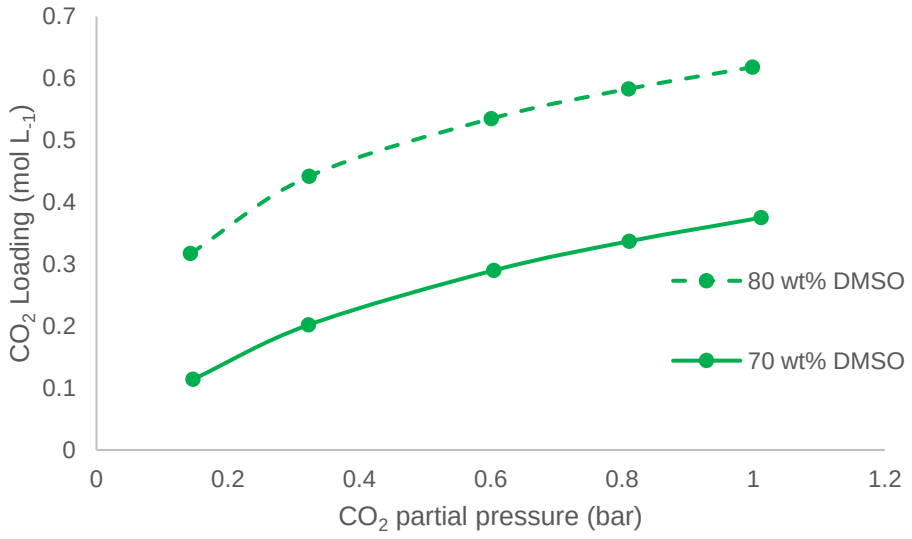

Figure 5.17: CO_2 absorption curves for solutions containing 1 M potassium acetate dissolved in either 70/30 or 80/20 wt% mixtures of DMSO and water, with increasing partial pressures.

CO_2 capture into solution is clearly significant, far in excess of the concentrations that could be obtained through physical solvation at such low pressure, and improved by the reduction of solvent water content. Furthermore, a noticeable amount of potassium bicarbonate precipitate was observed in solution. This offers confirmation that reactive absorption is occurring (Scheme 5.7)

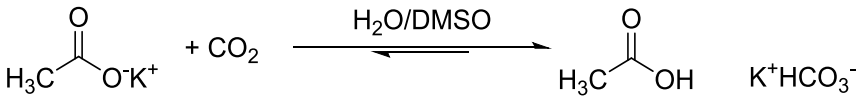

Scheme 5.7: CO_2 capture by potassium acetate in DMSO/water mixtures.

Absorption is far from stoichiometric in the solution containing 70 wt% DMSO, but is significantly improved in 80% DMSO. In one sense this supports the earlier finding that acetic acid and carbon dioxide have very similar pK_a values in this system, and therefore absorption is very much an equilibrium process. However, the pK_a values measured above were quite far apart in this region. For example, in 80% DMSO the pK_a of acetic acid is 1.47 units lower than that of CO_2, scarcely different from that in pure water.

The cause of this divergent behaviour likely lies in the ionic strength of the capture solvent, which is an order of magnitude higher than that used in the potentiometric experiments. In order to probe this further, a variety of other carboxylic acids were also examined. Hence, solutions of 1 M potassium propionate and potassium pivalate were carboxylated in the same manner, demonstrating uniformly better CO_2 capacity than acetate (Figure 5.18), a trend which appears to increase with size of the carboxylate.

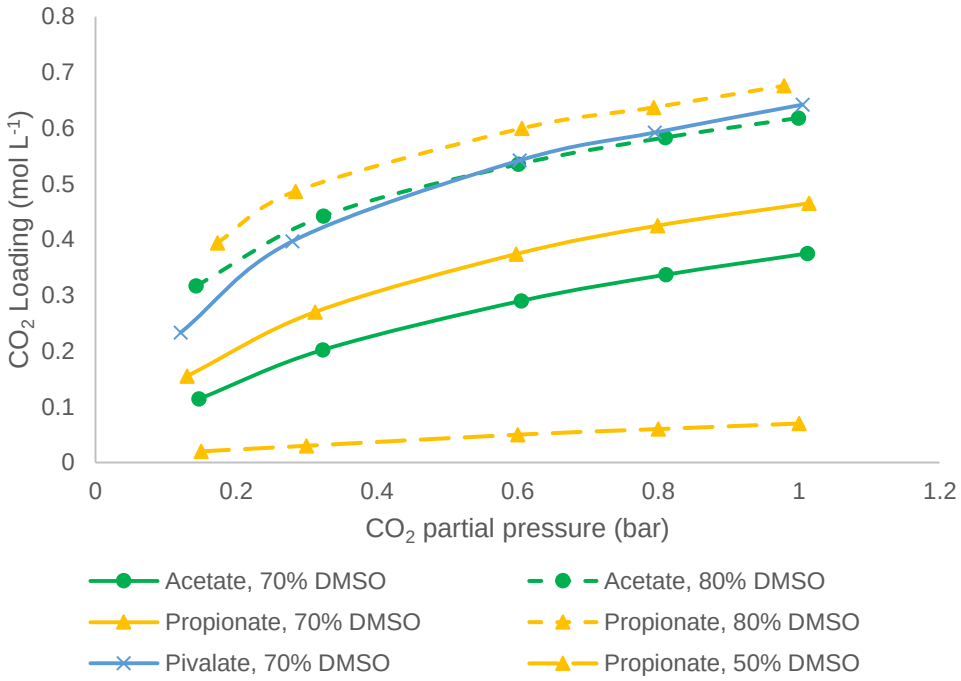

Figure 5.18: CO_2 absorption curves for solutions containing 1 mol L^{-1} potassium salt of the given carboxylate, dissolved in either 70/30 or 80/20 wt% mixtures of DMSO and water, with increasing partial pressures.

In order to provide a suitable negative control, further absorption experiments were performed with potassium propionate in 50% DMSO/50% water and in pure water solutions. In the former case, CO_2 absorption was very small indeed, while none was measured in the pure water solution. This suggests that the pK_a gap between carbonic acid and acetic acid is much closer together in the capture compositions measured above than potentiometric experiments would suggest, as exact reflection of idealised values would lead to either CO_2 absorption by carboxylate salts in pure water, or minimal/no CO_2 absorption in 80% DMSO.

Concurrently, the pK_a values of these additional carboxylic acids were measured via *potentiometric titration (*

Table 5.4) in DMSO/water mixtures. The values thus produced were higher than acetic acid, though not especially dissimilar from one another. In particular pivalic acid was observed to (barely) cross over with the pK_{a1}' of carbon dioxide.

Table 5.4: Measured pK_a values for carboxylic acids and CO_2 in DMSO/water mixtures.

DMSO (wt%)	pK_a (acetic acid)	pK_{a1}' (carbon dioxide)	pK_a (propionic acid)	pK_a (pivalic acid)
0 (water)	4.76	6.32	4.87	5.03
80	6.85	8.32	7.34	7.41
90	9.03	9.62	9.52	9.66
95	10.22	10.76	10.63	10.82

It is quite clear that there is a strong divergence between the pK_a values measured under idealised conditions, and the observed carbon dioxide capture behaviour at molar concentrations, with capture proving somewhat more favourable, at higher water concentrations, than the pK_a measurements would suggest. This implies that CO_2 absorption is favoured by an additional effect which has not been considered thus far, a concern which will be explored in depth in Chapter 6.

5.4 Conclusions

In summary, this section reports the first comprehensive study of the acid-base chemistry of CO_2 outside aqueous solution. The acidity of CO_2 is peculiarly insensitive to reductions in water content compared to a carboxylic acid, a fact which may be exploited for CO_2 capture purposes. Such a capture system produces a comparatively low CO_2 capacity in comparison to amine solutions. The amine and phenoxide-containing solutions studied in the preceding chapters are all capable of equimolar CO_2 absorption, while the best-performing carboxylate solution studied here (1 M potassium propionate in 80% DMSO) can absorb only 68 mol% CO_2. However, the capture capacity of amine solutions is limited in practice by the very slow rate of absorption into these solutions when significant amounts of CO_2 have already been absorbed (since there is no free amine available and absorption in such solutions occurs *via* the decomposition of carbamate).

Furthermore, the relatively low capture capacity of carboxylate solutions points to a relatively weak thermodynamic driving force for absorption, which is likely to reduce the cost of thermal

desorption significantly. The use of an organic solvent in place of water is likely to reduce this cost further, by lowering the heat capacity of the capture solvent, though some water is necessary for solvation of the carboxylate salts.

Carboxylate-based capture solvents may also be released by the addition of water, a pathway unique to this capture system, driving the equilibrium back toward neutralisation of bicarbonate by a carboxylic acid. The advantage of this approach is that both CO_2 absorption and desorption would then be energetically favourable, with the thermodynamically disfavoured step being the removal of this water in order to reset the capture solvent. Since drying of solvents is an extremely common operation on which a vast amount of industrial experience has been built, this may enable the overall process to be carried out with greater efficiency, in comparison with amine-based capture solvents where the energetically demanding step (desorption) is still being improved upon.

Energetic evaluations carried out by C-Capture Ltd. suggest that the energy requirements of a carboxylate-based capture system are significantly lower than existing systems in use. Energy demand is typically measured in gigajoules per ton of CO_2 captured. The most advanced existing amine blend-based systems require approximately 2-2.5 GJ/t, whereas it is estimated that a carboxylate-based CO_2 capture system would require as little as 0.2 GJ/t.[15,197]

Furthermore, a carboxylate-based system is likely to be far more stable than one based on amines, since the major cause of solvent degradation is oxidation (by oxygen present in the flue gas stream) to which carboxylates are not susceptible, being already highly-oxidised species. Not only would this bring benefits in terms of solvent lifetime (thus reducing the cost associated with replacing degraded solvent) but this also eliminates the danger of environmental pollution caused by amine degradation products such as nitrosamine and nitramine compounds.

6 Chemical Basis of pK_a-swing Absorption

6.1 Introduction

In the previous chapter, it was shown that the acidity of CO_2 is less sensitive to changes in its solvent environment than carboxylic acids, a fact which allows the capture of CO_2 by solutions of carboxylate salts in certain solvent mixtures. The reason for this behaviour is, however, unknown, and will be discussed more thoroughly in this chapter.

The interconversion of CO_2 with bicarbonate is, of course, not a simple Brønsted-Lowry dissociation as is the case for a carboxylic acid, but consists of two successive equilibria: the hydration of carbon dioxide to form carbonic acid, and the subsequent dissociation of carbonic acid into bicarbonate and a proton. While important to practical applications due to its implications for the rate of absorption, this fact is irrelevant from a thermodynamic viewpoint, since the overall equilibrium constant (pK_{a1}') is dependent only on the free energy difference between the reactants and products, not on any intermediate species. However, since the aqueous dissociation constant of carbonic acid is known ($pK_{a1} = 3.45$) appreciation of these underlying equilibria may aid in understanding the differences between CO_2 and carboxylic acids.

An obvious difference between CO_2 and carboxylic acids is that water is required for the dissociation of the former, which might be expected to become significant in solvent mixtures containing relatively little water such as those studied above. Since water is required for *dissociation*, the effect of a lack of water would be anticipated to drive the equilibrium toward association – in other words, a *higher* pK_a than would be observed for a comparable carboxylic acid. This, of course, is the opposite of what we have observed experimentally.

6.2 Free energy analysis

For the study of pK_a-swing absorption, we are not directly interested in the behaviour of the individual acid dissociation equilibria, but in the solvent-dependent behaviour of the overall equilibrium:

$$AcOK + CO_2 + H_2O \rightleftharpoons AcOH + KHCO_3$$

This can be discussed more rigorously in terms of energetics. The Gibbs free energy of this equilibrium may be defined from the relevant free energies of formation, hence:

$$\Delta G = \Delta G_{AcOH} + \Delta G_{KHCO_3} - \Delta G_{AcOK} - \Delta G_{CO_2} - \Delta G_{H_2O} \quad (6)$$

Let us define ΔG_{aq} as the Gibbs free energy of the equilibrium in aqueous solution. A value for ΔG_{aq} of +8.90 kJ mol^{-1} was trivially determined from the known aqueous pK_a values of acetic acid and CO_2 (i.e. the two equilibria from which the above is composed) since the Gibbs free energy of an equilibrium is related to the equilibrium constant by the relation $\Delta G = RT \ln K$. To treat the behaviour of the equilibrium in solvents other than water, it is easiest to consider this in terms of a change from aqueous values, since then the change in free energy may be broken down in terms of the free energy of transfer for each individual species involved. The free energy of transfer, ΔG_{tr}, is defined as the free energy change associated with moving a species from aqueous solution to another solvent.[168] Hence:

$$\Delta G - \Delta G_{aq} = \Delta G_{tr}(AcOH) + \Delta G_{tr}(KHCO_3) - \Delta G_{tr}(AcOK) - \Delta G_{tr}(CO_2) - \Delta G_{tr}(H_2O) \quad (7)$$

This perspective is particularly useful since it permits an appreciation of the contribution of the thermodynamics of solvation of each species toward the observed behaviour. It may therefore aid solvent selection by providing information on which solvent characteristics are most beneficial. The value of ΔG_{tr} for a given species is most easily determined from the solubility difference, since the free energy of solution of a substance, ΔG_s, is relatable to its molar solubility, S_o. For neutral compounds, this relation is:

$$\Delta G_s = -RT \ln S_o$$

This relation is derived from standard thermodynamic relations, since the equilibrium constant defining solubility is equal to S_o. For salts which dissociate into ions, the solubility product $K_{sp} = S_o^2$ must be used, and hence in this case the relation is:

$$\Delta G_s = -2RT \ln S_o$$

Alternative means beside solubility may also be used to determine ΔG_{tr}, including partition coefficients (when the two solvents in question are immiscible), vapour pressure measurements (for neutral substances), and specifically designed electrochemical cells (for ionic species). A number of studies have sought to establish ΔG_{tr} values for individual ions, using tetraphenylarsonium or tetraphenylborate salts (depending on the charge of the ion in question) with the convention that $[Ph_4As]^+$ and $[BPh_4]^-$ have the same free energy of transfer.[198]

The scientific literature contains a wealth of information relevant to ΔG_{tr} for most of the species above, including solubility studies and specific studies of the free energy of transfer. It must be noted that such studies deal almost exclusively with pure solvents, rather than the mixed solvents studied experimentally in the previous chapter. Since theoretical treatment of mixed solvents is extremely complex, however, it is useful to use the idealised situation of a pure organic solvent as a starting point.[168,199]

Relatively few experimental studies of this nature have been conducted on potassium bicarbonate, or any other bicarbonate salt, in solvents outside water. This paucity of information will be the primary limitation on this line of analysis. Conveniently, a recent study by Marcos et al. computed the free energy of solvation of the bicarbonate ion in a range of solvents.[200] These computed values are shown in Table 6.1.

Table 6.1: Gibbs free energies of solution of bicarbonate ion in the given solvents, along with Gibbs free energies of transfer from water. Experimentally determined value in water reported by Marcus.[201] *Other values calculated by Marcos et al. using SM8 solvation model.*[200]

	HCO_3^-	
Solvent	ΔG_s/kJ mol^{-1}	ΔG_{tr}/kJ mol^{-1}
H_2O	-335	0
MeOH	-308	27.1
EtOH	-294	40.9
^{i}PrOH	-285	50.5
DMSO	-259	76.4
MeCN	-253	81.9

As might be expected, large increases in the Gibbs energy are observed in solvents of decreasing polarity, due to these solvents' inability to effectively solvate anions as well as water does due to diminished hydrogen bonding. The very low solubility of bicarbonate salts in nonaqueous solutions is related to this effect.

Table 6.2 shows the same values for the potassium ion. In this case, the free energy changes are less significant, and the trend less distinct. Notably, potassium is better solvated in DMSO than in water due to the comparatively high basicity of this solvent, and better solvated in acetonitrile than any of the alcohols for similar reasons. It is worth mentioning that the free energy changes for potassium cancel one another out in the equilibrium under consideration, since if it is assumed that all ionic species are dissociated then this is merely a spectator ion. However, the latter assumption must be treated with care in nonaqueous solutions.

Table 6.2: Gibbs free energy of transfer of potassium ion from water to the given solvent. Values experimentally determined and reported in the scientific literature.[198,199,202–204]

	K^+
Solvent	ΔG_{tr}/kJ mol^{-1}
H_2O	0
MeOH	10.0
EtOH	16.0
^{i}PrOH	22.5
DMSO	-12.0
MeCN	8.0

ΔG_{tr} values for the acetate ion are shown below in Table 6.3. While the observable trends are similar to those seen with bicarbonate (both being relatively small anions) it is highly noteworthy that the magnitude of free energy changes in acetate are somewhat less than their bicarbonate equivalents.

Table 6.3: Gibbs free energy of transfer of acetate ion from water to the given solvent. Values experimentally determined and reported in the scientific literature.[198,199,202–204]

	AcO^-
Solvent	ΔG_{tr}/kJ mol^{-1}
H_2O	0
MeOH	16.0
EtOH	36.9
^{i}PrOH	31.0
DMSO	61.1
MeCN	60.9

Table 6.4 shows ΔG_{tr} values for the neutral species in the equilibrium: acetic acid, CO_2 and water. It is noteworthy that all of the free energy changes observed in these species are significantly smaller than those observed in the anions above. Thus, the behaviour of these species is likely to have a relatively marginal effect on the overall equilibrium, which would be expected to be dominated by the large positive ΔG_{tr} values of the two anionic species.

Table 6.4: Gibbs free energy of transfer of neutral acetic acid and CO_2 respectively, from water to the given solvent. Values experimentally determined and reported in the scientific literature.[205,206]

	AcOH	**CO_2**
Solvent	ΔG_{tr}/kJ mol^{-1}	ΔG_{tr}/kJ mol^{-1}
H_2O	0	0
MeOH	0	-5.6
DMSO	-4.6	11.4
MeCN	2.3	10.1

Hence, for each solvent for which data is available, we may consider the total free energy difference from water and the effect of each of the relevant values quoted above. The contributions of each species to the overall Gibbs free energy of CO_2 absorption are compared in Figure 6.1 below. As predicted, the two anionic species appear to dominate the overall equilibrium due to the large magnitude of their transfer energies. However, the ΔG_{tr} values of these species are sufficiently close that they approximately cancel one another out, and thus the neutral species may also play some role. It must be re-emphasised that these are values for solvation in the pure organic solvents, and thus assume a concentration of water that is too small to affect the solvation environment.

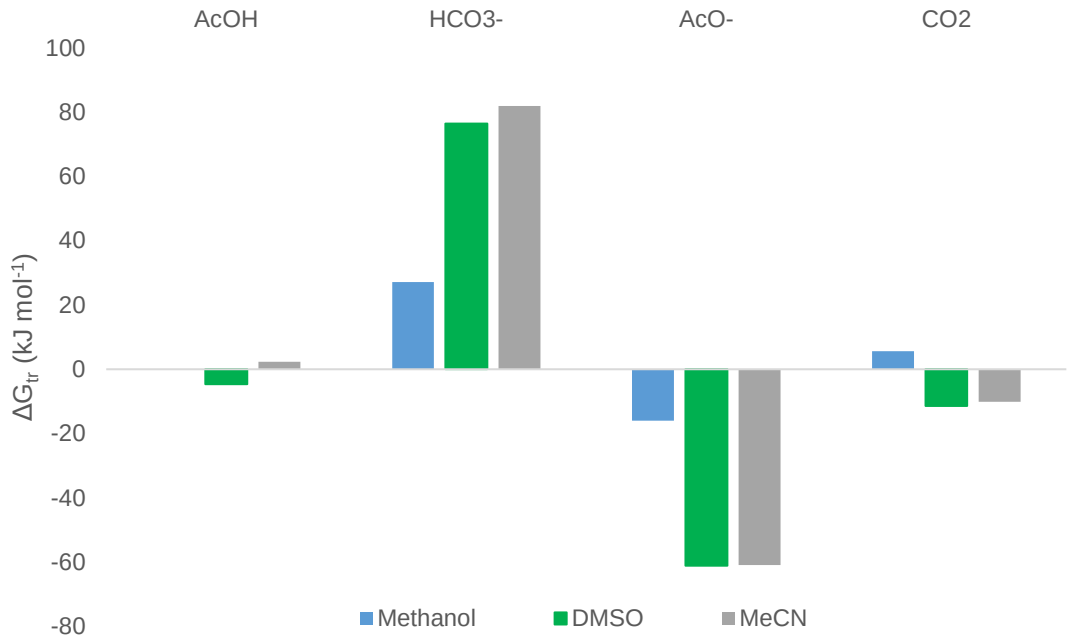

Figure 6.1: Graphical representation showing the major contributions, relative to aqueous solution, to equilibrium of CO_2 absorption in three different solvents.

The overall Gibbs free energies calculated by this method are all positive, and substantially so – only in DMSO is CO_2 absorption found to be more favourable than in water, and even there the margin amounts only to 0.7 kJ mol^{-1}. This is a highly intriguing finding, since based on these predictions the CO_2 absorption observed in the preceding chapter should not be possible. Since the broad thermodynamics seem to be opposed to such absorption, the logical conclusion to draw, once again, is that the chemical basis for pK_a-swing absorption must lie outside the straightforward examination presented thus far.

Table 6.5: Gibbs free energies of CO_2 absorption, both relative to that in water and as absolute values.

Solvent	$\Delta G - \Delta G_{aq}$ /kJ mol^{-1}	ΔG/kJ mol^{-1}
H_2O	0	8.90
MeOH	16.7	25.6
DMSO	-0.7	8.2
MeCN	13.2	22.1

Of course, it must also be considered that the analysis presented herein is based on the principle of investigating thermodynamics of absorption into pure organic solvents, an impossible scenario given that water is necessary for CO_2 hydration to bicarbonate. It is conceivable that in mixed solutions, even those which are moderately dry, the presence of a water solvation sphere radically

alters the energetics of the participating species. Available thermodynamic information on species dissolved in mixed solvents is decidedly limited. However, one point of comparison is available – the pK_a values measured in the preceding chapter.

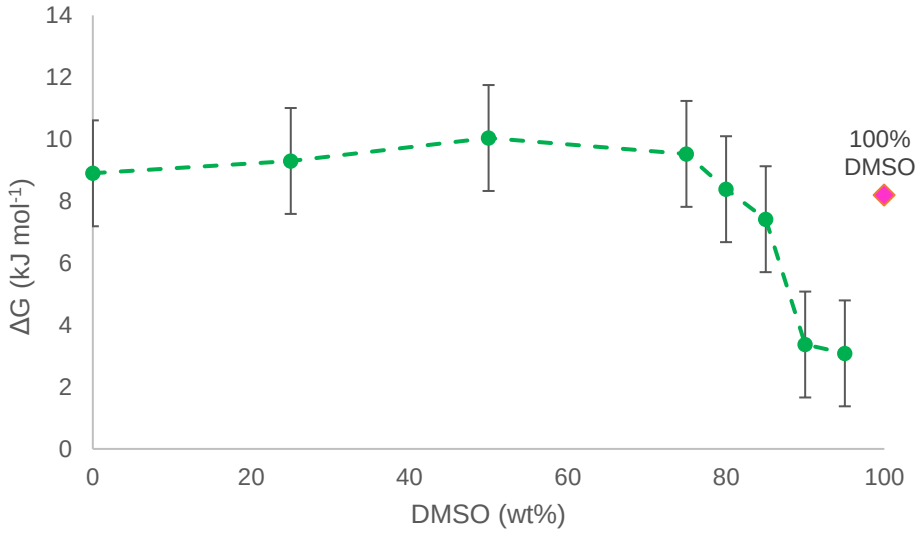

Figure 6.2: Experimentally derived ΔG of CO_2 absorption (this work) in DMSO mixtures of various compositions, together with the same for 100% DMSO, derived from published literature studies.

In Figure 6.2 above, the ΔG of CO_2 absorption has been calculated from the pK_a values previously measured, by addition of the relevant dissociation equilibria. In comparison with the value calculated for pure DMSO in this chapter, a "free energy trough" seems to be present in the region containing 85-99 wt% DMSO, in which CO_2 absorption is far more favourable than in other available compositions. Given the divergent behaviour already observed at higher concentrations, it is open to speculation as to whether this "trough" is universal or limited to lower concentrations.

6.3 Stoichiometry of water

It is well-known that solvation behaviour is usually dictated by inner-sphere solvation – the direct interactions between solute and solvent molecules. Since only a certain number of solvent molecules can do this, it would be expected that reducing the proportion of a particular solvent (in this case water, which preferentially solvates ions) below such a limit would exert a strong effect on the solvation environment experienced by the solute in question.

Such behaviour may be hypothesised to be the basis for pK_a-swing CO_2 capture. However, while such an argument might be plausible in real systems where concentrations of absorbent are very

high, it does not explain the rise in pK_a observed by the titration measurements in Chapter 5, wherein base concentration was at an extremely low level of 2.5 mmol L^{-1}. This fact is demonstrated by Figure 6.3, in which the measured pK_a values of CO_2 and acetic acid and DMSO are plotted, not against the wt% composition of the solvent, but against the number of moles of water relative to the number of moles of acid. As can be seen, even in the driest mixture, this ratio does not fall below 1000:1.

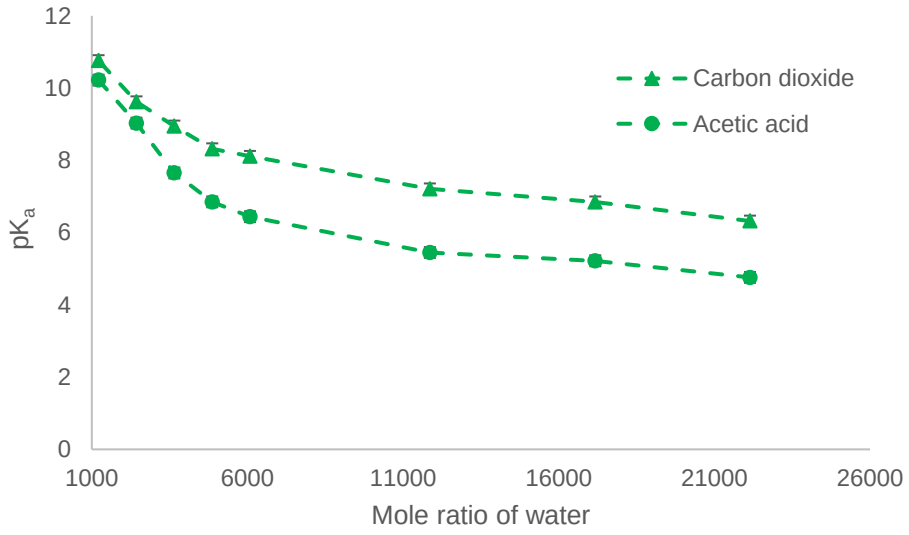

Figure 6.3: pK_a values of acetic acid and CO_2 in various DMSO/water mixtures, plotted against the molar ratio of water to the salt in question.

This evidence would appear to disprove the hypothesis that a limiting concentration of water is directly responsible for the observed pK_a-swing behaviour, since even outer-sphere coordination does not require hundreds of water-molecules. The implication therefore is that the effect of water content on the equilibria in question is more indirect, via the changing properties of the medium as a whole.

6.4 Ion clustering

Particularly in poorly-solvating nonaqueous solvents, it is possible for ionic species to engage in various clustering behaviours that may produce non-ideal outcomes. Such behaviour comes about when solute-solute interactions are sufficiently stronger than solute-solvent interactions to

overcome the additional statistical (entropic) barrier of there being many more molecules of solvent than of solute in the system.

A wide variety of possible modes of association exists, depending on the species in question. Some of those most commonly associated with carboxylic acids are shown in Scheme 6.1. These comprise ion pairing (in which ions of opposite charge are closely associated to form a neutral complex), homohydrogen bonding (in which a carboxylic acid and carboxylate share the former's proton between them, reducing charge density overall) and dimerization between two carboxylic acid molecules.[160,207] In addition to these bimolecular interactions, larger and less well-defined clustering behaviour has been observed for acetic acid, even in aqueous solution.[208]

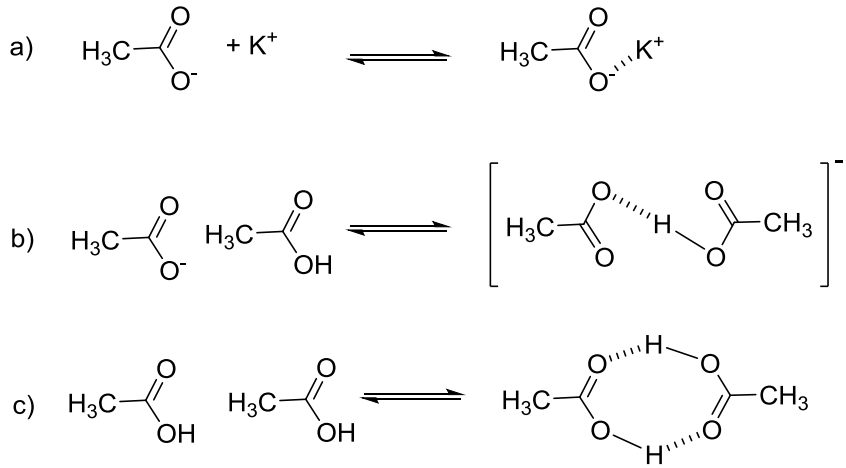

Scheme 6.1: Non-ideal behaviour of acetic acid: a)ion pairing; b) homohydrogen bonding; c) dimerization.

All of these behaviours may affect wider equilibria in which they are not taken into account, by sequestering species from the system. One must particularly note the preponderance of protonated species in these equilibria. A system favouring dimerization or homohydrogen bonding could help to drive CO_2 absorption, for example, by providing a sink for acetic acid, which then drives the equilibrium toward further protonation, and raising the effective pK_a of acetic acid. An illustration of how this might function is shown in Scheme 6.2.

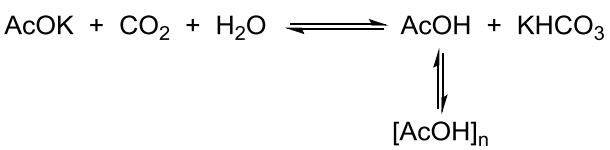

Scheme 6.2: Proposed thermodynamic assistance to CO_2 absorption by clustering of acetic acid in primarily organic solvent mixtures.

It has not been reported whether bicarbonate takes part in similar cluster behaviour, though this may be more a symptom of the generally poor understanding of nonaqueous carbonate chemistry rather than evidence of this behaviour's absence. While the structure of bicarbonate appears highly favourable toward such clustering, being both a hydrogen-bond donor and acceptor, bicarbonate-bicarbonate clustering is likely disfavoured by charge repulsion. However, the presence of bicarbonate-acetic acid clustering is a plausible possibility and would further favour CO_2 absorption. While it is likely that carbonic acid could also form such clusters, it is present in too small a concentration to have a significant effect. CO_2, on the other hand, lacks a dipole moment and is not readily deprotonated directly, due to the necessity of going through a hydration step first. Thus, CO_2 is set apart from carboxylic acids in that it likely cannot undergo such clustering behaviour.

This, therefore, may provide a reasonable explanation for why the pK_a of carbon dioxide is much closer to acetic acid in certain solvent systems than one might expect from aqueous behaviour or idealised thermodynamic predictions. When placed in a solvent system that disfavours anion formation, carboxylate dissociation is additionally suppressed due to the tendency for its neutral form to join dimers and clusters. On the other hand, the acidity of CO_2 is not so suppressed, and possibly even enhanced due to the ability of bicarbonate to take part in such clustering behaviour.

6.5 Mechanistic considerations

Though the thermodynamic analysis presented thus far bypasses questions of the mechanism of CO_2 absorption observed in the pK_a-swing process, that topic is of significant interest since the usual assumptions that hold true in aqueous solution may not apply in the organic solutions discussed in this work.

According to the conventional assumptions, two acid-base equilibria operate in tandem – CO_2 is hydrated to carbonic acid, followed by dissociation to bicarbonate and a solvated proton, and this equilibrium is pulled toward absorption by the favourable capture of solvated protons by carboxylate to make a carboxylic acid (Scheme 6.3a).

However, the availability of solvated protons in organic solution is likely to be relatively restricted, due to lack of available water, which may act to disfavour such a mechanism. Furthermore, such a mechanism would likely lead to a very slow rate of absorption, since the rate-determining step would be limited by the slow and unfavourable formation of carbonic acid. Though this work does not present detailed kinetic measurements, it must be noted that work by C-Capture Ltd. has found absorption to be noticeably faster than that seen in tertiary amine solutions which are believed to operate by this mechanism.[159]

Analogously to the concerted mechanism of carbamate formation discussed in chapter 2, we may therefore envisage a hypothetical concerted mechanism in which hydrolysis occurs directly through a loosely bound encounter complex, with participation of the potassium cation in a six-membered cyclic transition state (Scheme 6.3).

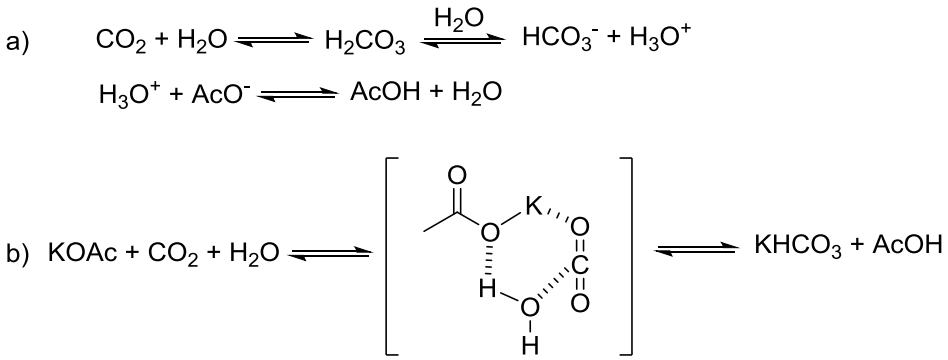

Scheme 6.3: Possible mechanisms for pK_a-swing CO_2 absorption: a) carbonic acid-mediated tandem equilibria; b) concerted addition.

Determination of the true mechanism of this process is not possible from the data available, but could be the objective of a future kinetic study.

6.6 Conclusions

This chapter has begun to probe the basis underlying the CO_2 absorption by carboxylate solutions observed in Chapter 5. The thermodynamic analysis herein showed that such absorption is not explainable by conventional energetics, at least not in idealised pure solvents, but did indicate that this behaviour may require a relatively specific solvent environment. It is proposed that this phenomenon is instead caused by clustering behaviour common to carboxylates in unfavourable solvent systems, but of which CO_2 is incapable.

The possibility of such clustering could be further probed with a conductometric study, since such techniques are sensitive to the nature and type of ionic species in solution, and could swiftly disprove or confirm the hypothesis. One other area of key interest is the concentration dependence of the equilibria in question, since the high-concentration absorption operated far more effectively than predicted by low-concentration titrations. This could be another effect of the cluster behaviour (since such behaviour is well-known to be common at high concentrations) but it is also possible that other, unknown effects may be at play.

7 Conclusions and Future Work

This work has explored the behaviour of three major solvent systems for the capture of CO_2 on an industrial scale. First, the aqueous amine solutions used in most conventional work were studied for their speciation using a novel ^1H NMR method in which concentration of bicarbonate, normally unquantifiable by proton NMR, was calculated based on the charge balance of the solution. This could be done either with ^1H NMR alone (allowing all species to be measured with a single spectrum) or with an additional gasometric measurement (which provides better accuracy and reliability, especially in more complex systems). Relatively large amounts of carbamate were observed in the amine capture solvents studied, which is likely to lead to difficult CO_2 desorption. The methods detailed therein are suitable for employment in a more wide-ranging study, examining in detail the speciation of either a large number of different amines, combinations of amines, or compositional screening.

The same approach was then applied to CO_2 absorption into aqueous mixtures of potassium phenoxide and MEA. The novel use of a phenoxide salt filled the same role as a tertiary amine would in other blends, while reducing the amount of amine that would be used in the capture process (and thus likely emissions of amine degradation products). The speciation study appeared to show that phenoxide also provides improved CO_2 absorption performance relative to comparable blends, with reduced carbamate formation. Significant scope now exists to extend this study to other phenoxide salts and blends with other amines, though the poor aqueous solubility of most phenol derivatives may be an obstacle. The high toxicity of phenol may also pose issues on an industrial scale.

Chapter 5 turned to the fundamentals of the acid-base behaviour of CO_2 itself. Despite its commonplace importance, outside pure aqueous solution this behaviour is remarkably poorly understood and this work made major strides in seeking to understand how the pK_a of CO_2 varies based on solvent composition. It was found that while CO_2 behaves like a carboxylic acid in that it is orders of magnitude less acidic in the presence of organic solvents, it much less sensitive to

its solvation environment than are simple carboxylic acids, and the normally very different pK_a values converge in very organic solutions (<20% H_2O). On this basis a completely amine-free CO_2 capture system was demonstrated that employed a solution of a carboxylate salt dissolved in a DMSO/water mixture. Not only does such a system completely avoid the issues of carbamate formation observed in prior chapters, but it allows for a novel form of desorption with the addition of water, which pushes the acid-base equilibria back toward aqueous norms. Further work could now seek to explore the limits of this behaviour, encompassing the innumerable carboxylate salt and solvent combinations that may be available.

In particular, deeper study is needed into the energetic basis for the observed convergence in pK_a. Chapter 6 presented a superficial thermodynamic analysis of the question, and concluded that existing theory contradicts the experimentally observations reported herein. It was suggested that non-ideal behaviour caused by carboxylate clustering may be the reason for the observed capture behaviour, but a dedicated study into this area, perhaps a computational analysis, is needed before any firm conclusions can be drawn.

This work has primarily focused upon the thermodynamics of CO_2 absorption, but the kinetics are also of fundamental importance in practical applications as they determine the size and cost of absorber unit. In particular, since the carboxylate-based systems represent new chemistry with great potential for improvement over existing systems, it is recommended that a full kinetic study of these capture solvents be carried out in conjunction with any future screening efforts.

8 Experimental Details

8.1 General considerations

8.1.1 Chemicals

Monoethanolamine and *N*-methyldiethanolamine were distilled at reduced pressure from 4A molecular sieves and stored over the same. Potassium acetate, piperazine, phenol (supplied as a mixture with 10 wt% water), hydrochloric acid (37% aqueous), glacial acetic acid and 2-amino-2-methyl-1-propanol were used as supplied. Potassium propionate, potassium pivalate, potassium isobutyrate and potassium *n*-butyrate were prepared from the relevant carboxylic acid by neutralisation with KOH in ethanol solution, the ethanol and residual acid distilled off, and the solid dried and recrystallized from ethanol. Potassium hexafluorophosphate was recrystallized from alkaline water before use. Dimethylsulfoxide, diglyme, and ethylene glycol butyl ether were each stirred over 4A molecular sieves for 24 hours, then distilled from KOH at reduced pressure. Distilled water used was of a minimum resistance of 18 MΩ.

8.1.2 Instruments

^{1}H, ^{13}C, ^{19}F and ^{31}P NMR spectra were recorded on a Brucker 300 MHz spectrometer. Reported ^{1}H and ^{13}C chemical shifts are referenced to the 9H peak of sodium 4,4-dimethyl-4-silapentane-1-sulfonate (DSS), present as an internal reference in all such samples unless otherwise stated. NMR-scale pH measurements were made using a Hanna Instruments 1093B electrode, calibrated by a three-point calibration using aqueous buffer solutions (of pH 4.010, 7.010 and 10.010 respectively) supplied by Hanna Instruments. Other pH measurements were made using a Jenway 924005 electrode, calibrated in the same manner. A 25 ml glass burette was used for the titrations. Water content measurements were made using a Mettler-Toledo V20 volumetric Karl-Fischer titrator.

8.1.2.1 Description of small vapour-liquid equilibrium cell (VLE1)

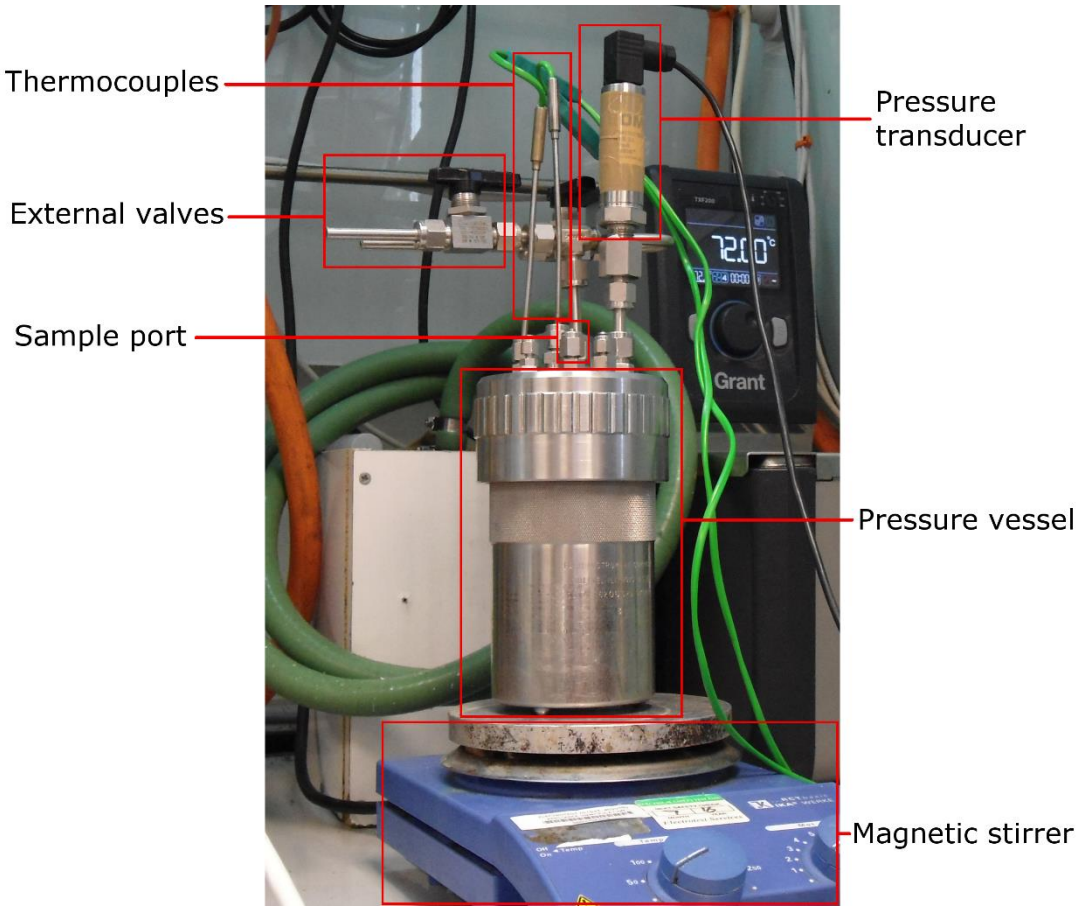

Figure 8.1: Vapour-liquid equilibrium cell designated VLE1

The vapour-liquid equilibrium cell designated VLE1 (Figure 8.1) was originally designed by C-Capture Ltd.[159] and consisted of a Parr 1108 stainless-steel vessel, equipped with a custom-built lid containing the following:

- Thermocouple (K-type) located at top of vessel for temperature monitoring of vapour phase;
- Thermocouple (K-type) extending to base of vessel for temperature monitoring of liquid phase;
- Omega 0-3.5 bar (absolute) pressure transducer;
- Sample port for attachment to gas chromatograph (not used in this work);
- Sample port for addition/removal by syringe, equipped with rubber septum and sealed when not in use;
- Dual inlet/outlet for gas or vacuum supply.

Stirring was provided via a magnetic stir bar placed inside the cell. Instrument output was monitored using the LabVIEW environment developed by National Instruments.[209] The sample port septum was regularly replaced after every 3-4 experiments. Prior to each use, the cell was pressure-tested by application of a vacuum to the interior of the cell followed by sealing of all ports. Only if this internal vacuum could be sustained did experimental work proceed.

8.1.2.2 Description of large vapour-liquid equilibrium cell (VLE2)

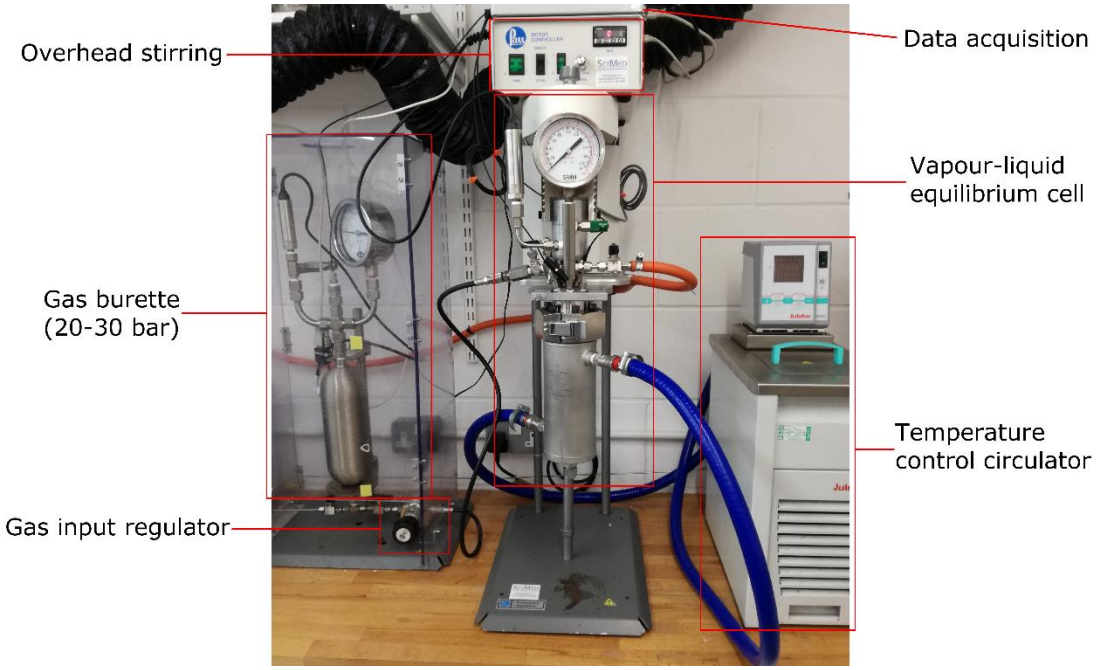

Figure 8.2: Vapour-liquid equilibrium cell designated VLE2 (whole apparatus).

The vapour-liquid equilibrium cell designated VLE2 (Figure 8.2, Figure 8.3) was originally developed by C-Capture Ltd. and consists of a stainless steel vessel equipped with a heating jacket, insulation and overhead stirring incorporating a gas impeller. Pressure and temperature in the cell are continuously monitored with built-in thermocouples and a pressure transducer. The cell is connected through a needle valve and gas regulator to a gas burette from which CO_2 is supplied. The cell also contains an external port for venting and pressure-testing.

Prior to every experimental run, the cell was pressure-tested by evacuating the interior and then sealing all ports. Only if the standing vacuum was retained did experimental work proceed.

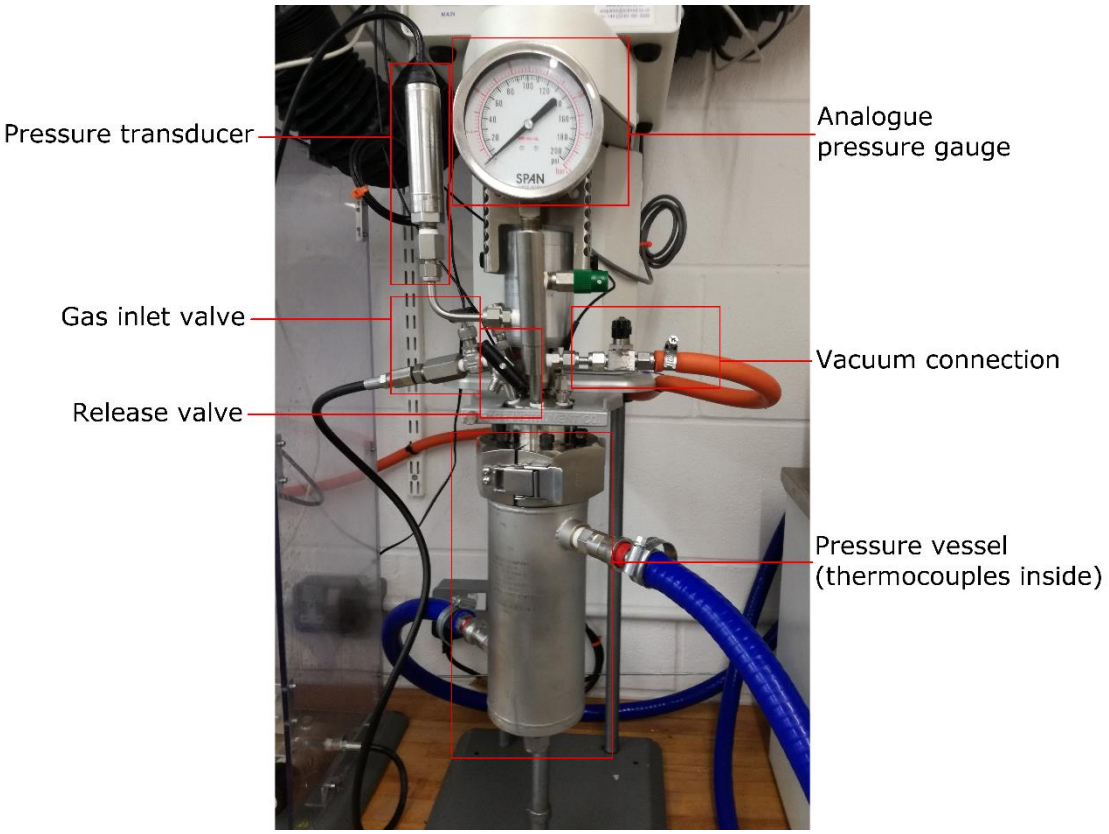

Figure 8.3: Vapour-liquid equilibrium cell designated VLE2 (the cell itself). Additional insulation surrounding the pressure vessel not shown here.

8.2 CO_2 absorption with aqueous amine solutions

8.2.1 Procedures

8.2.1.1 Preparation of solutions

8.2.1.1.1 Preparation of amine solutions

Amine capture solutions were prepared in 250 ml batch solutions. The appropriate amine(s) were dissolved in distilled water at the required concentration, along with DSS (0.27 g, 1.3 mmol, for a concentration of 5 mmol L^{-1}) and made up to 250 ml in a volumetric flask. The solutions prepared in this manner are listed in Table 8.1.

Table 8.1: Amine solutions prepared in this work.

Amine 1	Amine 1 conc. (mol L^{-1})	Amine 1 mass (g)	Amine 2	Amine 2 conc. (mol L^{-1})	Amine 2 mass (g)
MEA	5	76.35	n/a	n/a	n/a
MDEA	3	89.37	MEA	1	15.27
AMP	3	66.86	MEA	1	15.27
AMP	3	66.86	PZ	1	21.54

8.2.1.1.2 Preparation of phenoxide solutions

Phenoxide capture solutions were prepared in 250 mL batch solutions. The appropriate amount of 90.1% aqueous phenol was neutralised at 0 °C *in situ* by equimolar potassium hydroxide dissolved in *ca.* 25 mL water, then the appropriate amount (if any) of monoethanolamine added, along with DSS (0.27 g, 1.3 mmol, for a concentration of 5 mmol L^{-1}), and the solution made up to 250 mL in a volumetric flask. The solutions prepared in this manner are listed in Table 8.2.

Table 8.2: Phenoxide solutions prepared in this work.

Required KOPh (mol L^{-1})	90.1% aqueous phenol (g)	KOH (g)	MEA conc. (mol L^{-1})	MEA mass (g)
1	26.11	14.03	n/a	n/a
1	26.11	14.03	1	15.27
2	52.23	28.06	1	15.27
2	52.23	28.06	2	30.54
3	78.34	42.08	1	15.27
1	26.11	14.03	2	30.54

8.2.1.2 CO_2 absorption procedure

CO_2 absorption was carried out in a 50 mL graduated cylinder equipped with magnetic stirring and maintained at a constant 25 °C with the use of a water bath. The solution of interest (30 mL) was added to the cylinder and incubated for 30 minutes. Pure CO_2 was introduced through a syringe needle at the base of the cylinder, at a constant flow rate of 0.3 L min^{-1} (measured using a rotameter connected to the CO_2 supply), for a set time. For each solution studied, seven samples were exposed to CO_2 in this manner for 1, 5, 10, 15, 30, 60 and 90 minutes respectively.

Sampling of the carboxylated solution depended upon its physical properties, as those containing > 1 mol potassium phenoxide tended to separate into two phases, and in some cases also a white precipitate was produced, identified as $KHCO_3$. Any precipitate was decanted, dried under vacuum over H_2SO_4 and weighed. For biphasic solutions, the mixture was stirred at a high rate, and a sample **(c)** withdrawn. The two phases were then allowed to fully separate and the volume of each phase measured using the graduations on the cylinder. A sample of the organic upper phase **(b)** was withdrawn by syringe, with care taken not to disturb the phase boundary. Then, a sample of the aqueous lower phase **(a)** was withdrawn by syringe.

8.2.1.3 General procedure for measurement of absorbed CO_2 concentration

The concentration of CO_2 absorbed into solution was measured using the VLE1 (see 8.1.2.1). The analyte (2 ml) was injected through the sample port by syringe, and the vessel then sealed. Acetic acid (1 ml) was injected through the sample port with stirring. Concentration of absorbed CO_2 was calculated from the resultant pressure increase using the ideal gas law, with the volume nearly constant (1 ml subtracted for the volume of acetic acid) and the pressure and temperature measured by the instrument.

In cases where the amount of CO_2 released was very small, the experiment was repeated using 5 ml of analyte and 2 ml of acetic acid.

8.2.1.4 Procedure for carboxylated species determination

The procedure for determining the concentrations of carboxylated species necessarily differed depending on the physical behaviour of the solution under study.

8.2.1.4.1 Monophasic solutions

A sample (0.5 mL) of the solution under study was slightly diluted with D_2O (75 µL) and the ^1H NMR spectrum (300 MHz, 298K) recorded. The concentration of any carbamate species was determined by integration of the carbamate peaks as a mole fraction of the concentration of the amine. The initial concentration of the amine is a known quantity from solution preparation. The concentration of bicarbonate was then calculated by subtracting the carbamate concentration from the total absorbed CO_2 concentration (measured as per 8.2.1.3). This neglects that other non-carbamate species (chiefly carbonate) are present, but the concentration of these is very small (<1 mol%).[78]

8.2.1.4.2 Multiphasic solutions

Many phenoxide-containing compositions produced two phases upon carboxylation – a dark, phenol-rich upper phase and a colourless lower phase. Three samples, comprising the aqueous **(a)**, organic **(b)** and total mixture of phases **(c)**, were obtained as described in 8.2.1.2. The amount of absorbed CO_2 in each was measured using the VLE1 (see 8.2.1.3).

A ^{1}H NMR spectrum of the aqueous phase **(a)** was recorded and the amount of any carbamates determined as a mole fraction of amine by integration of the carbamate and amine peaks. For each of the remaining two samples **(b)** and **(c)**, a small amount (0.5 µL) was dissolved in D_2O (0.5 mL) and the ^{1}H NMR spectra recorded.

The ratios of amine (including carbamate) to phenol was measured in each sample via integration of the 1H NMR spectra. From this the amount of each phase was calculated as a mole fraction, by virtue of the fact that the ratio of amine to phenol in the total (mixed) solution is an average of this ratio in each phase, weighted by the amount of each phase. The mole fraction of carbamate within the aqueous phase was then converted to a mole fraction of the solution as a whole, and thence to concentration using the known concentration of the capture agents.

8.2.2 Speciation studies of amine and phenolate-based CO_2 capture solvents

8.2.2.1 5 mol L^{-1} monoethanolamine and CO_2

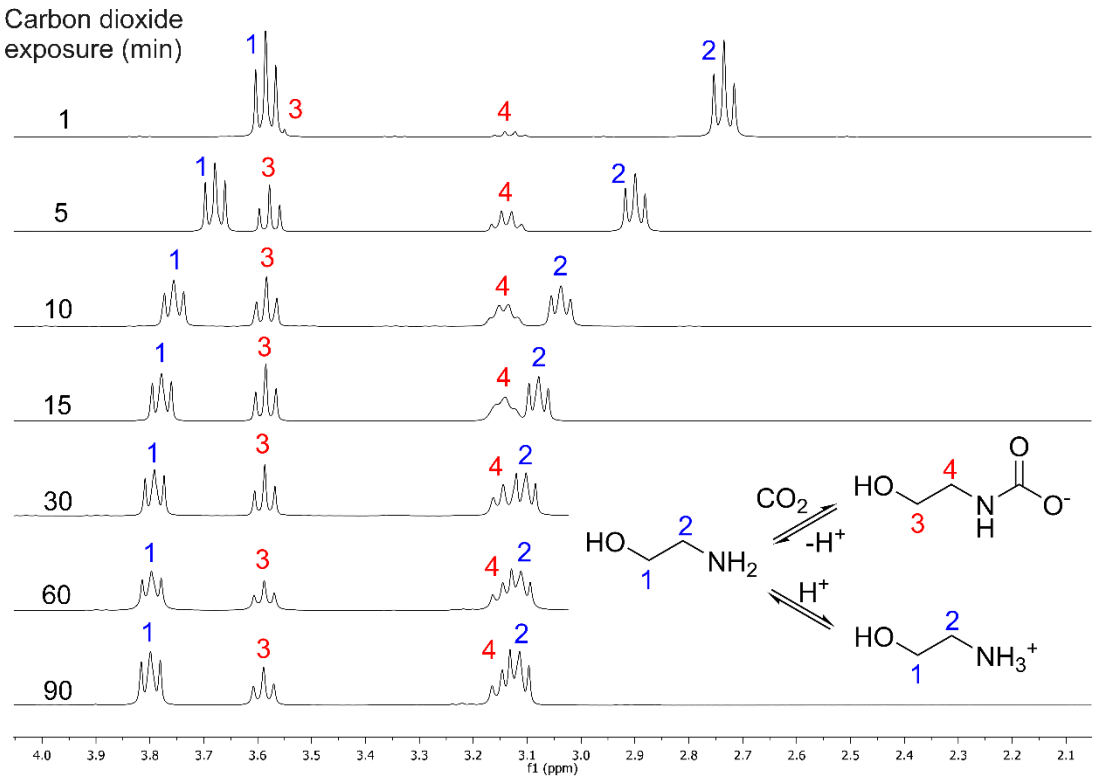

Figure 8.4: ^{1}H NMR stacked plot following carboxylation of 5 mol L^{-1} monoethanolamine.

Table 8.3: ^{1}H NMR data from carboxylation of 5 mol L^{-1} monoethanolamine.

Sample	CO_2 exposure (min)	MEA/carbamate integral ratio (^{1}H NMR)	δ MEA O-CH_2	δ MEA N-CH_2	δ $MEACO_2^-$ O-CH_2	δ $MEACO_2^-$ N-CH_2
1	1	0.93	3.58	2.73	3.57	3.13
2	5	0.68	3.68	2.90	3.58	3.14
3	10	0.57	3.76	3.04	3.58	3.15
4	15	0.55	3.78	3.08	3.58	3.14
5	30	0.58	3.79	3.10	3.59	3.13
6	60	0.63	3.80	3.11	3.59	3.14
7	90	0.65	3.80	3.11	3.59	3.14

Table 8.4: Calculated speciation for carboxylation of 5 mol L^{-1} monoethanolamine.

Time (min)	Acid-recoverable CO_2 (mol L^{-1})[a]	Carbamate (mol L^{-1})[b]	Bicarbonate (mol L^{-1})[c]
1	0.37	0.35	0.02
5	1.59	1.60	-
10	2.33	2.15	0.18
15	2.46	2.25	0.21
30	2.67	2.10	0.57
60	3.08	1.85	1.23
90	3.15	1.75	1.40

[a]*Calculated from the amount of CO_2 released following addition of excess acetic acid.*

[b]*Measured as a mole fraction of total MEA concentration using ^{1}H NMR.*

[c]*Calculated as the difference between total CO_2 concentration and carbamate concentration.*

8.2.2.2 Carboxylation of 3 mol L^{-1} N-methyldiethanolamine, 1 mol L^{-1} monoethanolamine

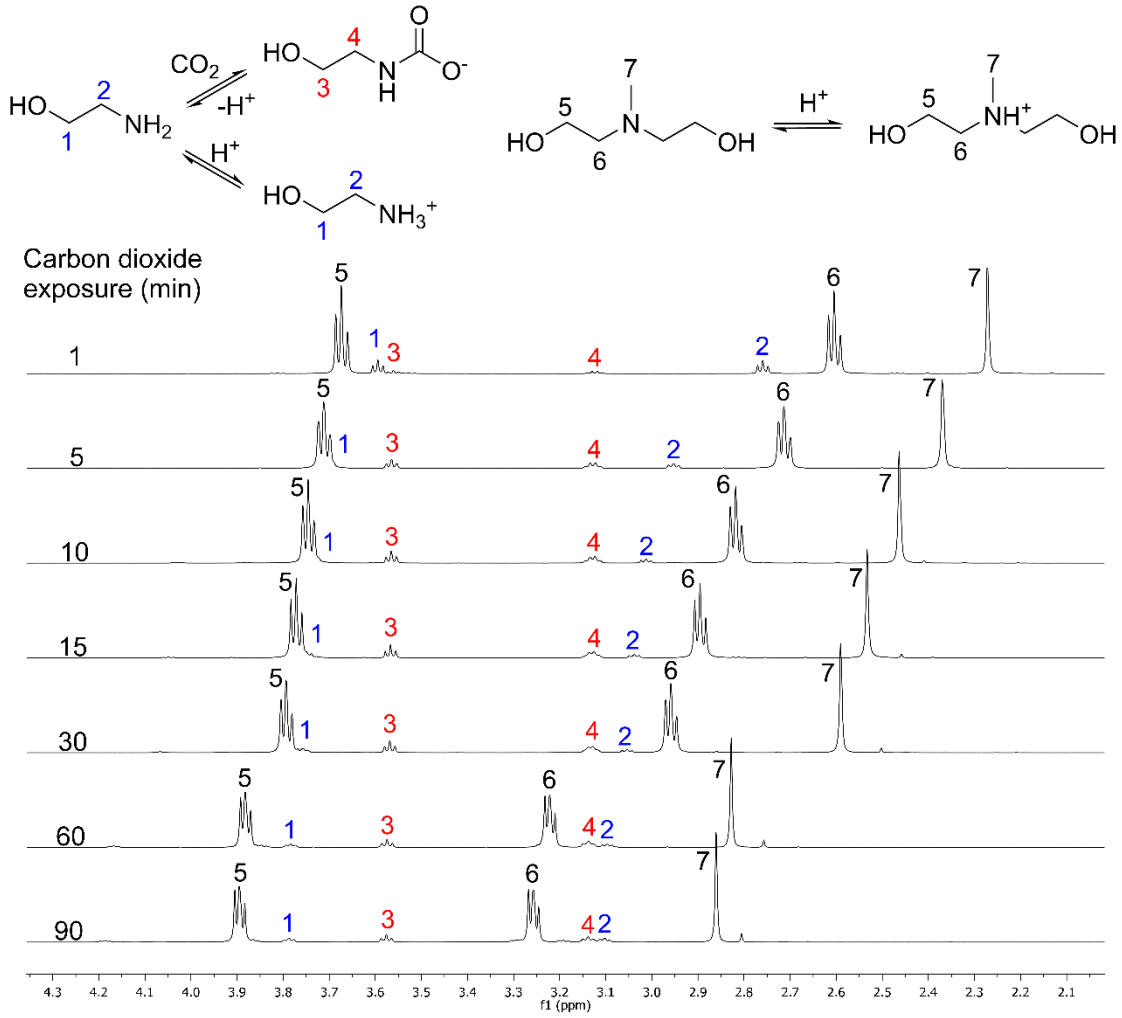

Figure 8.5: ^{1}H NMR stacked plot following carboxylation of solutions containing 3 mol L^{-1} N-methyldiethanolamine and 1 mol L^{-1} monoethanolamine.

Table 8.5: ^{1}H NMR data from carboxylation of solutions containing 3 mol L^{-1} N-methyldiethanolamine and 1 mol L^{-1} monoethanolamine

Sample	CO_2 exposure (min)	MEA/ carbamate ratio	δ MEA O-CH_2	δ MEA N-CH_2	δ $MEACO_2^-$ O-CH_2	δ $MEACO_2^-$ N-CH_2	δ MDEA O-CH_2	δ MDEA N-CH_2	δ MDEA N-CH_3
1	1	0.83	3.59	2.76	3.56	3.13	3.67	2.6	2.27
2	5	0.41	3.71	2.95	3.56	3.13	3.71	2.71	2.37
3	10	0.30	3.75	3.01	3.57	3.13	3.75	2.82	2.46
4	15	0.30	3.77	3.04	3.57	3.14	3.77	2.90	2.53
5	21	0.27	3.76	3.05	3.57	3.14	3.79	2.96	2.59
6	60	0.37	3.78	3.1	3.57	3.14	3.88	3.22	2.83
7	90	0.41	3.79	3.10	3.58	3.14	3.90	3.26	2.86

Table 8.6: Calculated speciation for carboxylation of solutions containing 3 mol L^{-1} N-methyldiethanolamine and 1 mol L^{-1} monoethanolamine.

Time (min)	Acid-recoverable CO_2 (mol L^{-1})[a]	Carbamate (mol L^{-1})[b]	Bicarbonate (mol L^{-1})[c]
1	0.20	0.11	0.09
5	0.62	0.38	0.24
10	1.05	0.45	0.6
15	1.29	0.45	0.84
30	1.58	0.47	1.11
60	2.68	0.40	2.28
90	2.90	0.38	2.52

[a]*Calculated from the amount of CO_2 released following addition of excess acetic acid.*

[b]*Measured as a mole fraction of total base concentration using ^1H NMR.*

[c]*Calculated as the difference between total CO_2 concentration and carbamate concentration.*

8.2.2.3 Carboxylation of 3 mol L^{-1} 2-amino-2-methyl-1-propanol and 1 mol L^{-1} monoethanolamine

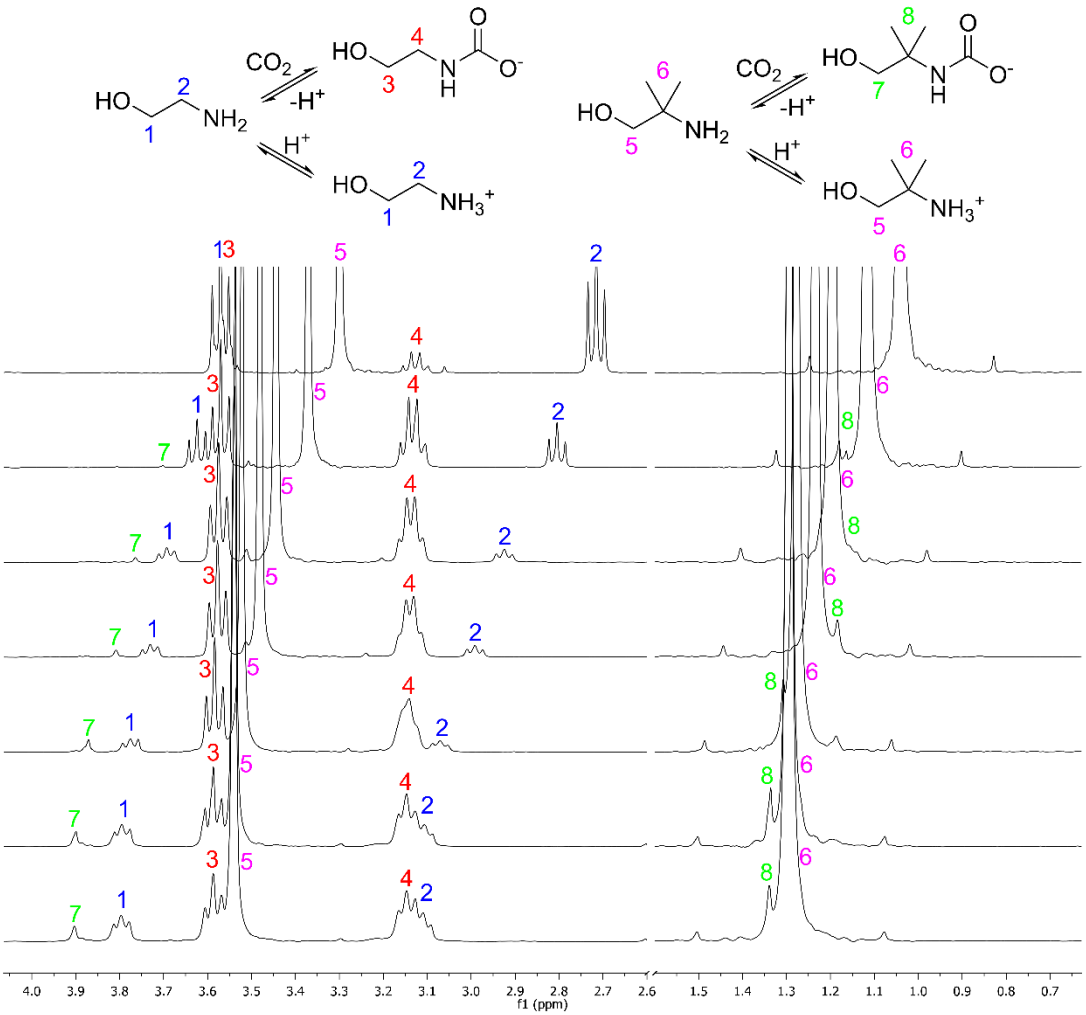

Figure 8.6: ^1H NMR stacked plot following carboxylation of solutions containing 3 mol L^{-1} 2-amino-2-methyl-1-propanol and 1 mol L^{-1} monoethanolamine.

Table 8.7: Calculated speciation for carboxylation of solutions containing 3 mol L^{-1} 2-amino-2-methyl-1-propanol and 1 mol L^{-1} monoethanolamine.

Time (min)	Acid-recoverable CO_2 (mol L^{-1})[a]	Carbamate (mol L^{-1})[b]	Bicarbonate (mol L^{-1})[c]
1	0.21	0.11	0.10
5	0.98	0.50	0.48
10	1.54	0.61	0.93
15	1.98	0.61	1.37
30	2.35	0.57	1.78
60	3.01	0.49	2.52
90	2.95	0.51	2.44

[a]*Calculated from the amount of CO_2 released following addition of excess acetic acid.*

[b]*Measured as a mole fraction of total base concentration using ^1H NMR.*

[c]*Calculated as the difference between total CO_2 concentration and carbamate concentration.*

8.2.2.4 Carboxylation of 3 mol L^{-1} 2-amino-2-methyl-1-propanol and 1 mol L^{-1} piperazine

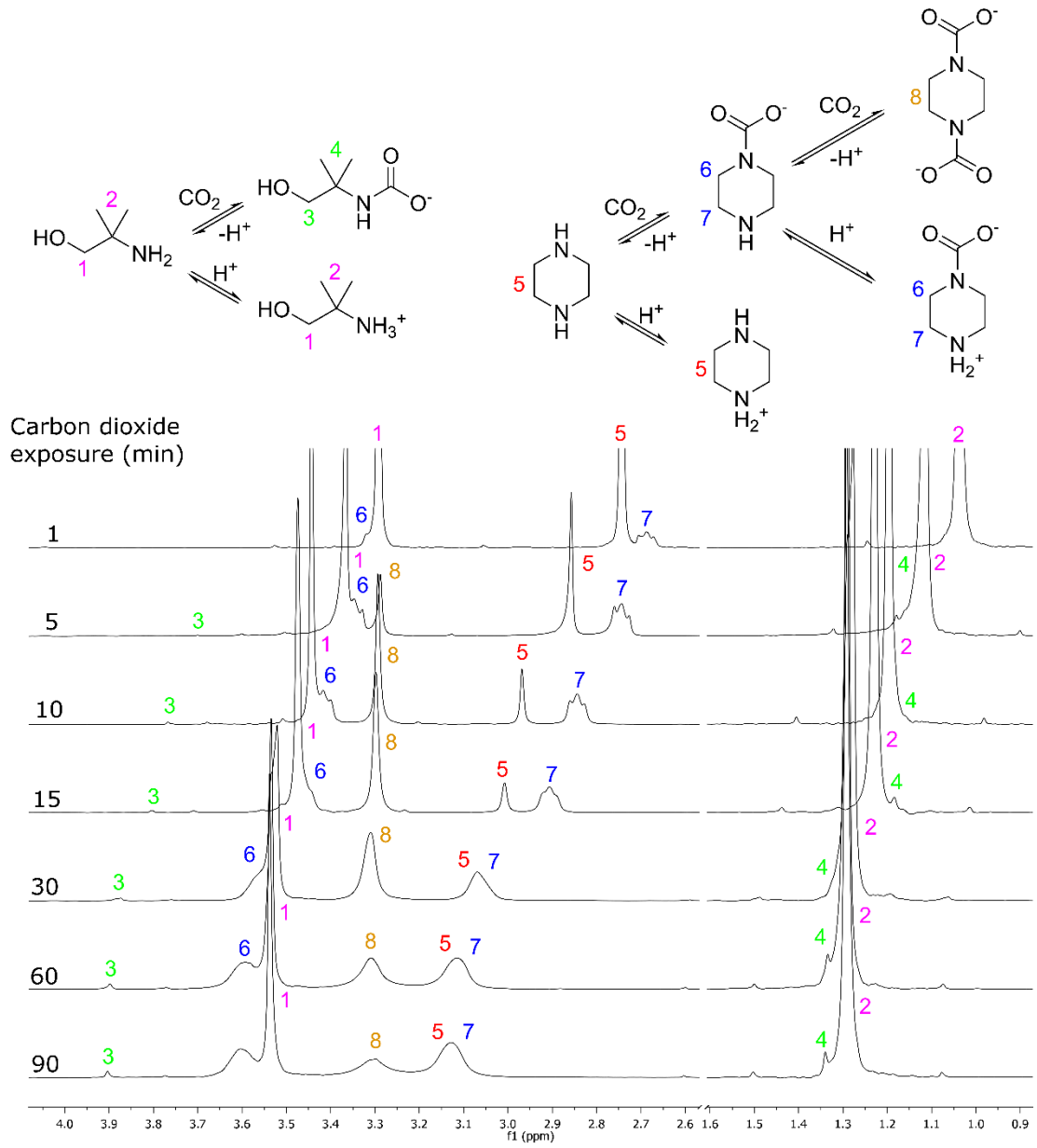

Figure 8.7: ^{1}H NMR stacked plot following carboxylation of solutions containing 3 mol L^{-1} 2-amino-2-methyl-1-propanol and 1 mol L^{-1} piperazine.

Table 8.8: Calculated speciation for carboxylation of solutions containing 3 mol L^{-1} 2-amino-2-methyl-1-propanol and 1 mol L^{-1} piperazine.

Time (min)	Acid-recoverable CO_2 (mol L^{-1})[a]	PZ monocarbamate (mol L^{-1})[b]	PZ bis(carbamate) (mol L^{-1})[c]	Bicarbonate (mol L^{-1})[d]
1	0.38	0.20	-	0.18
5	0.99	0.59	0.16	0.08
10	1.85	0.55	0.54	0.22
15	2.18	0.51	0.60	0.47
30	2.98	0.48	0.63	1.24
60	3.29	0.67	0.44	1.75
90	3.51	0.77	0.33	2.07

[a]*Calculated from the amount of CO_2 released following addition of excess acetic acid.*

[b]*Measured as a mole fraction of total base concentration using ^1H NMR. Comprises both PZ monocarbamate and the equivalent ammonium zwitterion.*

[c]*Measured as a mole fraction of total base concentration using ^1H NMR.*

[d]*Calculated as the difference between total CO_2 concentration and carbamate concentration.*

8.2.2.5 Carboxylation of 1 mol L^{-1} potassium phenoxide

Table 8.9: Absorption of CO_2 into solutions containing 1 mol L^{-1} potassium phenoxide.

Time (min)	Acid-recoverable CO_2 (mol L^{-1})[a]
1	0.04
5	0.18
10	0.37
15	0.56
30	0.92
60	0.89
90	0.92

[a]*Calculated from the amount of CO_2 released following addition of excess acetic acid.*

8.2.2.6 Carboxylation of 1 mol L^{-1} potassium phenoxide and 1 mol L^{-1} monoethanolamine

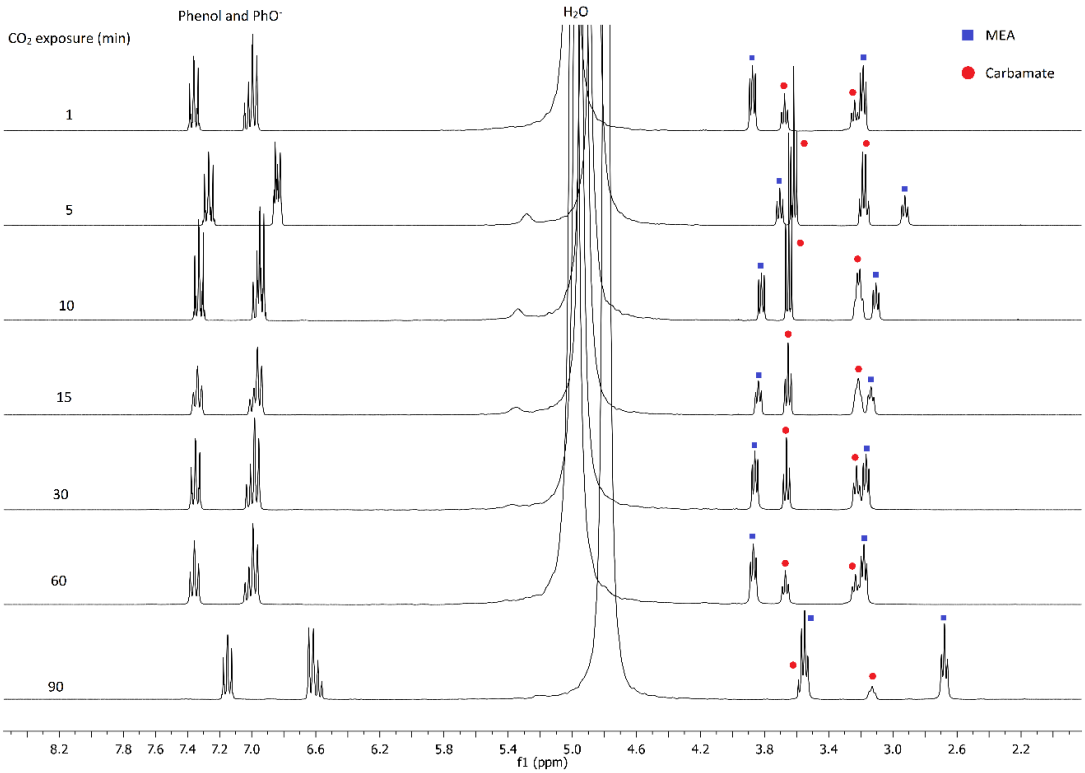

Figure 8.8: ^{1}H NMR stacked plot following carboxylation of solutions containing 1 mol L^{-1} potassium phenoxide and 1 mol L^{-1} monoethanolamine.

Table 8.10: ^{1}H NMR data from carboxylation of solutions containing 1 mol L^{-1} potassium phenoxide and 1 mol L^{-1} monoethanolamine.

Sample	CO_2 exposure (min)	MEA/ carbamate ratio	δ MEA O-CH_2	δ MEA N-CH_2	δ $MEACO_2^-$ O-CH_2	δ $MEACO_2^-$ N-CH_2	δ PhOH *meta*-H	δ PhOH *ortho*-H	δ PhOH *para*-H
1	1	0.82	3.55	2.68	3.57	3.13	7.15	6.63	6.59
2	5	0.31	3.71	2.93	3.62	3.18	7.27	6.84	6.84
3	10	0.34	3.82	3.11	3.65	3.22	7.33	6.94	6.97
4	15	0.40	3.84	3.14	3.65	3.21	7.34	6.95	6.98
5	30	0.56	3.86	3.17	3.66	3.23	7.35	6.97	7.01
6	60	0.68	3.87	3.18	3.67	3.23	7.36	6.98	7.02
7	90	0.69	3.88	3.18	3.68	3.24	7.36	6.98	7.02

Table 8.11: Calculated speciation for carboxylation of solutions containing 1 mol L^{-1} potassium phenoxide and 1 mol L^{-1} monoethanolamine.

Time (min)	Acid-recoverable CO_2 (mol L^{-1})[a]	Carbamate (mol L^{-1})[b]	Bicarbonate (mol L^{-1})[c]
1	0.21	0.23	0.00
5	0.90	0.87	0.03
10	1.13	0.84	0.29
15	1.28	0.76	0.52
30	1.57	0.56	1.01
60	1.66	0.41	1.25
90	1.64	0.39	1.25

[a]*Calculated from the amount of CO_2 released following addition of excess acetic acid.*

[b]*Measured as a mole fraction of total base concentration using ^1H NMR.*

[c]*Calculated as the difference between total CO_2 concentration and carbamate concentration.*

8.2.2.7 Carboxylation of 2 mol L^{-1} potassium phenoxide and 1 mol L^{-1} monoethanolamine

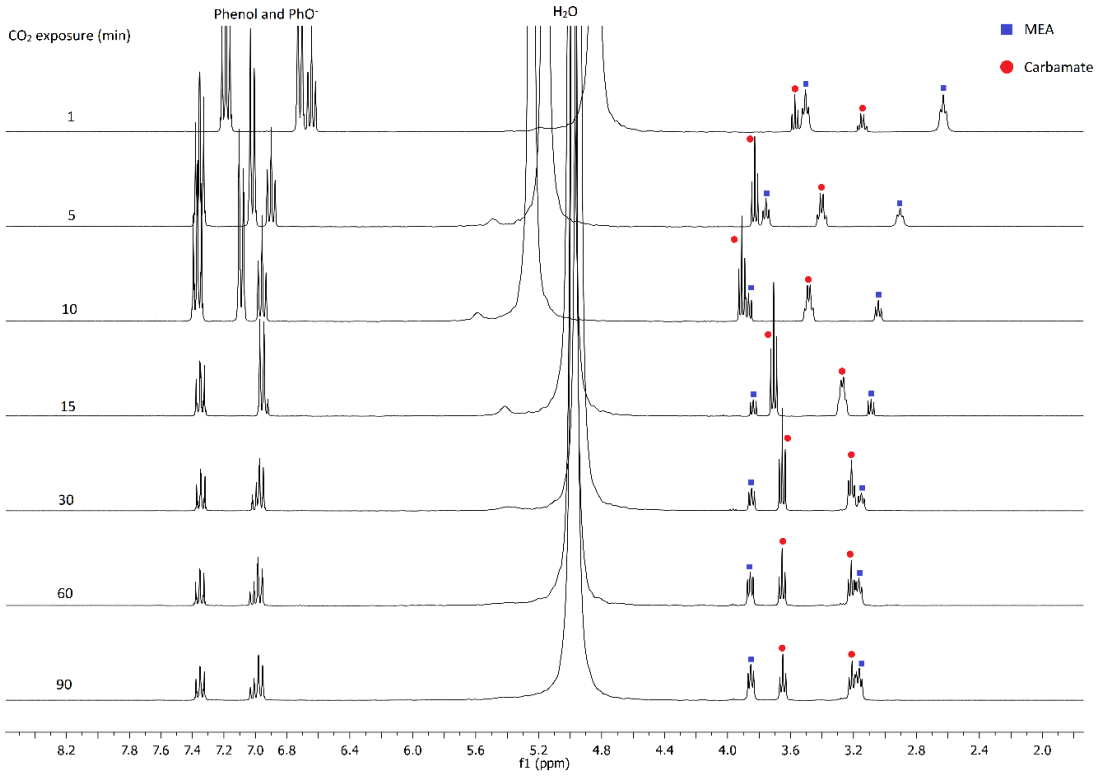

Figure 8.9: ^1H NMR stacked plot following carboxylation of solutions containing 2 mol L^{-1} potassium phenoxide and 1 mol L^{-1} monoethanolamine. Where multiple phases were produced (from 15 mins onwards) the spectrum shown is that of the aqueous phase.

Table 8.12: Relevant ^{1}H NMR integral ratios from carboxylation of solutions containing 2 mol L^{-1} potassium phenoxide and 1 mol L^{-1} monoethanolamine.

Sample	Time (min)	MEA/KOPh ratio (aqueous)	MEA/KOPh ratio (organic)	MEA/KOPh ratio (overall)	MEA/carbamate ratio
1	1	0.28	-	0.28	0.77
2	5	0.27	-	0.27	0.41
3	10	0.27	-	0.27	0.28
4	15	0.55	0.05	0.27	0.16
5	30	0.66	0.04	0.27	0.31
6	60	0.67	0.05	0.27	0.5
7	90	0.68	0.05	0.27	0.54

Table 8.13: ^{1}H NMR chemical shifts in aqueous phase of carboxylated solutions containing 2 mol L^{-1} potassium phenoxide and 1 mol L^{-1} monoethanolamine.

Sample	Time (min)	δ MEA(H^+) O-CH_2	δ MEA(H^+) N-CH_2	δ $MEACO_2^-$ O-CH_2	δ $MEACO_2^-$ N-CH_2	δ PhO(H) *meta*-H	δ PhO(H) *ortho*-H	δ PhO(H) *para*-H
1	1	3.51	2.63	3.57	3.14	7.18	6.72	6.64
2	5	3.76	2.9	3.83	3.4	7.35	7.02	6.9
3	10	3.87	3.04	3.91	3.49	7.37	7.09	6.96
4	15	3.84	3.09	3.71	3.27	7.35	6.96	6.95
5	30	3.85	3.15	3.65	3.21	7.35	6.96	7
6	60	3.86	3.17	3.65	3.21	7.35	6.97	7.01
7	90	3.85	3.16	3.65	3.21	7.35	6.97	7.01

Table 8.14: Concentrations of carboxylated species following carboxylation of solutions containing 2 mol L^{-1} potassium phenoxide and 1 mol L^{-1} monoethanolamine.

	Aqueous phase				Organic phase		Solution total		
Time (min)	Vol%	Carbamate (mol L^{-1})[a]	Acid-recoverable CO_2 (mol L^{-1})[b]	Bicarbonate (mol L^{-1})[c]	Vol%	Acid-recoverable CO_2 (mol L^{-1})[b]	Carbamate (mol L^{-1})[a]	Bicarbonate (mol L^{-1})[c]	Acid-recoverable CO_2 (mol L^{-1})[b]
1	100	0.23	0.19	-	0	-	0.23	-	0.19
5	100	0.56	0.88	0.32	0	-	0.56	0.32	0.88
10	100	0.68	1.19	0.51	0	-	0.68	0.51	1.19
15	80	0.86	1.84	0.98	20	0.35	0.71	0.82	1.49
30	79	0.72	2.42	1.70	21	0.24	0.59	1.41	2.06
60	81	0.50	2.83	2.33	19	0.31	0.42	1.95	2.29
90	79	0.47	2.84	2.37	21	0.38	0.38	1.96	2.36

[a]*Measured as a mole fraction of total base concentration using 1H NMR.*

[b]*Calculated from the amount of CO2 released following addition of excess acetic acid.*

[c]*Calculated as the difference between total CO2 concentration and carbamate concentration in this phase.*

8.2.2.8 Carboxylation of 3 mol L^{-1} potassium phenoxide and 1 mol L^{-1} monoethanolamine

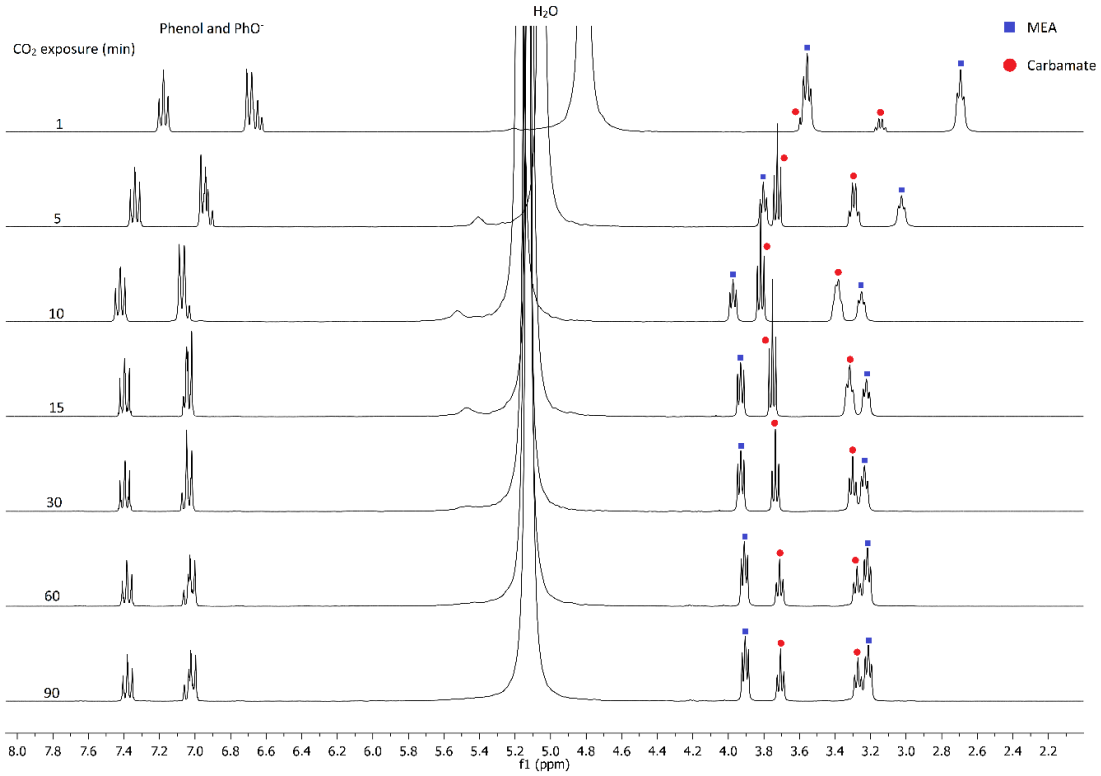

Figure 8.10: ^{1}H NMR stacked plot following carboxylation of solutions containing 3 mol L^{-1} potassium phenoxide and 1 mol L^{-1} monoethanolamine.

Table 8.15: Relevant ^{1}H NMR integral ratios from carboxylation of solutions containing 3 mol L^{-1} potassium phenoxide and 1 mol L^{-1} monoethanolamine.

Sample	MEA/KOPh ratio (aqueous)	MEA/KOPh ratio (organic)	MEA/KOPh ratio (overall)	MEA/ carbamate ratio	Precipitate /g
1	0.19	-	0.19	0.96	-
2	0.19	-	0.19	0.58	-
3	0.19	-	0.19	0.41	-
4	0.21	-	0.21	0.32	-
5	0.67	0.13	0.44	0.45	-
6	0.73	0.13	0.44	0.15	1.76
7	0.72	0.13	0.44	0.37	6.01

Table 8.16: ^{1}H NMR chemical shifts from aqueous phase of carboxylated solutions containing 3 mol L^{-1} potassium phenoxide and 1 mol L^{-1} monoethanolamine.

Sample	δ MEA O-CH_2	δ MEA N-CH_2	δ $MEACO_2^-$ O-CH_2	δ $MEACO_2^-$ N-CH_2	δ PhO(H) *meta*-H	δ PhO(H) *ortho*-H	δ PhO(H) *para*-H
1	3.43	2.55	3.55	3.13	7.17	6.72	6.62
2	3.61	2.72	3.76	3.34	7.29	6.96	6.81
3	3.67	2.79	3.83	3.41	7.30	7.03	6.85
4	3.71	2.83	3.87	3.46	7.29	7.06	6.87
5	3.79	3.04	3.63	3.21	7.31	6.89	6.88
6	3.82	3.11	3.63	3.19	7.33	6.94	6.95
7	3.85	3.15	3.65	3.21	7.35	6.97	7.00

Table 8.17: Calculated concentrations of carboxylated species in carboxylation of solutions containing 3 mol L^{-1} potassium phenoxide and 1 mol L^{-1} monoethanolamine.

	Aqueous phase				Organic phase		Solution total		
Time (min)	Vol%	Carbamate (mol L^{-1})[a]	Acid-recoverable CO_2 (mol L^{-1})[b]	Bicarbonate (mol L^{-1})[c]	Vol%	Acid-recoverable CO_2 (mol L^{-1})[b]	Carbamate (mol L^{-1})[a]	Bicarbonate (mol L^{-1})[c]	Acid-recoverable CO_2 (mol L^{-1})[b]
1	100	0.04	0.19	0.16	-	-	0.04	0.16	0.19
5	100	0.38	0.85	0.47	-	-	0.38	0.47	0.85
10	100	0.54	1.14	0.60	-	-	0.54	0.60	1.14
15	100	0.68	1.36	0.68	-	-	0.68	0.68	1.36
30	48	0.86	2.52	1.66	52	0.34	0.57	1.09	1.85
60	46	0.94	2.95	2.01	54	0.45	0.61	1.73	2.58
90	39	0.73	2.91	2.18	61	0.36	0.45	2.81	3.50

[a]*Measured as a mole fraction of total base concentration using ^{1}H NMR.*

[b]*Calculated from the amount of CO_2 released following addition of excess acetic acid.*

[c]*Calculated as the difference between total CO_2 concentration and carbamate concentration in this phase.*

8.2.2.9 Carboxylation of 2 mol L^{-1} potassium phenoxide and 2 mol L^{-1} monoethanolamine

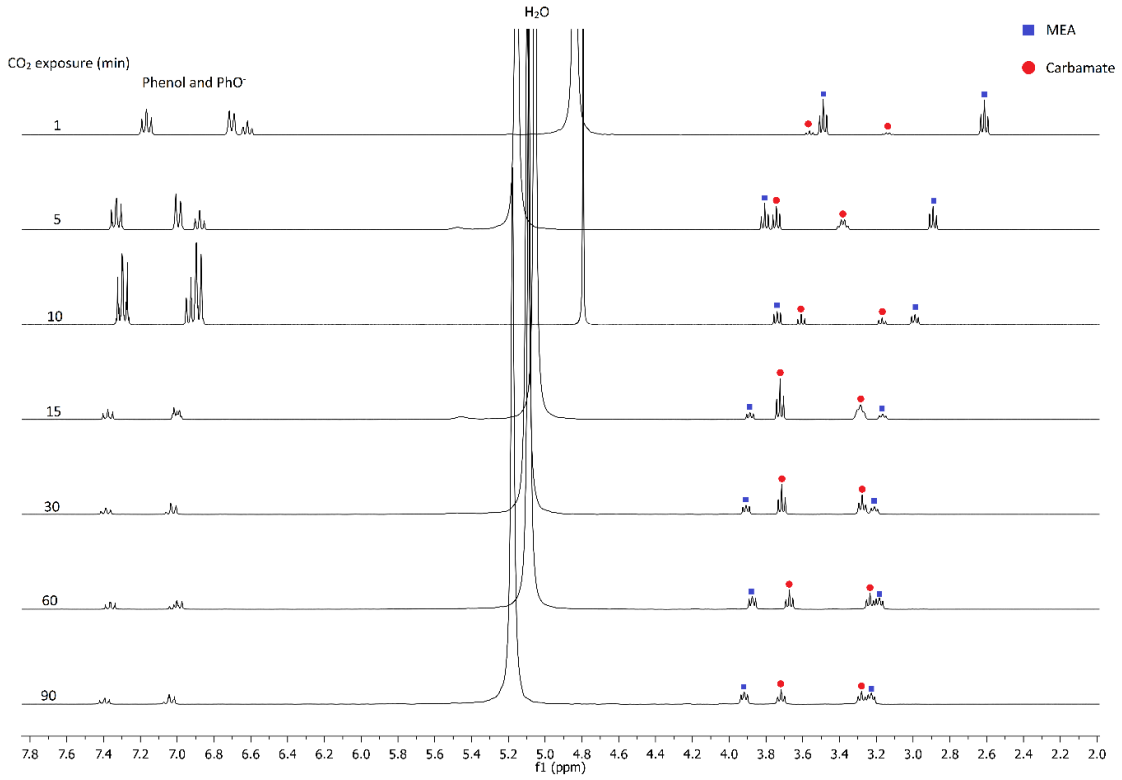

Figure 8.11: ^{1}H NMR stacked plot following carboxylation of solutions containing 2 mol L^{-1} potassium phenoxide and 2 mol L^{-1} monoethanolamine. Where multiple liquid phases were produced (>10 mins) the spectrum shown is that of the aqueous phase.

Table 8.18: Relevant ^{1}H NMR integral ratios from carboxylation of solutions containing 2 mol L^{-1} potassium phenoxide and 2 mol L^{-1} monoethanolamine.

Sample	MEA/KOPh ratio (aqueous)	MEA/KOPh ratio (organic)	MEA/KOPh ratio (overall)	MEA/carbamate ratio
1			0.44	0.89
2			0.43	0.51
3			0.44	0.23
4	0.73	0.14	0.44	0.24
5	0.78	0.14	0.44	0.36
6	0.8	0.13	0.44	0.51
7	0.79	0.13	0.44	0.54

Table 8.19: ^{1}H NMR chemical shifts from aqueous phase of carboxylated solutions containing 2 mol L^{-1} potassium phenoxide and 2 mol L^{-1} monoethanolamine.

Sample	δ MEA(H^+) O-CH_2	δ MEA(H^+) N-CH_2	δ $MEACO_2^-$ O-CH_2	δ $MEACO_2^-$ N-CH_2	δ PhO(H) *meta*-H	δ PhO(H) *ortho*-H	δ PhO(H) *para*-H
1	3.49	2.61	3.56	3.14	7.17	6.71	6.62
2	3.74	2.89	3.81	3.38	7.33	7	6.88
3	3.91	3.15	3.8	3.37	7.4	7.04	7
4	3.89	3.17	3.72	3.29	7.38	7.01	7
5	3.9	3.21	3.71	3.27	7.38	7.02	7.03
6	3.87	3.18	3.67	3.23	7.37	6.99	7.02
7	3.92	3.23	3.72	3.28	7.4	7.03	7.05

Table 8.20: Calculated concentrations of carboxylated species in carboxylation of solutions containing 2 mol L^{-1} potassium phenoxide and 2 mol L^{-1} monoethanolamine.

	Aqueous phase				Organic phase		Solution total		
Time (min)	Vol%	Carbamate (mol L^{-1})[a]	Acid-recoverable CO_2 (mol L^{-1})[b]	Bicarbonate (mol L^{-1})[c]	Vol%	Acid-recoverable CO_2 (mol L^{-1})[b]	Carbamate (mol L^{-1})[a]	Bicarbonate (mol L^{-1})[c]	Acid-recoverable CO_2 (mol L^{-1})[b]
1	100	0.22	0.25	0.03	-	-	0.22	0.03	0.25
5	100	0.95	1.19	0.24	-	-	0.95	0.24	1.19
10	100	1.56	2.10	0.54	-	-	1.25	0.43	1.81
15	75	1.59	2.45	0.86	25	0.77	1.27	0.69	2.03
30	74	1.33	2.99	1.66	26	0.78	1.05	1.31	2.51
60	72	1.04	3.30	2.26	28	0.99	0.82	1.77	2.75
90	75	0.96	3.25	2.29	25	0.94	0.77	1.83	2.65

[a]*Measured as a mole fraction of total base concentration using ^{1}H NMR.*

[b]*Calculated from the amount of CO_2 released following addition of excess acetic acid.*

[c]*Calculated as the difference between total CO_2 concentration and carbamate concentration in this phase.*

8.2.2.10 Carboxylation of 2 mol L^{-1} monoethanolamine and 1 mol L^{-1} potassium phenoxide

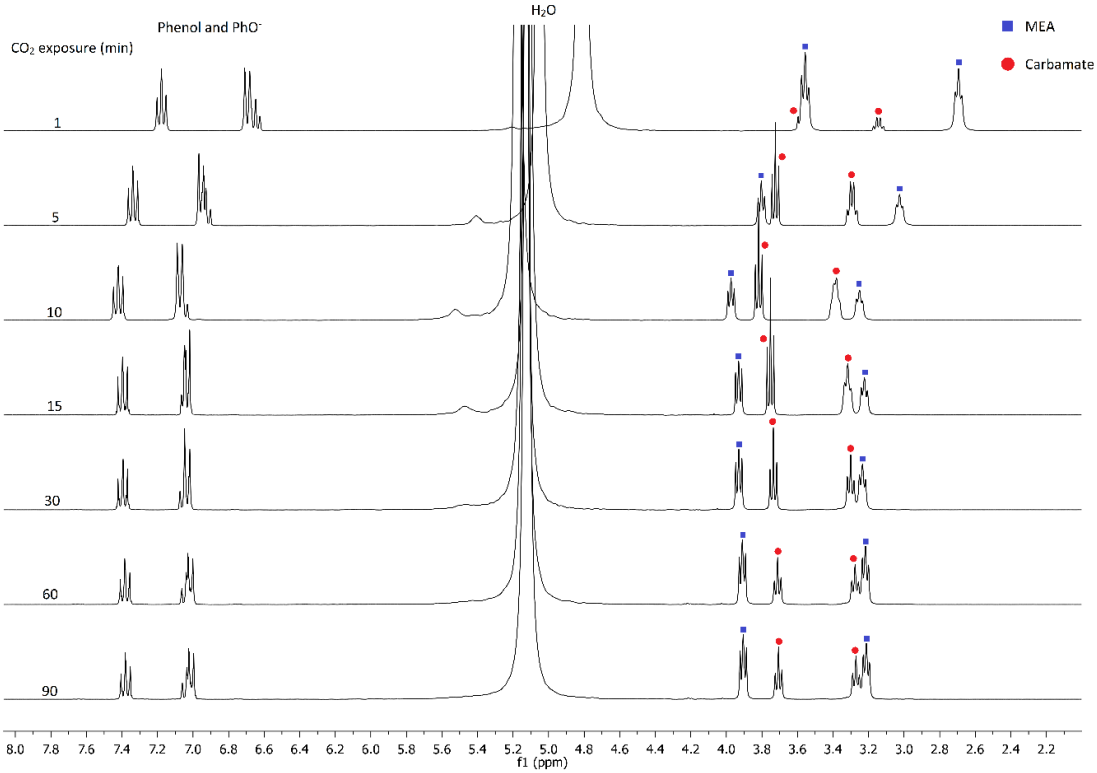

Figure 8.12: ^{1}H NMR stacked plot following carboxylation of solutions containing 2 mol L^{-1} monoethanolamine and 1 mol L^{-1} potassium phenoxide. Where multiple liquid phases were produced (>10 mins) the spectrum shown is that of the aqueous phase.

Table 8.21: Relevant ^{1}H NMR integral ratios from carboxylation of solutions containing 2 mol L^{-1} monoethanolamine and 1 mol L^{-1} potassium phenoxide.

Sample	MEA/KOPh ratio (aqueous)	MEA/KOPh ratio (organic)	MEA/KOPh ratio (overall)	MEA/carbamate ratio
1	1	0	0.61	0.86
2	1	0	0.61	0.47
3	1	0	0.62	0.41
4	0.68	0.15	0.61	0.43
5	0.70	0.13	0.61	0.55
6	0.71	0.12	0.61	0.63
7	0.72	0.13	0.61	0.62

Table 8.22: ^{1}H NMR chemical shifts from aqueous phase of carboxylated solutions containing 2 mol L^{-1} monoethanolamine and 1 mol L^{-1} potassium phenoxide.

Sample	δ MEA(H^+) O-CH_2	δ MEA(H^+) N-CH_2	δ $MEACO_2^-$ O-CH_2	δ $MEACO_2^-$ N-CH_2	δ PhO(H) *meta*-H	δ PhO(H) *ortho*-H	δ PhO(H) *para*-H
1	3.56	2.69	3.58	3.14	7.18	6.7	6.65
2	3.8	3.03	3.72	3.29	7.34	6.96	6.93
3	3.97	3.25	3.82	3.38	7.42	7.08	7.06
4	3.93	3.22	3.75	3.32	7.4	7.04	7.05
5	3.93	3.23	3.74	3.3	7.39	7.04	7.05
6	3.91	3.22	3.71	3.28	7.38	7.02	7.04
7	3.9	3.21	3.71	3.27	7.38	7.02	7.04

Table 8.23: Calculated concentrations of carboxylated species in carboxylation of solutions containing 2 mol L^{-1} monoethanolamine and 1 mol L^{-1} potassium phenoxide.

	Aqueous phase				Organic phase		Solution total		
Time (min)	Vol%	Carbamate (mol L^{-1})[a]	Acid-recoverable CO_2 (mol L^{-1})[b]	Bicarbonate (mol L^{-1})[c]	Vol%	Acid-recoverable CO_2 (mol L^{-1})[b]	Carbamate (mol L^{-1})[a]	Bicarbonate (mol L^{-1})[c]	Acid-recoverable CO_2 (mol L^{-1})[b]
1	100	0.22	0.25	0.03	-	-	0.22	0.03	0.25
5	100	0.95	1.19	0.24	-	-	0.95	0.24	1.19
10	100	1.56	2.10	0.54	-	-	1.25	0.43	1.81
15	75	1.59	2.45	0.86	25	0.77	1.27	0.69	2.03
30	74	1.33	2.99	1.66	26	0.78	1.05	1.31	2.51
60	72	1.04	3.30	2.26	28	0.99	0.82	1.77	2.75
90	75	0.96	3.25	2.29	25	0.94	0.77	1.83	2.65

[a]*Measured as a mole fraction of total base concentration using ^{1}H NMR.*

[b]*Calculated from the amount of CO_2 released following addition of excess acetic acid.*

[c]*Calculated as the difference between total CO_2 concentration and carbamate concentration in this phase.*

8.3 Determination of pK_a of CO_2 and carboxylates in nonaqueous solutions

8.3.1 Solution preparation

Stock solutions (250g) were prepared gravimetrically from an organic solvent and water. Organic solvents used were: DMSO, ethanol, 1,4-dioxane, ethylene glycol butyl ether (EGBE) and

diglyme. For each solvent, stock solutions were prepared containing, respectively: 5, 10, 15, 30 and 50 wt% water.

8.3.1.1 Titrant preparation

Titrant solutions (50 ml) were prepared by dissolving concentrated hydrochloric acid (37%, 0.1 g, for a concentration of 0.02 M) and potassium hexafluorophosphate (4.60 g, for a concentration of 0.1 M) in a stock solution prepared as above, with additional organic solvent added in order to offset the water content of the hydrochloric acid.

8.3.1.2 Analyte preparation

Analyte solutions (50 ml) were prepared from a potassium carboxylate (used as a 1 wt% aqueous solution, for a concentration of 2.5 mM) and potassium hexafluorophosphate (4.60 g, for a concentration of 0.1 M) in a stock solution prepared as above, with additional organic solvent added in order to offset the water content of the potassium carboxylate solution.

When the organic solvent was DMSO, the following potassium carboxylates were employed: potassium acetate, potassium propionate, potassium *n*-butyrate, potassium isobutyrate and potassium pivalate. For other organic solvents (ethanol, 1,4-dioxane, EGBE and diglyme), only potassium acetate was used.

Analyte solutions were also prepared from potassium carbonate in the same manner as described above, containing only 1.25 mM potassium carbonate in order to retain the same total base concentration.

8.3.2 Potentiometric titration procedure

To a three-necked round-bottomed flask (100 ml) was added the analyte solution (50 ml), which was then stirred and maintained at a constant 25 °C. A pH electrode (Jenway 924005 glass electrode with internal Ag/AgCl reference) was inserted into the solution and allowed to incubate until the measured potential stabilised. Titrant solution (prepared with the same organic solvent/water content as the analyte) was then added in 0.2 ml aliquots from a 25 mL glass burette. The electrode potential was allowed to stabilise between each addition and recorded together with

the solution temperature. Addition continued until no significant change in electrode potential was observed. The total volume of titrant added in this manner was *ca.* 9 ml.

8.3.3 Gran function analysis of titration curves

Each titration produced a sigmoidal curve of electrode potential against the volume of addition, from which the pK_a of the analyte was calculated using Gran's method.[192,193] For the titration of a monoprotic base, A^-, by a strong acid, it can be shown that, when all A^- has been neutralised:

$$F_1 = (V_0 + v)[H^+] = (v - v_{eq})t \quad (8)$$

Wherein V_0 is the initial volume of the analyte solution, v is the volume of titrant added, v_{eq} is the volume of titrant added at the equivalence point, and t is the concentration of the titrant. Hence, a plot of the Gran function $F_1 = (V_0 + v)[H^+]$ against v produces a straight line that has a v-intercept at $v = v_{eq}$.

Furthermore, prior to the equivalence point:

$$F_2 = \frac{(v_{eq} - v)}{K_a} = \frac{v}{[H^+]} \quad (9)$$

Hence, a plot of the Gran function $F_2 = \frac{v}{[H^+]}$ against v produces a straight line that has a gradient of $\frac{-1}{K_a}$ and a v-intercept at $v = v_{eq}$. Note that in both cases the Gran plots are not truly linear when v is very close to the equivalence point, as the assumptions underlying their derivation are untrue within this region, and therefore in practice the v-intercept is determined by extrapolation.

Thus, the equivalence point of the titration and pK_a of the acid can be determined by plots of F_1 and F_2, calculating the equivalence point from the v-intercept (F_1 is preferred for this as it depends only on the properties of the strong acid and therefore is independent of the properties of the base) and the pK_a from the gradient of F_2.

For the titration of a diprotic base such as carbonate, four Gran equations, and hence four Gran plots, are produced:

$$F_1 = (V_0 - v)[H^+] = \left(v - v_{eq}\right)t \tag{10}$$

$$F_2 = \left(v_{eq} - v\right)[H^+] = (v - v_w)K'_{a1} \tag{11}$$

$$F_3 = \frac{(v - v_w)}{[H^+]} = \frac{(v_{eq} - v)}{K'_{a1}} \tag{12}$$

$$F_4 = \frac{(v_{eq} - 2v_w + v)}{[H^+]} = \frac{v_w - v}{K_{a2}} \tag{13}$$

Wherein v_w is the titration volume at the first equivalence point. Note that a Gran plot based on F_2 requires knowledge of v_w, a plot based on F_3 requires knowledge of F_1, and a plot of F_4 requires knowledge of both. Thus, analysis of a titration curve of this nature is carried out in the following manner.

First, a Gran plot of F_1 is used to determine v_{eq}. A Gran plot of F_3 is then made using this value, in order to determine v_w and K_{a1}. F_2 and F_4 can then be freely plotted, with F_2 providing a second estimate for K_{a1}, and F_4 used to calculate K_{a2}.

In order to use the above method, it is necessary to determine the pH (and thereby $[H^+]$) from the electrode potential measured in the titration. The pH glass electrode obeys the Nernst equation:

$$E = E_0 - \frac{2.303RT}{F}pH \tag{14}$$

Where:

- E is the measured electrode potential;
- E_0 is the standard potential of the cell;
- F is the Faraday constant (96,485 C mol^{-1}).

The standard electrode potential is determined by calibration and will vary significantly depending on the solvent used. A correct value of E_0 is not required for calculation of the equivalence volume (as this is simply the location of the inflection point of the titration curve on the *volume* axis) but it is absolutely necessary for determination of pK_a values. Since the solvent is not pure water, standard calibration with aqueous buffers is inappropriate, and instead the calibration was performed *in situ* using the titration end point and the concentration of HCl in the titrant solution, in a method derived from one originally developed by Grunwald et al.[178]

A Gran plot of F_1 was employed to calculate the equivalence volume, using values of $[H^+]$ derived via the Nernst equation with E_0 set at 400 mV. From the equivalence point onwards, it is assumed that HCl suppresses dissociation of the analyte, and therefore that addition of further acid is equivalent to addition of H^+ into neutral solution, and hence that the true pH is equal to the negative logarithm of the concentration of HCl in solution. In other words:

$$pH = -\log\left(\frac{t(v - v_{eq})}{V_0 + v}\right) \quad (15)$$

Such assumptions are not valid when very close to the equivalence point, where dissociation of the analyte is still significant relative to the small concentration of HCl, but otherwise proved to be highly robust.

Hence, E_0 was determined by fitting of the pH determined via the Nernst equation from experimentally measured potentials, to the true pH as determined above from the volume of HCl addition, in the region >1.5 ml beyond the equivalence point. This was accomplished using a generalised reduced gradient algorithm to minimise the root-mean-square deviation (RMSD) of these values as a function of E_0. In this manner, a value of E_0 was determined for each individual titration.

Given E_0, the pH was then calculated from the measured potential for the whole range of the titration curve. pK_a of the analyte was then determined using Gran's method as already described.

8.3.4 Potentiometric titration – worked example

Titration of potassium acetate with HCl in DMSO containing 10 wt% water yields the following titration curve:

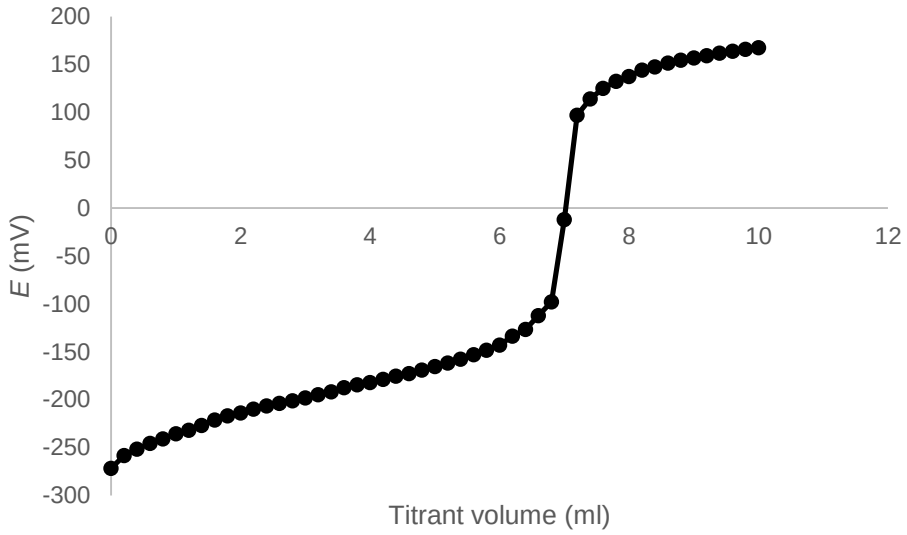

Figure 8.13: Potentiometric titration curve from titration of 2.5 mM potassium acetate against 0.02 M HCl, dissolved in a mixture of DMSO (90 wt%) and water (10 wt%). Conditions: V_0 = 50 ml, 25 °C, I = 0.1 M KPF_6.

Gran function plot of $F_1 = (V_0 + v)[H^+]$, calculating [H^+] from the Nernst equation (equation (14)), has a v-intercept at the equivalence point, where v = 7.05 ml:

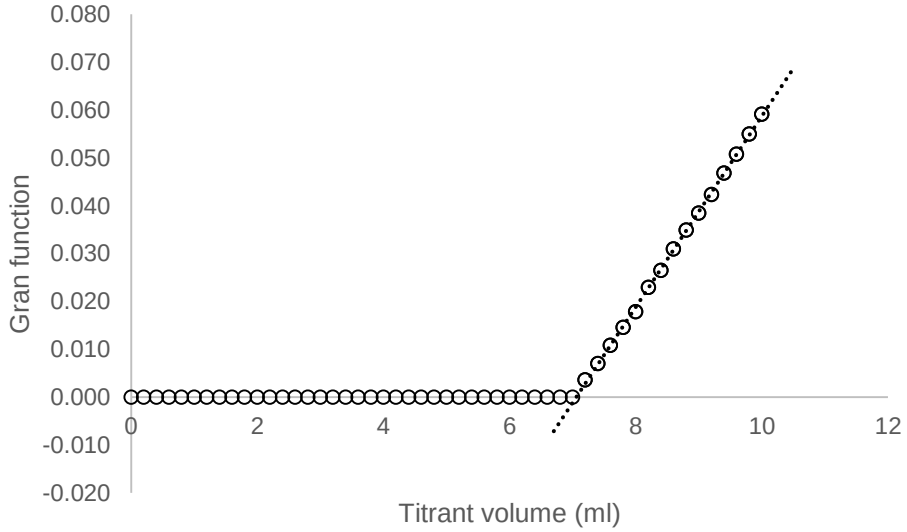

Figure 8.14: Plot of Gran function F_1 for titration curve of potassium acetate against HCl in 90 wt% DMSO. The trendline highlights the linear portion of the curve, which intersects the v-axis at the equivalence volume.

The theoretical pH beyond the equivalence point was then calculated based on equation (15). The value of E_0 was fitted to these values using the Nernst equation and the experimentally measured electrode potentials within the region $v - v_{eq} > 1.5$ where equation (15) holds well. A close fit was achieved at E_0 = 345.9 mV, with RMSD = 0.0026.

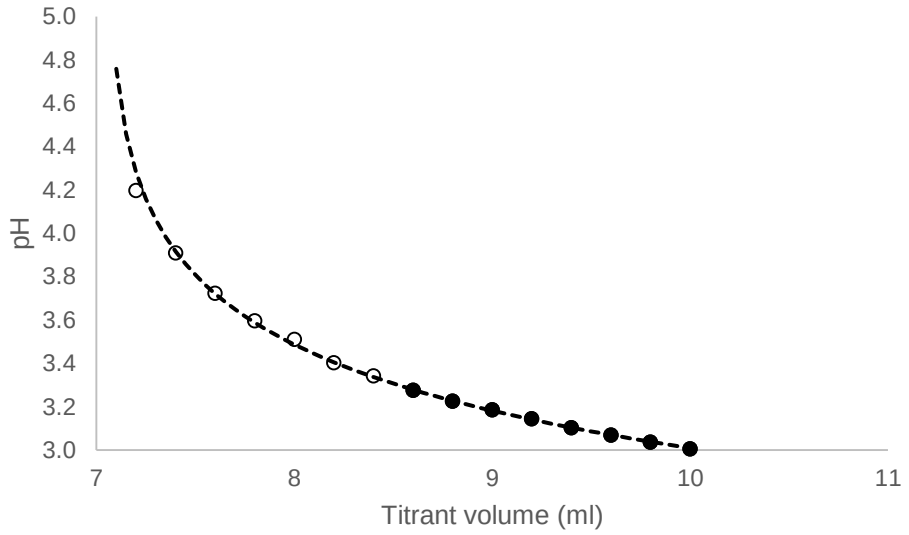

Figure 8.15: Plot showing (dashed line) theoretical pH and (data points) pH calculated from experimentally measured potentials via the Nernst equation, with E_0 = 345.9 mV. Hollow data points (where $v - v_{eq} < 1.5$) were not used in fitting of E_0 to the theoretical values, as the theoretical and experimental values are both less accurate within this region.

Given the value of E_0, the whole titration curve was calculated in terms of pH using the Nernst equation, and the Gran functions F_1 and F_2 calculated. The slope of the Gran F_2 function is equal to $\frac{-1}{K_a}$, and from this the pK_a of potassium acetate was determined to be 9.03 under these conditions.

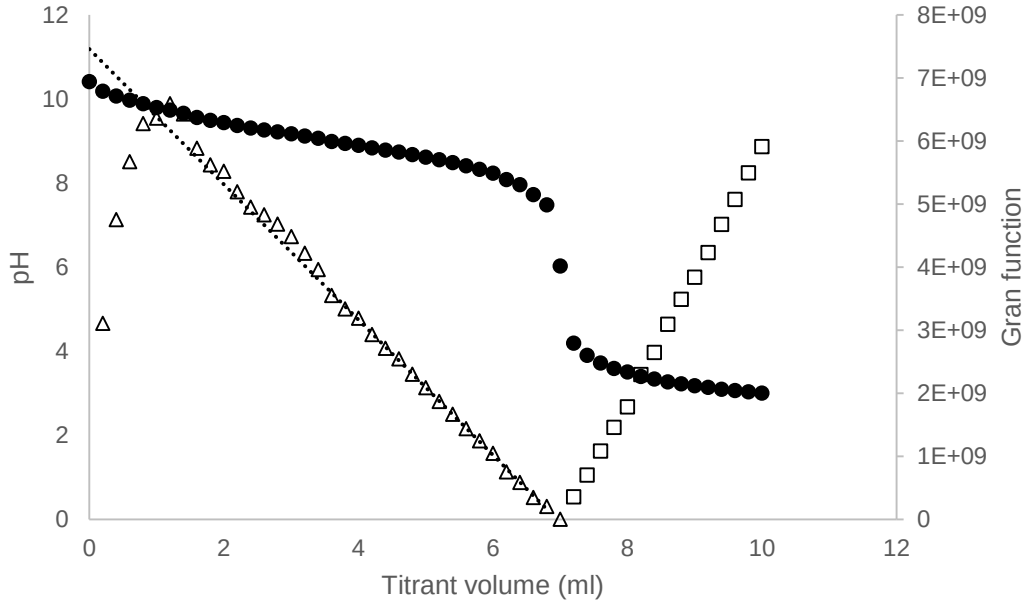

Figure 8.16: Plot showing: (primary axis, filled circles) pH titration curve of potassium acetate against HCl in 90% DMSO; (secondary axis, hollow squares) normalised Gran F_1 function of the same; (secondary axis, hollow triangles) Gran F_2 function of the same.

8.3.5 Potentiometric titration data

Table 8.24: Measured pK_a values from titrations carried out in mixed solutions of water and the specified weight percentage of ethanol.

%	AcO^-	HCO_3^-
0	4.76	6.32
25	4.98	7.10
50	5.43	7.71
75	6.15	8.44
80	6.31	8.75
85	6.71	9.02
90	7.63	9.6
95	8.52	10.6

Table 8.25: Measured pK_a values from titrations carried out in mixed solutions of water and the specified weight percentage of 1,4-dioxane.

%	AcO^-	HCO_3^-
0	4.76	6.32
25	5.01	7.11
50	6.02	7.74
75	7.74	9.69
80	8.1	9.99
85	8.47	10.60
90	9.9	11.2
95	12.8	12.2

Table 8.26: Measured pK_a values from titrations carried out in mixed solutions of water and the specified weight percentage of EGBE.

%	AcO^-	HCO_3^-
0	4.76	6.32
25	4.88	7.05
50	5.61	7.62
75	6.21	7.8
80	6.38	8.10
85	6.89	8.63
90	7.56	9.22
95	8.43	10.24

Table 8.27: Measured pK_a values from titrations carried out in mixed solutions of water and the specified weight percentage of diglyme.

%	AcO^-	HCO_3^-
0	4.76	6.32
25	5.03	7.12
50	5.67	7.79
75	7.34	9.12
80	7.85	9.61
85	8.91	10.28
90	10.34	11.00
95	12.15	12.3

Table 8.28: Measured pK_a values from titrations carried out in mixed solutions of water and the specified weight percentage of DMSO.

%	AcO^-	HCO_3^-
0	4.76	6.32
25	5.22	6.85
50	5.45	7.21
75	6.44	8.11
80	6.85	8.32
85	7.65	8.95
90	9.03	9.62
95	10.22	10.76

8.4 CO_2 absorption with nonaqueous carboxylate solutions

8.4.1 Solution preparation

Stock solutions (500 g) were prepared gravimetrically from DMSO and the desired weight percentage of water. Solutions were prepared containing, respectively: 5, 10, 20, 30 and 50 wt% water. Carboxylate salt solutions were then prepared by dissolving a carboxylate salt (0.25 mol, for a concentration of 1 mol L^{-1}) in either the requisite stock solution or distilled water and making the solution up to 250 ml with the same.

8.4.2 Procedure for CO_2 absorption in VLE2

150 ml of a carboxylate salt solution prepared in the above manner was added to the vapour-liquid equilibrium cell, and allowed to attain thermal equilibrium at 25 °C. A vacuum was briefly applied to the solution, before air was slowly introduced into the cell to achieve a total pressure of 500 mbar, and again the solution was allowed to equilibrate. The connection to the gas burette (via regulator preset to 650 mbar) was then opened, releasing 150 mbar CO_2 into the cell, and the cell allowed to reach equilibrium. The partial pressure of CO_2 in the cell was then increased to 300 mbar by increasing the regulator pressure. Once equilibrium was attained, the partial pressure of CO_2 was increased to 600 mbar, then 800 mbar, then 1000 mbar, each time allowing the pressure and temperature in the cell to stabilise before a further increase.

The amount (if any) of CO_2 absorbed into the solution at each partial pressure was then calculated based on the amount of CO_2 remaining in the gas burette at each equilibrium point.

8.4.3 Vapour-liquid equilibrium data

Table 8.29: Equilibrium pressure and CO_2 loading values for absorption of CO_2 into 1 M KOAc in 70% DMSO/30% water.

Pressure	P(CO_2)	Loading
0.646	0.147	0.114
0.822	0.323	0.202
1.104	0.605	0.29
1.31	0.811	0.337
1.511	1.012	0.375

Table 8.30: Equilibrium pressure and CO_2 loading values for absorption of CO_2 into 1 M KOAc in 80% DMSO/20% water.

Pressure	P(CO_2)	Loading
0.646	0.143	0.317
0.827	0.324	0.442
1.104	0.601	0.535
1.313	0.81	0.583
1.502	0.999	0.618

Table 8.31: Equilibrium pressure and CO_2 loading values for absorption of CO_2 into 1 M potassium propionate in 70% DMSO/30% water.

Pressure	$P(CO_2)$	Loading
0.63	0.13	0.155
0.812	0.312	0.27
1.098	0.598	0.374
1.299	0.799	0.425
1.514	1.014	0.465

Table 8.32: Equilibrium pressure and CO_2 loading values for absorption of CO_2 into 1 M potassium propionate in 80% DMSO/20% water.

Pressure	P(CO2)	Loading
0.674	0.173	0.394
0.785	0.284	0.487
1.106	0.606	0.600
1.294	0.793	0.637
1.479	0.979	0.676

Table 8.33: Equilibrium pressure and CO_2 loading values for absorption of CO_2 into 1 M potassium pivalate in 70% DMSO/30% water.

Pressure	P(CO2)	Loading
0.623	0.121	0.233
0.782	0.28	0.397
1.105	0.603	0.542
1.297	0.795	0.592
1.507	1.005	0.642

9 References

1 J. G. Crowther, *Scientists of the industrial revolution: Joseph Black, James Watt, Joseph Priestley, Henry Cavendish*, Cresset Press, London, 1962.

2 B. P. Sullivan, K. Krist and H. E. Guard, *Electrochemical and Electrocatalytic Reactions of Carbon Dioxide*, Elsevier, Amsterdam, 1993.

3 C. D. Keeling, S. C. Piper, T. P. Whorf and R. F. Keeling, *Tellus, Ser. B Chem. Phys. Meteorol.*, 2011, **63**, 1–22.

4 C. D. Carver, *The Coblentz Society Desk Book of Infrared Spectra*, The Coblentz Society, Kirkwood (Missouri), 1982.

5 S. Arrhenius, *Philos. Mag. J. Sci. (Fifth Ser.)*, 1896, **41**, 237–279.

6 R. A. Hanel, B. J. Conrath, V. G. Kunde, C. Prabhakara, I. Revah, V. V. Salomonson and G. Wolford, *J. Geophys. Res.*, 1972, **77**, 2629–2641.

7 J. R. Petit, J. Jouzel, D. Raynaud, N. I. Barkov, J.-M. Barnola, I. Basile, M. Bender, J. Chappellaz, M. Davis, G. Delaygue, M. Delmotte, V. M. Kotlyakov, M. Legrand, V. Y. Lipenkov, C. Lorius, L. Pépin, C. Ritz, E. Saltzman and M. Stievenard, *Nature*, 1999, **399**, 429–436.

8 J. Jouzel, N. I. Barkov, J. M. Barnola, M. Bender, J. Chappellaz, C. Genthon, V. M. Kotlyakov, V. Lipenkov, C. Lorius, J. R. Petit, D. Raynaud, G. Raisbeck, C. Ritz, T. Sowers, M. Stievenard, F. Yiou and P. Yiou, *Nature*, 1993, **364**, 407–412.

9 J. Jouzel, C. Waelbroeck, B. Malaize, M. Bender, J. R. Petit, M. Stievenard, N. I. Barkov, J. M. Barnola, T. King, V. M. Kotlyakov, V. Lipenkov, C. Lorius, D. Raynaud, C. Ritz and T. Sowers, *Clim. Dyn.*, 1996, **12**, 513–521.

10 J. Jouzel, C. Lorius, J. R. Petit, C. Genthon, N. I. Barkov, V. M. Kotlyakov and V. M. Petrov, *Nature*, 1987, **329**, 403–408.

11 T. A. Boden, G. Marland and R. J. Andres, *Global, Regional, and National Fossil-Fuel CO2 Emissions*, Carbon Dioxide Information Analysis Center, Oak Ridge National Laboratory, U.S. Department of Energy, Oak Ridge, Tenn., USA, 2010.

12 Intergovernmental Panel on Climate Change, *Climate Change 2014 Synthesis Report. Contribution of Working Groups I, II and III to the Fifth Assessment Report of the Intergovernmental Panel on Climate Change*, IPCC, Geneva, 2014.

13 Intergovernmental Panel on Climate Change, *Carbon Dioxide Capture and Storage*, Cambridge University Press, Cambridge, 2005.

14 R. S. Haszeldine, *Science*, 2009, **325**, 1647–52.

15 M. E. Boot-Handford, J. C. Abanades, E. J. Anthony, M. J. Blunt, S. Brandani, N. Mac Dowell, J. R. Fernández, M.-C. Ferrari, R. Gross, J. P. Hallett, R. S. Haszeldine, P. Heptonstall, A. Lyngfelt, Z. Makuch, E. Mangano, R. T. J. Porter, M. Pourkashanian, G. T. Rochelle, N. Shah, J. G. Yao and P. S. Fennell, *Energy Environ. Sci.*, 2014, **7**, 130–189.

16 J. Kemper, *Int. J. Greenh. Gas Control*, 2015, **40**, 401–430.

17 M. M. J. Knoope, W. Guijt, A. Ramírez and A. P. C. Faaij, *Int. J. Greenh. Gas Control*, 2014, **22**, 25–46.

18 O. Eiken, P. Ringrose, C. Hermanrud, B. Nazarian, T. A. Torp and L. Høier, *Energy Procedia*, 2011, **4**, 5541–5548.

19 K. Michael, A. Golab, V. Shulakova, J. Ennis-King, G. Allinson, S. Sharma and T. Aiken, *Int. J. Greenh. Gas Control*, 2010, **4**, 659–667.

20 G. P. D. De Silva, P. G. Ranjith and M. S. A. Perera, *Fuel*, 2015, **155**, 128–143.

21 C. M. White, B. R. Strazisar, E. J. Granite, J. S. Hoffman and H. W. Pennline, *J. Air Waste Manage. Assoc.*, 2003, **53**, 645–715.

22 S. Bachu, *Prog. Energy Combust. Sci.*, 2008, **34**, 254–273.

23 D. Y. C. Leung, G. Caramanna and M. M. Maroto-Valer, *Renew. Sustain. Energy Rev.*, 2014, **39**, 426–443.

24 C. Descamps, C. Bouallou and M. Kanniche, *Energy*, 2008, **33**, 874–881.

25 J. Davison, *Energy*, 2007, **32**, 1163–1176.

26 D. Zhang, Z. Wang, J. Sun, L. Zhang and Z. Li, *Energy Convers. Manag.*, 2012, **55**, 127–135.

27 J. M. Matter, M. Stute, S. Ó. Snæbjörnsdottir, E. H. Oelkers, S. R. Gislason, E. S. Aradottir, B. Sigfusson, I. Gunnarsson, H. Sigurdardottir, E. Gunnlaugsson, G. Axelsson, H. Alfredsson, D. Wolff-Boenisch, K. Mesfin, D. Fernandez de la Reguera Taya, J. Hall, K. Dideriksen and W. S. Broecker, *Science*, 2016, **352**, 1312–1314.

28 C.-H. Yu, C.-H. Huang and C.-S. Tan, *Aerosol Air Qual. Res.*, 2012, **12**, 745–769.

29 I. Kim and H. F. Svendsen, *Ind. Eng. Chem. Res.*, 2007, **46**, 5803–5809.

30 J. Oexmann and A. Kather, *Int. J. Greenh. Gas Control*, 2010, **4**, 36–43.

31 J. H. Meldon, *Curr. Opin. Chem. Eng.*, 2011, **1**, 55–63.

32 C. Sun, S. Wang, S. Zhou and C. Chen, *Int. J. Greenh. Gas Control*, 2014, **23**, 98–104.

33 G. Hochgesand, *Ind. Eng. Chem.*, 1970, **62**, 37–43.

34 M. B. Miller, D. Chen, D. R. Luebke, J. K. Johnson and R. M. Enick, *J. Chem. Eng. Data*, 2011, **56**, 1565–1572.

35 W. Bucklin, *Energy Prog.*, 1984, **4**, 137–142.

36 F. Karadas, M. Atilhan and S. Aparicio, *Energy & Fuels*, 2010, **24**, 5817–5828.

37 S. Baj, A. Siewniak, A. Chrobok, T. Krawczyk and A. Sobolewski, *J. Chem. Technol. Biotechnol.*, 2013, **88**, 1220–1227.

38 M. Ramdin, T. W. De Loos and T. J. H. Vlugt, *Ind. Eng. Chem. Res.*, 2012, **51**, 8149–

8177.

39 B. E. Gurkan, J. C. de la Fuente, E. M. Mindrup, L. E. Ficke, B. F. Goodrich, E. a Price, W. F. Schneider and J. F. Brennecke, *J. Am. Chem. Soc.*, 2010, **132**, 2116–7.

40 X. Luo, Y. Guo, F. Ding, H. Zhao, G. Cui, H. Li and C. Wang, *Angew. Chemie Int. Ed.*, 2014, **53**, 7053–7057.

41 E. I. Privalova, P. Mäki-Arvela, D. Y. Murzin and J. P. Mikkhola, *Russ. Chem. Rev.*, 2012, **81**, 435–457.

42 H. G. Joglekar, I. Rahman and B. D. Kulkarni, *Chem. Eng. Technol.*, 2007, **30**, 819–828.

43 L. Li, N. Zhao, W. Wei and Y. Sun, *Fuel*, 2013, **108**, 112–130.

44 K. E. Gutowski and E. J. Maginn, *J. Am. Chem. Soc.*, 2008, **130**, 14690–14704.

45 L. A. Blanchard, Z. Gu and J. F. Brennecke, *J. Phys. Chem. B*, 2001, **105**, 2437–2444.

46 B. Wu, W. Liu, Y. Zhang and H. Wang, *Chem. Eur. J.*, 2009, **15**, 1804–1810.

47 M. C. Bubalo, K. Radošević, I. R. Redovniković, J. Halambek and V. G. Srček, *Ecotoxicol. Environ. Saf.*, 2014, **99**, 1–12.

48 R. Thiruvenkatachari, S. Su, H. An and X. X. Yu, *Prog. Energy Combust. Sci.*, 2009, **35**, 438–455.

49 M. T. Ho, G. W. Allinson and D. E. Wiley, *Ind. Eng. Chem. Res.*, 2008, **47**, 4883–4890.

50 D. Aaron and C. Tsouris, *Sep. Sci. Technol.*, 2005, **40**, 321–348.

51 A. Sayari, Y. Belmabkhout and R. Serna-Guerrero, *Chem. Eng. J.*, 2011, **171**, 760–774.

52 K. Sumida, D. L. Rogow, J. A. Mason, T. M. McDonald, E. D. Bloch, Z. R. Herm, T.-H. Bae and J. R. Long, *Chem. Rev.*, 2012, **112**, 724–781.

53 W. Hage, A. Hallbrucker and E. Mayer, *J. Am. Chem. Soc.*, 1993, **115**, 8427–8431.

54 M. Weller, T. Overton, J. Rourke and F. Armstrong, *Inorganic Chemistry (Sixth Edition)*, Oxford University Press, Oxford, 2014.

55 P. G. Barash, B. F. Cullen, R. K. Stoelting, M. K. Cahalan and M. C. Stock, *Clinical Anesthesia*, Lippincott Williams & Wilkins, Philadelphia, 2009.

56 F. S. Zeman and K. S. Lackner, *World Resour. Rev.*, 2004, **16**, 157–172.

57 M. Caplow, *J. Am. Chem. Soc.*, 1968, **90**, 6795–6803.

58 P. V. Danckwerts, *Chem. Eng. Sci.*, 1979, **34**, 443–446.

59 J. E. Crooks and J. P. Donnellan, *J. Chem. Soc. Perkin Trans. 2*, 1989, 331–333.

60 C. J. T. de Grotthuss, *Ann. Chim.*, 1806, **58**, 54–74.

61 G. S. Hwang, H. M. Stowe, E. Paek and D. Manogaran, *Phys. Chem. Chem. Phys.*, 2015, **17**, 831–839.

62 H. Nakai, Y. Nishimura, T. Kaiho, T. Kubota and H. Sato, *Chem. Phys. Lett.*, 2016, **647**, 127–131.

63 C. A. Guido, F. Pietrucci, A. G. Gallet and W. Andreoni, *J. Chem. Theory Comput.*, 2013, **9**, 28–32.

64 H. M. Stowe, L. Vilčiauskas, E. Paek and G. S. Hwang, *Phys. Chem. Chem. Phys.*, 2015, **17**, 29184–29192.

65 G. Sartori and D. W. Savage, *Ind. Eng. Chem. Fundam.*, 1987, **22**, 239–249.

66 N. McCann, D. Phan, X. Wang, W. Conway, R. Burns, M. Attalla, G. Puxty and M. Maeder, *J. Phys. Chem. A*, 2009, **113**, 5022–5029.

67 Y. Matsuzaki, H. Yamada, F. A. Chowdhury, T. Higashii and M. Onoda, *J. Phys. Chem. A*, 2013, **117**, 9274–9281.

68 D. M. Kern, *J. Chem. Educ.*, 1960, **37**, 14–23.

69 F. Christensson, H. C. S. Koefoed, A. C. Petersen and K. Rasmussen, *Acta Chem. Scand. A*, 1978, 32, 15–17.

70 J. Gabrielsen, H. F. Svendsen, M. L. Michelsen, E. H. Stenby and G. M. Kontogeorgis,

Chem. Eng. Sci., 2007, **62**, 2397–2413.

71 P. Jackson, K. Robinson, G. Puxty and M. Attalla, *Energy Procedia*, 2009, **1**, 985–994.

72 P. W. J. Derks, P. J. G. Huttenhuis, C. van Aken, J.-H. Marsman and G. F. Versteeg, *Energy Procedia*, 2011, **4**, 599–605.

73 G. L. Samarakoon P. A., N. H. Andersen, C. Perinu and K.-J. Jens, *Energy Procedia*, 2013, **37**, 2002–2010.

74 S. K. Bharti and R. Roy, *Trends Anal. Chem.*, 2012, **35**, 5–26.

75 D. J. Cookson and B. E. Smith, *J. Magn. Reson.*, 1984, **57**, 355–368.

76 A. F. Ciftja, A. Hartono and H. F. Svendsen, *Int. J. Greenh. Gas Control*, 2013, **16**, 224–232.

77 A. K. Chakraborty, G. Astarita and K. B. Bischoff, *Chem. Eng. Sci.*, 1986, **41**, 997–1003.

78 J. P. Jakobsen, J. Krane and H. F. Svendsen, *Ind. Eng. Chem. Res.*, 2005, **44**, 9894–9903.

79 A. F. Ciftja, A. Hartono and H. F. Svendsen, *Energy Procedia*, 2013, **37**, 1605–1612.

80 A. F. Ciftja, A. Hartono and H. F. Svendsen, *Chem. Eng. Sci.*, 2014, **107**, 317–327.

81 A. F. Ciftja, A. Hartono and H. F. Svendsen, *Chem. Eng. Sci.*, 2013, **102**, 378–386.

82 A. F. Ciftja, A. Hartono and H. F. Svendsen, *Energy Procedia*, 2013, **37**, 1605–1612.

83 Q. Yang, M. Bown, A. Ali, D. Winkler, G. Puxty and M. Attalla, *Energy Procedia*, 2009, **1**, 955–962.

84 T. Suda, T. Iwaki and T. Mimura, *Chem. Lett.*, 1996, **25**, 777–778.

85 D. M. Austgen, G. T. Rochelle and C. Chen, *Ind. Eng. Chem. Res.*, 1991, **30**, 543–555.

86 W. Böttinger, M. Maiwald and H. Hasse, *Fluid Phase Equilib.*, 2008, **263**, 131–143.

87 C. Perinu, B. Arstad and K.-J. Jens, *Int. J. Greenh. Gas Control*, 2014, **20**, 230–243.

88 N. S. Matin, J. E. Remias, J. K. Neathery and K. Liu, *Ind. Eng. Chem. Res.*, 2012, **51**,

6613–6618.

89 Y. Zhang, H. Que and C. C. Chen, *Fluid Phase Equilib.*, 2011, **311**, 67–75.

90 G. Puxty, R. Rowland, A. Allport, Q. Yang, M. Bown, R. Burns, M. Maeder and M. Attalla, *Environ. Sci. Technol.*, 2009, **43**, 6427–33.

91 C. Perinu, G. Saramakoon, B. Arstad and K.-J. Jens, *Energy Procedia*, 2014, **63**, 1144–1150.

92 J. H. Choi, S. G. Oh, Y. Il Yoon, S. K. Jeong, K. R. Jang and S. C. Nam, *J. Ind. Eng. Chem.*, 2012, **18**, 568–573.

93 R. J. Hook, *Ind. Eng. Chem. Res.*, 1997, **36**, 1779–1790.

94 F. Bougie and M. C. Iliuta, *J. Chem. Eng. Data*, 2012, **57**, 635–669.

95 S. Gangarapu, G. J. Wierda, A. T. M. Marcelis and H. Zuilhof, *ChemPhysChem*, 2014, **15**, 1880–1886.

96 S. A. Freeman, R. Dugas, D. Van Wagener, T. Nguyen and G. T. Rochelle, *Energy Procedia*, 2009, **1**, 1489–1496.

97 S. Bishnoi and G. T. Rochelle, *Chem. Eng. Sci.*, 2000, **55**, 5531–5543.

98 D. Fernandes, W. Conway, X. Wang, R. Burns, G. Lawrance, M. Maeder and G. Puxty, *J. Chem. Thermodyn.*, 2012, **51**, 97–102.

99 R. J. Littel, W. P. M. Van Swaaij and G. F. Versteeg, *AIChE J.*, 1990, **36**, 1633–1640.

100 F. A. Chowdhury, H. Yamada, T. Higashii, K. Goto and M. Onoda, *Ind. Eng. Chem. Res.*, 2013, **52**, 8323–8331.

101 F. A. Chowdhury, H. Okabe, S. Shimizu, M. Onoda and Y. Fujioka, *Energy Procedia*, 2009, **1**, 1241–1248.

102 D. P. Hagewiesche, S. S. Ashour, H. A. Al-Ghawas and O. C. Sandall, *Chem. Eng. Sci.*, 1995, **50**, 1071–1079.

103 A. A. Olajire, *Energy*, 2010, **35**, 2610–2628.

104 B. Dutcher, M. Fan and A. G. Russell, *ACS Appl. Mater. Interfaces*, 2015, **7**, 2137–2148.

105 J. Fang-Yuan, F. D. Otto and A. E. Mather, *Ind. Eng. Chem. Res.*, 1994, **33**, 2002–2005.

106 J. Xiao, C.-W. Li and M.-H. Li, *Chem. Eng. Sci.*, 2000, **55**, 161–175.

107 T. Wang and K.-J. Jens, *Energy Procedia*, 2013, **37**, 306–313.

108 W. Conway, S. Bruggink, Y. Beyad, W. Luo, I. Melián-Cabrera, G. Puxty and P. Feron, *Chem. Eng. Sci.*, 2015, **126**, 446–454.

109 S.-Y. Horng and M.-H. Li, *Ind. Eng. Chem. Res.*, 2002, **41**, 257–266.

110 R. Idem, M. Wilson, P. Tontiwachwuthikul, A. Chakma, A. Veawab, A. Aroonwilas and D. Gelowitz, *Ind. Eng. Chem. Res.*, 2006, **45**, 2414–2420.

111 G. Rochelle, E. Chen, S. Freeman, D. Van Wagener, Q. Xu and A. Voice, *Chem. Eng. J.*, 2011, **171**, 725–733.

112 D. Tong, G. C. Maitland, M. J. P. Trusler and P. S. Fennell, *Chem. Eng. Sci.*, 2013, **101**, 851–864.

113 W.-J. Choi, K.-C. Cho, S.-S. Lee, J.-G. Shim, H.-R. Hwang, S.-W. Park and K.-J. Oh, *Green Chem.*, 2007, **9**, 594–598.

114 H. Li, L. Li, T. Nguyen, G. T. Rochelle and J. Chen, *Energy Procedia*, 2013, **37**, 340–352.

115 G. Fytianos, S. Ucar, A. Grimstvedt, A. Hyldbakk, H. F. Svendsen and H. K. Knuutila, *Int. J. Greenh. Gas Control*, 2016, **46**, 48–56.

116 Z. Liang, W. Rongwong, H. Liu, K. Fu, H. Gao, F. Cao, R. Zhang, T. Sema, A. Henni, K. Sumon, D. Nath, D. Gelowitz, W. Srisang, C. Saiwan, A. Benamor, M. Al-Marri, H. Shi, T. Supap, C. Chan, Q. Zhou, M. Abu-Zahra, M. Wilson, W. Olson, R. Idem and P. Tontiwachwuthikul, *Int. J. Greenh. Gas Control*, 2015, **40**, 26–54.

117 P. Wattanaphan, T. Sema, R. Idem, Z. Liang and P. Tontiwachwuthikul, *Int. J. Greenh.*

Gas Control, 2013, **19**, 340–349.

118 S. Srinivasan, A. Veawab and A. Aroonwilas, *Energy Procedia*, 2013, **37**, 890–895.

119 A. Bello and R. O. Idem, *Ind. Eng. Chem. Res.*, 2006, **45**, 2569–2579.

120 C. Gouedard, D. Picq, F. Launay and P.-L. Carrette, *Int. J. Greenh. Gas Control*, 2012, **10**, 244–270.

121 B. R. Strazisar, R. R. Anderson and C. M. White, *Energy and Fuels*, 2003, **17**, 1034–1039.

122 T. Wang and K.-J. Jens, *Int. J. Greenh. Gas Control*, 2014, **24**, 98–105.

123 A. J. Reynolds, T. V. Verheyen, S. B. Adeloju, E. Meuleman and P. Feron, *Environ. Sci. Technol.*, 2012, **46**, 3643–3654.

124 K. Veltman, B. Singh and E. G. Hertwich, *Environ. Sci. Technol.*, 2010, **44**, 1496–1502.

125 N. Dai and W. A. Mitch, *Environ. Sci. Technol.*, 2013, **47**, 13175–13183.

126 A. K. Voice, A. Hill, N. A. Fine and G. T. Rochelle, *Int. J. Greenh. Gas Control*, 2015, **39**, 329–334.

127 L. Onel, M. A. Blitz and P. W. Seakins, *J. Phys. Chem. Lett.*, 2012, **3**, 853–856.

128 L. Onel, M. A. Blitz, J. Breen, A. R. Rickard and P. W. Seakins, *Phys. Chem. Chem. Phys.*, 2015, **17**, 25342–25353.

129 R. K. Harris, E. D. Becker, S. M. Cabral de Menezes, P. Granger, R. E. Hoffman and K. W. Zilm, *Pure Appl. Chem.*, 2008, **80**, 59–84.

130 A. De Marco, *J. Magn. Reson.*, 1977, **26**, 527–528.

131 R. G. Bryant, *J. Chem. Educ.*, 1983, **60**, 933–935.

132 D. H. Williams and I. Fleming, *Spectroscopic Methods in Organic Chemistry*, McGraw-Hill, New York, 2007.

133 J. C. Schink, J. H. Stockwell and R. A. Ellis, *J. Sediment. Res.*, 1979, **49**, 651–653.

134 A. Vrachnos, G. Kontogeorgis and E. Voutsas, *Ind. Eng. Chem. Res.*, 2006, **45**, 5148–5154.

135 B. P. Mandal, M. Guha, A. K. Biswas and S. S. Bandyopadhyay, *Chem. Eng. Sci.*, 2001, **56**, 6217–6224.

136 B. P. Mandal and S. S. Bandyopadhyay, *Chem. Eng. Sci.*, 2006, **61**, 5440–5447.

137 Y. Du, Y. Yuan and G. T. Rochelle, *Chem. Eng. Sci.*, 2016, **155**, 397–404.

138 A. Wilk, L. Wiêcław-Solny, D. Spiewak, T. Spietz and H. Kierzkowska-Pawlak, *Chem. Process Eng.*, 2015, **36**, 49–57.

139 O. Lawal, A. Bello and R. Idem, *Ind. Eng. Chem. Res.*, 2005, **44**, 1874–1896.

140 V. Ermatchkov, A. P.-S. Kamps, D. Speyer and G. Maurer, *J. Chem. Eng. Data*, 2006, **51**, 1788–1796.

141 P. M. Dewick, *Essentials of Organic Chemistry: For Students of Pharmacy, Medicinal Chemistry and Biological Chemistry*, John Wiley & Sons Ltd., Chichester, 2006.

142 L. I. Helgesen and E. Gjernes, *Energy Procedia*, 2016, **86**, 239–251.

143 J. R. Pliego Jr and J. M. Riveros, *Phys. Chem. Chem. Phys.*, 2002, **4**, 1622–1627.

144 S. Bala, University of Leeds, 2013.

145 University of Leeds, Int. Pat., 2010/049739 A3, 2010.

146 Vetrocoke S.p.A., Br. Pat., 786 669 A, 1967.

147 Z. Marković, S. Marković and N. Begović, *J. Chem. Inf. Model.*, 2006, **46**, 1957–1964.

148 V. Barbarossa, F. Barzagli, F. Mani, S. Lai and G. Vanga, *J. CO2 Util.*, 2015, **10**, 50–59.

149 C. Wang, H. Luo, H. Li, X. Zhu, B. Yu and S. Dai, *Chem. Eur. J.*, 2012, **18**, 2153–2160.

150 C. Wang, H. Luo, D. Jiang, H. Li and S. Dai, *Angew. Chem. Int. Ed.*, 2010, **49**, 5978–5981.

151 W. W. Kaeding, *J. Org. Chem.*, 1964, **29**, 2556–2559.

152 A. Dreimanis, *J. Sediment. Petrol.*, 1962, **32**, 520–529.

153 P. D. Vaidya and E. Y. Kenig, *Chem. Eng. Technol.*, 2007, **30**, 1467–1474.

154 O. Söhnel and P. Novotny, *Densities of Aqueous Solutions of Inorganic Substances*, Elsevier, Amsterdam, 1985.

155 W. Conway, X. Wang, D. Fernandes, R. Burns, G. Lawrance, G. Puxty and M. Maeder, *J. Phys. Chem. A*, 2011, **115**, 14340–14349.

156 E. S. Hamborg, J. P. M. Niederer and G. F. Versteeg, *J. Chem. Eng. Data*, 2009, **54**, 1318–1328.

157 A. Tagiuri, M. Mohamedali and A. Henni, *J. Chem. Eng. Data*, 2016, **61**, 247–254.

158 F. Khalili, A. Henni and A. L. L. East, *J. Chem. Eng. Data*, 2009, **54**, 2914–2917.

159 C-Capture Ltd., Int. Pat., 2015/092427 A2, 2015.

160 B. G. Cox, *Org. Process Res. Dev.*, 2015, **19**, 1800–1808.

161 E. Raamat, K. Kaupmees, G. Ovsjannikov, A. Trummal, A. Kütt, J. Saame, I. Koppel, I. Kaljurand, L. Lipping, T. Rodima, V. Pihl, I. A. Koppel and I. Leito, *J. Phys. Org. Chem.*, 2013, **26**, 162–170.

162 F. Rived, M. Rosés and E. Bosch, *Anal. Chim. Acta*, 1998, **374**, 309–324.

163 F. G. Bordwell, *Acc. Chem. Res*, 1988, **21**, 456–463.

164 I. M. Kolthoff, M. K. Chantooni and S. Bhowmik, *J. Am. Chem. Soc.*, 1968, **90**, 23–28.

165 I. Kaljurand, A. Kutt, L. Soovali, T. Rodima, V. Maemets, I. Leito and I. A. Koppel, *J. Org. Chem.*, 2005, **70**, 1019–1028.

166 B. Gutbezahl and E. Grunwald, *J. Am. Chem. Soc.*, 1953, **75**, 559–565.

167 E. Grunwald and B. J. Berkowitz, *J. Am. Chem. Soc.*, 1951, **73**, 4939–4944.

168 B. G. Cox, *Acids and Bases: Solvent Effects on Acid-Base Strength*, Oxford University Press, Oxford, 2013.

169 R. Quinn, J. B. Appleby and G. P. Pez, *J. Am. Chem. Soc.*, 1995, **117**, 329–335.

170 G. N. Wang, Y. Dai, X. B. Hu, F. Xiao, Y. T. Wu, Z. B. Zhang and Z. Zhou, *J. Mol. Liq.*, 2012, **168**, 17–20.

171 F. G. Bordwell, J. C. Branca, D. L. Hughes and W. N. Olmstead, *J. Org. Chem.*, 1980, **45**, 3305–3313.

172 J. X. Mao, J. A. Steckel, F. Yan, N. Dhumal, H. Kim and K. Damodaran, *Phys. Chem. Chem. Phys.*, 2015, **18**, 1911–1917.

173 M. Kanakubo, T. Makino and T. Umecky, *J. Mol. Liq.*, 2016, **217**, 112–119.

174 G. Gurau, H. Rodríguez, S. P. Kelley, P. Janiczek, R. S. Kalb and R. D. Rogers, *Angew. Chemie Int. Ed.*, 2011, **50**, 12024–12026.

175 A. Yokozeki, M. B. Shiflett, C. P. Junk, L. M. Grieco and T. Foo, *J. Phys. Chem. B*, 2008, **112**, 16654–16663.

176 K. S. Alongi and G. C. Shields, *Annu. Rep. Comput. Chem.*, 2010, **6**, 113–138.

177 E. L. M. Miguel, P. L. Silva and J. R. Pliego, *J. Phys. Chem. B*, 2014, **118**, 5730–5739.

178 A. L. Bacarella, E. Grunwald, H. P. Marshall and E. L. Purlee, *J. Org. Chem.*, 1955, **20**, 747–762.

179 H. S. Harned and G. L. Kazanjian, *J. Am. Chem. Soc.*, 1936, **58**, 1912–1915.

180 S. H. Pine, *Organic Chemistry*, McGraw-Hill, New York, 5th ed., 1987.

181 J. Reijenga, A. van Hoof, A. van Loon and B. Teunissen, *Anal. Chem. Insights*, 2013, **8**, 53–71.

182 R. de Levie, *Aqueous Acid-Base Equilibria and Titrations*, Oxford University Press, Oxford, 1999.

183 G. P. Ertokus and A. H. Aktas, *Asian J. Chem.*, 2009, **21**, 3825–3835.

184 M. Jabbari, *J. Mol. Liq.*, 2015, **208**, 5–10.

185 K. Takács-Novák, K. J. Box and A. Avdeef, *Int. J. Pharm.*, 1997, **151**, 235–248.

186 E. Koort, P. Gans, K. Herodes, V. Pihl and I. Leito, *Anal. Bioanal. Chem.*, 2006, **385**, 1124–1139.

187 M. Li, D. Constantinescu, L. Wang, A. Mohs and J. Gmehling, *Ind. Eng. Chem. Res.*, 2010, **49**, 4981–4988.

188 C. O. Laoire, S. Mukerjee, K. M. Abraham, E. J. Plichta and M. A. Hendrickson, *J. Phys. Chem. C*, 2009, **113**, 20127–20134.

189 H. Wang and M. Yoshio, *J. Power Sources*, 2010, **195**, 1263–1265.

190 R. H. Crabtree, *Acc. Chem. Res.*, 1979, **12**, 331–337.

191 A. L. Bacarella, E. Grunwald, H. P. Marshall and E. L. Purlee, *J. Phys. Chem.*, 1958, **62**, 856–857.

192 G. Gran, *Acta Chem. Scand.*, 1950, 4, 559–577.

193 G. Gran, *Analyst*, 1952, **77**, 661–671.

194 C. Mehrbach, C. H. Culberson, J. E. Hawley and R. M. Pytkowicz, *Limnol. Oceanogr.*, 1973, **18**, 897–907.

195 S. Espinosa, E. Bosch and M. Rosés, *Anal. Chim. Acta*, 2002, **454**, 157–166.

196 F. Rived, I. Canals, E. Bosch and M. Rosés, *Anal. Chim. Acta*, 2001, **439**, 315–333.

197 Caspar Schoolderman, *Personal communication*, .

198 M. Johnsson and I. Persson, *Inorganica Chim. Acta*, 1987, **127**, 15–24.

199 I. M. Kolthoff and M. K. Chantooni, *J. Phys. Chem.*, 1972, **76**, 2024–2034.

200 R. Marcos, L. Xue, R. Sánchez-De-Armas and M. S. G. Ahlquist, *ACS Catal.*, 2016, **6**,

2923–2929.

201 Y. Marcus, *J. Chem. Soc., Faraday Trans.*, 1991, **87**, 2995–2999.

202 M. H. Abraham and Y. H. Zhao, *J. Org. Chem.*, 2004, **69**, 4677–4685.

203 M. H. Abraham and W. E. Acree, *J. Org. Chem.*, 2010, **75**, 1006–1015.

204 Y. Marcus, *Pure Appl. Chem.*, 1983, **55**, 977–1021.

205 D. Jiao and S. B. Rempe, *J. Chem. Phys.*, 2011, **134**, 224506.

206 A. Gennaro, A. A. Isse and E. Vianello, *J. Electroanal. Chem.*, 1990, **289**, 203–215.

207 K. M. Johansson, E. I. Izgorodina, M. Forsyth, D. R. MacFarlane and K. R. Seddon, *Phys. Chem. Chem. Phys.*, 2008, **10**, 2972–2978.

208 N. Nishi, T. Nakabayashi and K. Kosugi, *J. Phys. Chem. A*, 1999, **103**, 10851–10858.

209 C. Elliott, V. Vijayakumar, W. Zink and R. Hansen, *J. Lab. Autom.*, 2007, **12**, 17–24.